A Unitary RG-based Auxiliary Model Approach to Strongly-Correlated Electrons

Abhirup Mukherjee, Siddhartha Lal

Department of Physical Sciences, Indian Institute of Science Education
and Research-Kolkata, Mohanpur Campus, West Bengal 741246, India
(Dated: April 2, 2025)

CONTENTS

I.   WHAT IS THE MINIMAL IMPURITY MODEL FOR A MOTT METAL-INSULATOR TRANSITION?

The Hubbard model is one of the fundamental models for strong electronic correlation; in its simplest form, it features a single band of conduction electrons hopping on a lattice and interacting via local correlations that provide a cost U if any site is doubly occupied:

$$H_{\text{hubb}} = -t \sum_{\langle i,j \rangle, \sigma} \left(c_{i\sigma}^{\dagger} c_{j\sigma} + \text{h.c.} \right) + U \sum_i \hat{n}_{i\uparrow} \hat{n}_{i\downarrow} - \mu \sum_{i,\sigma} \hat{n}_{i\sigma} \ . \tag{1}$$

The model can be made particle-hole symmetric by choosing $\mu = U/2$:

$$H_{\text{hubb}} = -t \sum_{\langle i,j \rangle, \sigma} \left(c_{i\sigma}^\dagger c_{j\sigma} + \text{h.c.} \right) - \frac{U}{2} \sum_i (\hat{n}_{i\uparrow} - \hat{n}_{i\downarrow})^2$$

There are two trivial limits of the model. At $U = 0$, the bath consists of just a kinetic energy part, and the ground state is just a filled Fermi sea. At $t = 0$, each lattice site decouples from the rest and becomes a local moment, which under symmetry-breaking becomes a Néel antiferromagnet. This suggests that on increasing U/t beyond some critical value, the system might undergo a phase transition from a metallic state to an insulating state [1]. This transition is reflected in the local spectral function - while it has a well-defined zero energy peak in the metallic phase, it is gapped in the insulating phase.

One method of studying Hubbard models is through auxiliary models, described in the next section. Auxiliary models are simpler versions of the full Hamiltonian that are able to capture the essential physics. For example, a correlated impurity interacting with a conduction bath is a potential auxiliary model for the Hubbard Hamiltonian:

$$\mathcal{H}_{\text{SIAM}} = \epsilon_d \hat{n}_d + U \hat{n}_{d\uparrow} \hat{n}_{d\downarrow} - t \sum_{\langle i,j \rangle, \sigma} \left(c_{i\sigma}^\dagger c_{j\sigma} + \text{h.c.} \right) \\ + V \sum_\sigma \left(c_{d\sigma}^\dagger c_{0\sigma} + \text{h.c.} \right) \tag{2}$$

The impurity has onsite energy ϵ_d and an onsite correlation U. It hybridises into the bath through V.

If the impurity site hybridises with a *non-interacting* bath defined by a uniform density of states, the impurity spectral function is found to have a well-defined Kondo resonance at low temperatures. Increasing the impurity correlation U only serves to reduce the width of the central peak at the cost of the appearance of side bands at energy scales of the order of U, but the resonance never dies. The situation is however different if the impurity is embedded in a correlated conduction bath with a non-trivial density of states. For the case of a conduction band with the DOS shown in the right of the figure below, the impurity hybridises into a reduced bandwidth because of the correlation on the lattice [2].

This difference in the type of conduction baths is utilised in dynamical mean-field theory to describe various phases of the bulk system. This is done through the DMFT algorithm: one starts with a non-interacting bath, but depending on the value of U, the conduction bath then gets modified and we ultimately end up with something that is different from what we started with. For small U, the bath does not change much and we retain the central resonance of the impurity spectral function. This then describes a metal in the bulk. For larger values of U, however, the bath changes significantly such that its density of states becomes non-constant. Above a critical U_c, the impurity spectral function gets gapped out, and that then describes the insulating phase in the bulk. *This leaves open the following question: What is the minimal correlation one can insert into the non-interacting bath (of a single-impurity Anderson model) that can capture both the metallic and insulating phases of the bulk model?*
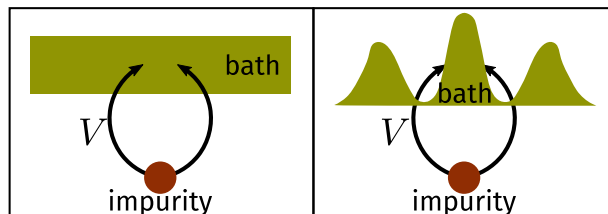
FIG. 1. Various kinds of bath that an impurity can hybridise into. The left panel shows a non-interacting conduction band with a flat density of states. The right panel shows an interacting bath with an energy-dependent density of states. In the latter case, the impurity "feels" a reduced effective bandwidth defined by the width of the central peak.

II. PHILOSOPHY OF AUXILIARY MODEL METHODS

The present method is a realisation of the general method of using simpler systems called auxiliary models to study bulk systems [3]. In general, a full Hamiltonian can be separated into the Hamiltonians for a particular subsystem S,

the rest of the system R, and the interactions between S and R.

$$\mathcal{H} = \mathcal{H}_S \left|S\right\rangle \left\langle S\right| + \mathcal{H}_R \left|R\right\rangle \left\langle R\right| + \mathcal{H}_{SR} \left|S\right\rangle \left\langle R\right|$$
$$+ \mathcal{H}_{RS} \left|S\right\rangle \left\langle R\right| = \begin{bmatrix} \mathcal{H}_R & \mathcal{H}_{RS} \\ \mathcal{H}_{RS}^* & \mathcal{H}_S \end{bmatrix} \quad (3)$$

where $\left|S\right\rangle$ and $\left|R\right\rangle$ actually represents sums over all basis kets of S and R respectively. As an example, we can split the Hubbard model Hamiltonian between a particular site $i = p$ and the rest of the lattice into three parts $H_{\text{hubb}} = H_S + H_R + H_{SR} + H_{RS}$ (fig. 2), where

$$H_S = U^H \hat{n}_{p\uparrow} \hat{n}_{p\downarrow} - \mu^H \sum_\sigma \hat{n}_{p\sigma}$$

$$H_R = U^H \sum_{i \neq p} \hat{n}_{i\uparrow} \hat{n}_{p\downarrow} - \mu^H \sum_{i \neq p, \sigma} \hat{n}_{i\sigma}$$
$$- t^H \sum_{\substack{\sigma, \langle i,j \rangle \\ i \neq p \neq j}} \left(c_{i\sigma}^\dagger c_{j\sigma} + \text{h.c.} \right) \quad (4)$$

$$H_{SR} + H_{Rs} = -t^H \sum_{\substack{\sigma, \\ i \in \text{N.N. of } p}} \left(c_{i\sigma}^\dagger c_{p\sigma} + \text{h.c.} \right) \ .$$

The Greens function of the full Hamiltonian can also be split in a similar fashion:

$$G(\omega) = \begin{bmatrix} G_S & G_{SR} \\ G_{RS} & G_R \end{bmatrix} \quad (5)$$

Each Greens function can be written in terms of the non-interacting counterpart and the self-energy through the Dyson equation: $\Sigma_i = 1/G_{i,0} - 1/G_i$.

The subsystem S is usually taken to be the "cluster", and consequently, R represents the "bath". The smaller system is typically chosen such that its eigenstates are known exactly. Progress is then made by choosing a simpler version of H_R and a simpler form also for its coupling H_{RS} with the smaller system. This combination of the cluster and the simpler bath is then called the *auxiliary system*. A typical auxiliary system for the Hubbard model would be the SIAM, where the impurity represents an arbitrary site p of the lattice, the bath represents the rest of the lattice sites and the hybridisation term between the impurity and the bath represents the coupling term H_{RS}. Such a construction is shown in fig. 2. *It should be noted that any reasonable choice of the cluster and bath would break the*
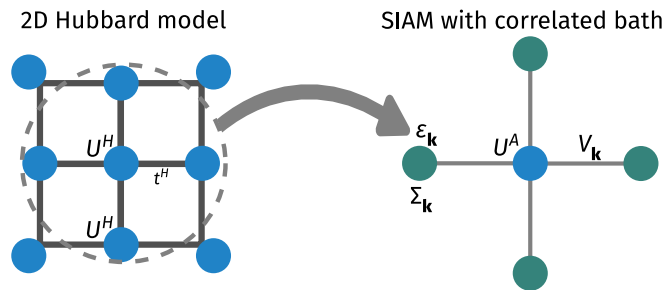
FIG. 2. *Left*: Full Hubbard model lattice with onsite repulsion U^H on all sites and hopping between nearest neighbour sites with strength t^H. *Right*: Extraction of the auxiliary (cluster+bath) system from the full lattice. The central site on left becomes the impurity site (red) on the right (with an onsite repulsion ϵ_d), while the rest of the $N - 1$ sites on the left form a conduction bath (green circles) (with dispersion ϵ_k and correlation modelled by the self-energy $\Sigma_k(\omega)$) that hybridizes with the impurity through the coupling V.

translational symmetry of the full model. To allow computing quantities, one would need to make the bath (which is a much larger system) simpler than the cluster (which is a single site). This distinction breaks the translational symmetry of the Hubbard model. For eg., if one chooses eq. 2 as the auxiliary system, then the fact that the impurity has an onsite correlation while the bath does not means we have broken the symmetry between the cluster and the bath.

Dynamical mean-field theory - an example of an auxiliary model approach

Dynamical mean-field theory is an approximation scheme that use impurity models to obtain Greens functions of bulk systems of strong correlation [4, 5]. The essential idea is to find the most suitable impurity model that replicates the full Hamiltonian. This is done through the following algorithm. Given a bulk Hamiltonian with on=site correlation U and a non-interacting $k-$space Greens function $G_{k,0}$ for the bath:

1. We first create an impurity model with on-site correlation U and non-interacting impurity Greens function $G_{i,0} = \sum_k G_{k,0}$.

$$\mathcal{H}_{\text{aux}} = H_{\text{imp}}(U) - t \sum_\sigma \left(c_{d\sigma}^\dagger c_{0\sigma} + \text{h.c.} \right) + H_{\text{bath}}\left(t, G_{i,0} \right)$$

2. This impurity model is solved using some method like numerical renormalisation group, and the self-energy Σ_{aux} of the impurity is obtained.

3. The impurity self-energy is now *equated* with the bath momentum-space self-energy:

$$\Sigma_k(\omega) = \Sigma_{\text{aux}}(\omega)$$

Since the impurity is purely local, this is an approximation that involves replacing a non-local quantity by its purely local component: $\Sigma_k(\omega) = \sum_{\mathbf{r}} e^{i\vec{k}\cdot\vec{r}} \Sigma_{\mathbf{r}}(\omega) \simeq \Sigma_{\mathbf{r}=0}(\omega)$. This approximation is a result of the single-site nature of the cluster of the chosen auxiliary model - larger clusters with more impurities can generate non-local components. This local approximation becomes exact in the limit of large system dimension w, because it can be shown that the non-local components of the self-energy scale as $w^{-3/2}$.

4. With this updated bath self-energy, we now create a new $k-$space Greens function for the bath:

$$\begin{aligned}
G_i(\omega) &= \sum_k G_k(\omega) \\
&= \sum_k \frac{1}{\omega - H_{\text{bath}}(k) - \Sigma_k(\omega)} \\
&= \sum_k \frac{1}{\omega - H_{\text{bath}}(k) - \Sigma_{\text{aux}}(\omega)}
\end{aligned} \tag{6}$$

This interacting Greens function is then used to obtain the updated non-interacting Greens function, using Dyson's equation:

$$G_{i,0} = \frac{1}{1/G_i + \Sigma_{\text{aux}}}$$

5. Repeat the algorithm from step 1 with the updated $G_{i,0}$, until Σ_{aux} stops changing.

The stopping condition is the consistency relation that makes the bath and impurity self-energies equal.
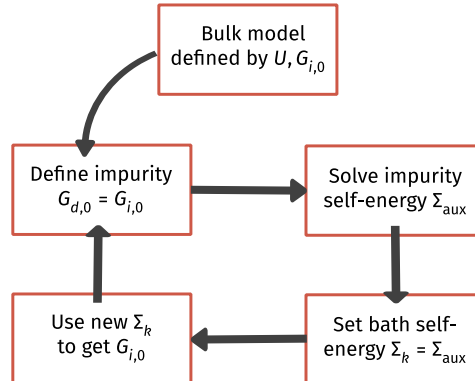
III.   A "BOTTOMS-UP" APPROACH TO USING AUXILIARY MODELS

As mentioned in the previous section, the question we are posing is the following: what is the simplest auxiliary model of impurity in a bath that can capture the metal-insulator transition in a Hubbard-like model of correlated electrons. We approach this problem in a constructionist/bottoms-up way: we first identity an appropriate quantum impurity model (fig. 2) that shows an impurity phase transition, and then create a bulk model out of this auxiliary model. The bulk model hence created will then show a metal-insulator transition.

The impurity models are studied using the recently-developed unitary renormalisation group method [6–11]. The leap to the bulk model is then made by applying lattice translation operators on the auxiliary model. This process, referred to as tiling here, relates the auxiliary model Hamiltonian with that of the bulk, and hence allows connecting the Greens functions and other related quantities across dimensions. One nice outcome is that since the auxiliary model has multiple sites, there is a real-space off-diagonal component of the self-energy, and this leads to a $k-$dependence in the self-energy of the bulk, which is in contrast with the lack of $k-$dependence in single-site DMFT.

In our approach, the auxiliary models can be chosen in various ways. The simplest choice is of course the single-impurity Anderson model of eq. 2:

$$\mathcal{H}_{\text{SIAM}} = \epsilon_d \hat{n}_d + U \hat{n}_{d\uparrow} \hat{n}_{d\downarrow} - t \sum_{\langle i,j \rangle, \sigma} \left(c_{i\sigma}^{\dagger} c_{j\sigma} + \text{h.c.} \right)$$
$$+ V \sum_{\sigma} \left(c_{d\sigma}^{\dagger} c_{0\sigma} + \text{h.c.} \right) \tag{7}$$

This model does not show any impurity phase transition - the impurity is always screened [12–14]. Correlation can be introduced into the auxiliary model in two ways:

1. The impurity or the bath can be made to have additional interaction:

$$\mathcal{H}_{\text{aux}} = H_{\text{SIAM}} + J \vec{S}_d \cdot \vec{s}_0 - \frac{1}{2} U_b \left(\hat{n}_{0\uparrow} - \hat{n}_{0\downarrow} \right)^2 \tag{8}$$

   The additional terms are (i) a spin-exchange interaction between the impurity site and the zeroth site, and (ii) a local correlation on the zeroth site.

2. The second method is to make the cluster itself more complicated. That is, one can introduce multiple impurity sites that are connected via the hopping:

$$\mathcal{H}_{\text{aux}} = -\frac{U}{2} \sum_{d_i} (\hat{n}_{d_i\uparrow} - \hat{n}_{d_i\downarrow})^2 + V \sum_{d_i} \sum_{\sigma} \left(c_{d_i\sigma}^{\dagger} c_{0\sigma} + \text{h.c.} \right)$$
$$+ \text{K.E.} - t \sum_{\sigma} \left(c_{d_1\sigma}^{\dagger} c_{d_2\sigma} + \text{h.c.} \right) \tag{9}$$
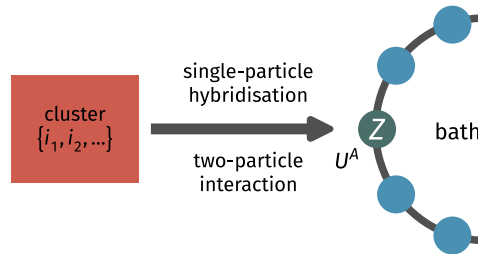
FIG. 3. Cluster+bath construction of auxiliary model. It consists of a cluster (red square) hybridising with a bath (ring) by hopping into and out of the zeroth site (pink). The other sites (green) form the rest of the bath. Just the cluster and the zeroth site have onsite correlations.

The next step in the programme is to tile the real-space lattice with this cluster+bath Hamiltonian $\tilde{H}$ to restore translational invariance (shown in a later section), and obtain a new bulk Hamiltonian for correlated electrons, $\tilde{H} = T \left[\mathcal{H}_{\text{aux}} \right] T^{-1}$, where T denotes the operator that performs the set of iterative real-space translations, and

enables the cluster-bath (auxiliary model) Hamiltonian to span the target real-space lattice. Given a general auxiliary model Hamiltonian $\mathcal{H}_{\text{aux}}$, the result of tiling can be written very generally as

$$\tilde{H} = \sum_{\{i_1, i_2, ...\}} \mathcal{H}_{\text{aux}}\left(\{i_1, i_2, ...\}\right) \tag{10}$$

where $\{i_1, i_2, ...\}$ represents the indices for the members of the cluster. To reiterate, what that means is that we have placed the cluster+bath system at all lattice point sets $\{i_1, i_2, ...\}$ to reconstruct a new model of correlated electrons. The answer to how closely $\tilde{H}$ approximates a target model of correlated electrons lies in (i) the choice of the cluster-bath construction of the auxiliary model, and (ii) the accuracy of the URG procedure on the auxiliary model.

The strategy, therefore, is to relate Hamiltonians, wavefunctions and hence correlation functions of the bulk model to those of the auxiliary model. One can then substitute the information obtained from solutions of the auxiliary model, and thereby calculate quantities on the bulk lattice model.

IV. EXTENDING THE ANDERSON MODEL TO A LATTICE-EMBEDDED IMPURITY MODEL

Crucial to our method is the choice of an impurity auxiliary model that is able to capture important aspects of the lattice model in a local sense. Some of us have shown in a previous work [15] that almost all aspects of the Mott metal-insulator transition on the infinite dimensional Hubbard model on the Bethe lattice (as seen, for example, from dynamical mean-field theory [16]) can be captured from a simple extension of the Anderson impurity model (eSIAM). The extension involves including a local attractive interacting U_b on the conduction bath site coupled to the impurity site; by tuning the ratio of $|U_b|$ and the Kondo coupling J, we obtained an impurity phase transition from a screened phase to an unscreened local moment phase. Since the impurity site of the auxiliary model is a representative of each correlated site on the lattice, the mapping to the lattice model then involves identifying the locally gapless impurity phase with the bulk gapless of the lattice model. In other words, the ability of the impurity site to participate in low-energy excitations corresponds to the ability of an electron, within the lattice model, to delocalise from one site into the rest of the lattice. In the same vein, a local moment phase of the impurity model maps to a gapped Mott insulating phase on the lattice model, where there's a charge gap to electron hopping processes.

In the present work, the goal is to tackle interacting fermions on a 2D square lattice, which makes it important for us to incorporate the effects of the lattice within the impurity model. More specifically, while the impurity-bath interactions on the infinite dimensional Bethe lattice are $s-$wave symmetric, that is not a realistic form for a 2D lattice. To make a realistic impurity model, we embed the impurity site into the lattice of a 2D conduction bath, and lower the $s-$wave symmetry of the interactions down to the C_4 symmetry of the 2D square lattice. A general structure of such a model is shown in fig. 4; one of the sites of the 2D square lattice is identified as the impurity (red), while the four nearest-neghbours (navy blue) interact directly with this impurity site through a C_4-symmetric interaction.
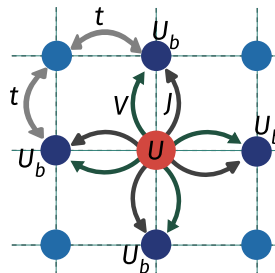

FIG. 4. General structure of an embedded extended SIAM, where the impurity site is a part of the 2D square lattice. The four nearest-neighbour sites (dark blue) interact with the impurity site through one or more processes, and can host local interactions. The other lattice sites (light blue) are completely non-interacting.

A. Hamiltonian

We consider an impurity spin $\vec{S}_d$ interacting with a two-dimensional tight-binding conduction bath through a highly localised interaction, described by the Hamiltonian

$$\mathcal{H} = H_{\text{cbath}} + H_{\text{imp-cbath}} + H_{\text{cbath-int}} \, , \tag{11}$$

where H_{cbath} is the kinetic energy arising out of nearest-neighbour hopping processes,

$$H_{\text{cbath}} = -2t \sum_{\mathbf{k}} \left[\cos(ak_x) + \cos(ak_y) \right] c_{\mathbf{k},\sigma}^{\dagger} c_{\mathbf{k},\sigma} \, . \tag{12}$$

For the impurity-bath interaction $H_{\text{imp-cbath}}$ and the local interaction $H_{\text{cbath-int}}$ in the bath, we take the simplest choices consistent with the 2D square lattice geometry:

$$H_{\text{imp-cbath}} = \frac{1}{2} J \sum_{\sigma_1, \sigma_2} \sum_Z \mathbf{S}_d \cdot c_{Z\sigma_1}^{\dagger} \boldsymbol{\tau}_{\sigma_1, \sigma_2} c_{Z\sigma_2} \, ,$$

$$H_{\text{cbath-int}} = -\frac{W}{2} \sum_Z \left(n_{Z\uparrow} - n_{Z\downarrow} \right)^2 \, , \tag{13}$$

where Z sums over all nearest-neighbour sites of the impurity site (navy blue circles in Fig. 4, henceforth referred to as bath zeroth sites). The impurity interacts with the bath zeroth sites in $H_{\text{imp-cbath}}$ through four local Kondo terms, of uniform strength. The other term $H_{\text{cbath-int}}$ represents local Hubbard interactions on the four zeroth sites, again of uniform strength.

The 2D structure of the impurity model and its distinction from the infinite-dimensional counterpart becomes apparent once we transform the Hamiltonian to momentum space:

$$J_{\mathbf{k},\mathbf{k}'} = \frac{J}{2} \left[\cos \left(\mathbf{k}_x - \mathbf{k}_x' \right) + \cos \left(\mathbf{k}_y - \mathbf{k}_y' \right) \right] \, ,$$

$$W_{\mathbf{k},\mathbf{k}',\mathbf{q},\mathbf{q}'} = W \left[\cos \left(\mathbf{k}_x - \mathbf{k}_x' + \mathbf{q}_x - \mathbf{q}_x' \right) + \cos \left(\mathbf{k}_y - \mathbf{k}_y' + \mathbf{q}_y - \mathbf{q}_y' \right) \right] \, . \tag{14}$$

where the subscripts x and y represent components of the momenta vector. This form shows that the Kondo coupling is no longer independent of the exchange momentum, and encodes information of the lattice geometry in it.

B. The unitary renormalisation group method

In order to obtain the various low-energy phases of our impurity model, we perform a scaling analysis of the associated Hamiltonian using the recently developed unitary renormalisation group (URG) method [8, 9]. The method has been applied successfully on a wide variety of problems of correlated fermions [6–11, 17–19]. The method proceeds by resolving quantum fluctuations in high-energy degrees of freedom, leading to a low-energy Hamiltonian with renormalised couplings and new emergent degrees of freedom. Typically, for a system with Fermi energy ϵ_F and bandwidth E_N, the sequence of isoenergetic shells $\left\{ E_{(j)} \right\}, E_j \in [E_0, E_N]$ define the states whose quantum fluctuations we sequentially resolve. The momentum states lying on shells E_N that are far away from the Fermi surface comprise the UV states, while those on shells near the Fermi surface comprise the IR states. This scheme is shown in Fig. (5).

As a result of the URG transformations, the Hamiltonian $H_{(j)}$ at a given RG step j involves scattering processes between the $k-$states that have energies lower than $D_{(j+1)}$. The unitary transformation $U_{(j)}$ is then defined so as to remove the number fluctuations of the currently most energetic set of states $D_{(j)}$ [8, 9]:

$$H_{(j-1)} = U_{(j)} H_{(j)} U_{(j)}^{\dagger} \, , \text{such that } \left[H_{(j-1)}, \hat{n}_j \right] = 0 \, . \tag{15}$$

The eigenvalue of $\hat{n}_j$ has, thus, been rendered an integral of motion (IOM) under the RG transformation.

The unitary transformations can be expressed in terms of a generator $\eta_{(j)}$ that has fermionic algebra [8, 9]:

$$U_{(j)} = \frac{1}{\sqrt{2}} \left(1 + \eta_{(j)} - \eta_{(j)}^{\dagger} \right) \, , \quad \left\{ \eta_{(j)}, \eta_{(j)}^{\dagger} \right\} = 1 \, , \tag{16}$$

where $\{\cdot\}$ is the anticommutator. The unitary operator $U_{(j)}$ that appears in Eq. (16) can be cast into the well-known general form $U = e^{\mathcal{S}}, \mathcal{S} = \frac{\pi}{4} \left(\eta_{(j)}^{\dagger} - \eta_{(j)} \right)$ that a unitary operator can take, defined by an anti-Hermitian operator $\mathcal{S}$.
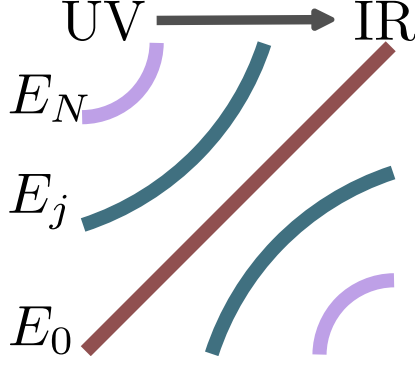
FIG. 5. High energy - low energy scheme defined and used in the URG method. The states away from the Fermi surface (E_N in the figure) form the UV subspace and are decoupled first, leading to a Hamiltonian which is more block-diagonal and comprised of only the IR states near the Fermi surface (E_0 in the figure).

The generator $\eta_{(j)}$ is given by the expression [8, 9]

$$\eta^\dagger_{(j)} = \frac{1}{\hat{\omega}_{(j)} - \mathrm{Tr}\left(H_{(j)}\hat{n}_j\right)} c^\dagger_j \mathrm{Tr}\left(H_{(j)} c_j\right) \; . \tag{17}$$

The operators $\eta_{(j)}, \eta^\dagger_{(j)}$ behave as the many-particle analogues of the single-particle field operators $c_j, c^\dagger_j$ - they change the occupation number of the single-particle Fock space $|n_j\rangle$. The important operator $\hat{\omega}_{(j)}$ originates from the quantum fluctuations that exist in the problem because of the non-commutation of the kinetic energy terms and the interaction terms in the Hamiltonian:

$$\hat{\omega}_{(j)} = H_{(j-1)} - H^i_{(j)} \; . \tag{18}$$

$H^i_{(j)}$ is the part of $H_{(j)}$ that commutes with $\hat{n}_j$ but does *not* commute with at least one $\hat{n}_l$ for $l < j$. The RG flow continues up to energy D^*, where a fixed point is reached from the vanishing of the RG function. Detailed comparisons of the URG with other methods (e.g., the functional RG, spectrum bifurcation RG etc.) can be found in Refs. [6, 8].

C. Unitary RG analysis of the embedded eSIAM

We studied the low-energy physics of this model through a unitary renormalisation group calculation that decouples the high-energy modes of the conduction bath and incorporates their effects in the form of renormalised Hamiltonian couplings. We find that the bath interaction W remains marginal (does not undergo any renormalisation), while the renormalisation in the momentum-resolved Kondo coupling $J^{(j)}$ at the jth step is of the form

$$\Delta J^{(j)}_{\mathbf{k}_1, \mathbf{k}_2} = - \sum_{\mathbf{q} \in \mathrm{PS}} \frac{J^{(j)}_{\mathbf{k}_2, \mathbf{q}} J^{(j)}_{\mathbf{q}, \mathbf{k}_1} + 4 J^{(j)}_{\mathbf{q}, \bar{\mathbf{q}}} W_{\bar{\mathbf{q}}, \mathbf{k}_2, \mathbf{k}_1, \mathbf{q}}}{\omega - \frac{1}{2}|\varepsilon_j| + J^{(j)}_{\mathbf{q}}/4 + W_{\mathbf{q}}/2} \; , \tag{19}$$

where ε_j is the energy of the shell being decoupled at the jth step, and the sum is over all momentum states $\mathbf{q}$ in the particle sector (PS) of the shell ε_j (that is, all states that are occupied at $T = 0$ and in the absence of any quantum fluctuations). The Kondo coupling and the RG equation as well have certain symmetries under transformations in the Brillouin zone. If any one of the momenta $\mathbf{k}_1$ or $\mathbf{k}_2$ are translated by π ($k_{1x} \to k_{1x} + \pi, k_{1y} \to k_{1y} + \pi$), the coupling as well as the RG equation changes sign. Translating both the momenta leads to the reversal of the sign change.

$$\Delta J^{(j)}_{\mathbf{k}_1 + \boldsymbol{\pi}, \mathbf{k}_2} = \Delta J^{(j)}_{\mathbf{k}_1, \mathbf{k}_2 + \boldsymbol{\pi}} = -\Delta J^{(j)}_{\mathbf{k}_1 + \boldsymbol{\pi}, \mathbf{k}_2 + \boldsymbol{\pi}} = -\Delta J^{(j)}_{\mathbf{k}_1, \mathbf{k}_2} \; . \tag{20}$$

These transformations involve translating one or both momenta through the center of the Brillouin zone.

With our chosen momentum-space dependence of the Kondo coupling and bath interaction, the form of the Kondo coupling morphs during the RG flow, allowing the emergence of new degrees of freedom that screen the impurity at low-energies. At the first step, the RG equation can be written down explicitly as

$$\Delta J^{(0)}_{\mathbf{k}, \mathbf{k}'} = - \sum_{\mathbf{q} \in \mathrm{PS}} \frac{J^2 \frac{1}{2} \sum_a \cos\left(\mathbf{k}'_a - \mathbf{q}_a\right) \frac{1}{2} \sum_a \cos\left(\mathbf{q}_a - \mathbf{k}_a\right) - 2JW \sum_a \cos\left(\mathbf{k}'_a - \mathbf{k}_a\right)}{\omega - \frac{1}{2}|\varepsilon_j| + \frac{J}{4} f_{\mathcal{D}}(\mathbf{q})^2 + \frac{W}{4}} \; , \tag{21}$$

where a sums over the x and y components of the momenta. We see that unlike the bare Kondo coupling $J_{\mathbf{k},\mathbf{k}'}$ that depends only on the momentum difference $\mathbf{k} - \mathbf{k}'$, the renormalisation $\Delta J^{(0)}$ depends on products of the momenta. This shows the form of the Kondo coupling continuously changes under renormalisation.

V. LOW-ENERGY DESCRIPTION OF THE EMBEDDED ESIAM

A. Zero temperature phase diagram and impurity site dynamics

The ground state phase diagram of the impurity model is shown in the left panel of Fig. 6. We find that upon tuning the ratio W/J of the bath interaction strength W and the Kondo coupling J, the impurity site undergoes a transition from a screened paramagnetic phase (dark green) to an unscreened local moment phase (yellow), through an intermediate pseudogapped regime (pink). The nature of pseudogapped phase will be clarified in the upcoming sections. The phase transition is seen through the evolution of the local spectral function (middle panel of Fig. 6); increasing the ratio W/J leads to the sharpening of the central Kondo resonance, indicating that the local Fermi liquid excitations are becoming poorer. At the transition, the extremely sharp peak disappears and we are left with a hard gap at zero frequency. A complimentary picture is painted by the imaginary part Σ'' of the impurity self-energy. The poles in Σ'' are the edges of the central Kondo resonance, and its sharpening leads to the coalescing of the poles.
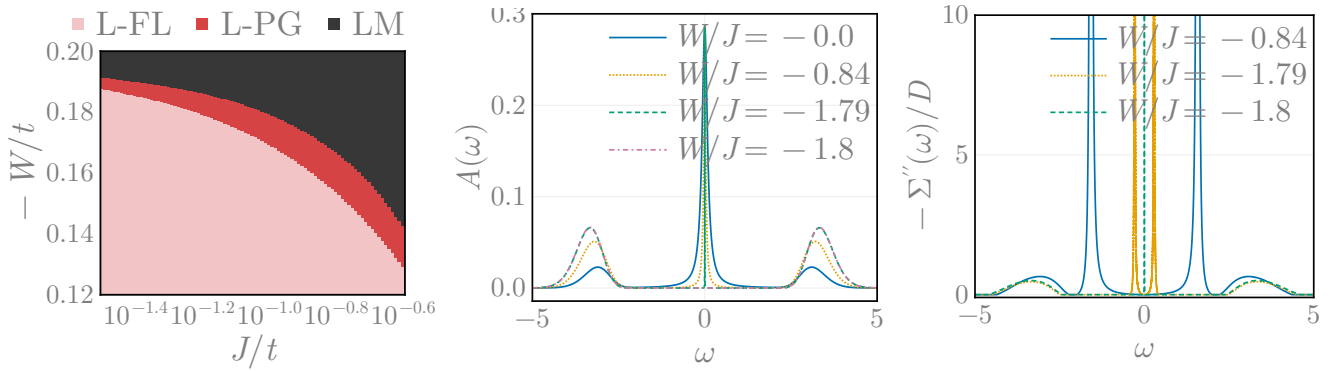
FIG. 6. **Left**: Zero temperature phase diagram of the embedded impurity model, obtained by tracking impurity-bath spin correlations. The pink phase is characterised by perfect Kondo screening and local Fermi liquid excitations (L-FL), leading to non-zero spin-correlations all over the Fermi surface of the conduction electrons. The red phase is a local pseudogap (L-PG) phase, where a part of the Fermi surface (starting from the antinodal regions) no longer participates in Kondo screening. This leads to "Fermi arc"-like behaviour in the spin-correlations and the $k-$space density of states. The black phase is a local moment (LM) phase, where the impurity is completely decoupled from the conduction electrons. **Middle**: Local spectral function of the impurity site. The blue curve is the normal Kondo resonance in the absence of any bath interaction. The yellow and green curves show the sharpening the spectral function through the locally pseudogapped phase, as momentum states are expelled from the Kondo cloud. The final pink curve shows the charge gap in the local moment phase. **Right:** Imaginary part of impurity self-energy. Poles represent the beginning of the optical gap between the central Kondo resonance and the Hubbard sidebands. Increasing the bath interaction leads to the coalescing of the poles (due to the sharpening of the Kondo resonance), ultimately leading to a zero frequency pole in the local moment phase.

B. Presence of a local pseudogapping transition with electronic differentiation in momentum space

We now discuss the intervening pseudogapped regime (pink region) of the phase diagram. We find that the process of Kondo breakdown in our model occurs anisotropically in our model - the transition starts through the removal, from the Kondo cloud, of the antinodal points of the conduction bath Fermi surface. This is followed by the sequential removal of points away from the antinodes, with the nodal points being removed at the very end. This electronic differentiation is a novel feature of this model that arises because of the more realistic embedding of the impurity site into the conduction bath lattice.

We quantify the removal of these points by the vanishing (up to a tolerance) of the average renormalised scattering

probability

$$\Gamma^*(\mathbf{k}) = \sum_{\mathbf{q} < \Lambda^*} \left(J^*_{\mathbf{k},\mathbf{q}} \right)^2 \ , \tag{22}$$

where the other momentum $\mathbf{q}$ is summed over all the momentum states that reside within the fixed point window. The quantity $\Gamma(\mathbf{k})$ therefore quantifies the degree to which the state $\mathbf{k}$ is participating in screening the impurity at low energies. The $k-$space forms of this quantity at various values of W/J is shown in fig. 7, and the difference in the behaviour of the nodal and antinodel points is apparent.
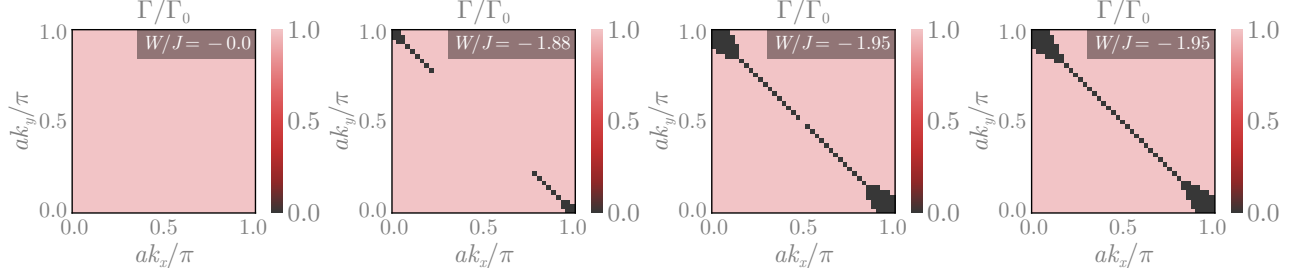
FIG. 7. Variation of the total scattering probability $\Gamma(\mathbf{k})$ (defined in the main text) as W/J is increased from left to right. Each plot shows whether $\Gamma(\mathbf{k})$ is RG-relevant (pink) or irrelevant (black). RG-relevant values of $\Gamma(\mathbf{k})$ indicate that the $k-$point participates in Kondo screening at low-energies, while an irrelevant value indicates that the $k-$point is decoupled from the impurity site. As W/J is made more negative, the antinodal points are the first state to be removed from the Kondo cloud, while the node is the last to be removed.

C. Spin-correlations across the pseudogap

In figure 8, we show the evolution of the spin-spin correlation $\chi_s(d, \vec{k}) = \left\langle \mathbf{S_d} \cdot \mathbf{S}_{\vec{k}} \right\rangle$ in $k-$space, as the system is tuned through the pseudogap. At vanishing value of the interaction W, the spin correlations are concentrated around the antinode, because of the $p-$wave nature of the Kondo interaction. At the entry into the pseudogap, the correlations become more pronounced near the nodes and become suppressed near the antinodes, signalling that the latter parts will gap out first. The last three figures ($W/J = -1.74, -1.83, -1.84$) show how $k-$points starting from the antinode progressively exit the Kondo cloud, the node being the last to decouple from the impurity.
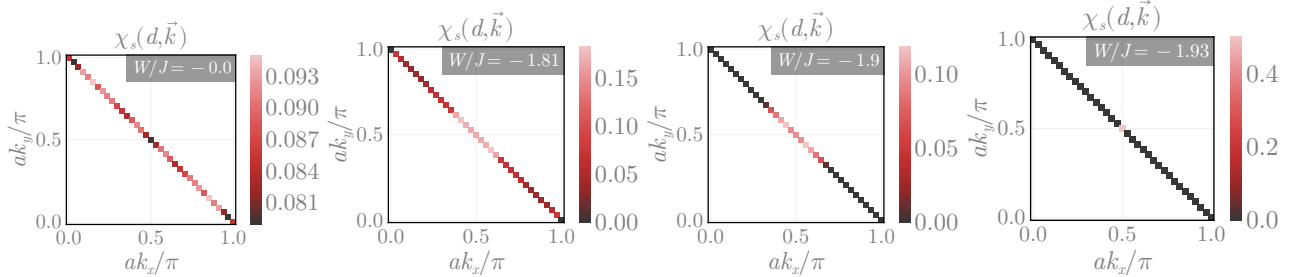
FIG. 8. $k-$space distribution of spin-spin correlation $\chi_s(d, \vec{k})$ (defined in the main text). The last three figures show how $k-$points starting from the antinode progressively exit the Kondo cloud, the node being the last $k-$point to decouple from the impurity.

D. Charge correlations

In order to study the mechanism behind the destabilisation of the Kondo cloud through the pseudogap, we calculate the $k-$space double occupancy $\left\langle n_{\vec{k}\uparrow} n_{\vec{k}\downarrow} \right\rangle$ and $k-$space charge-transfer correlation $\chi_c(\vec{k}, \vec{q}) = \left\langle c^\dagger_{\vec{k}\uparrow} c^\dagger_{\vec{k}\downarrow} c_{\vec{q}\downarrow} c_{\vec{q}\uparrow} \right\rangle$ (Fig. 9). We find that the entry into the pseudogap is marked by an increase of doubly-occupied states near the antinode in

comparison to $W = 0$. These pairs likely lead to the concomitant vanishing of spin-correlations near the antinode at the same value of W, as seen in Fig. 8. More insight on the nature of these correlations are obtained from the fluctuations $\chi_c(\vec{k}, \vec{q})$ starting from the node ($\vec{q} = k_N$) and antinode ($\vec{q} = k_{AN}$). Interestingly, we find strong pair-transfer interactions between the node and antinode. Within the pseudogap, this leads to charge-isospin flip correlations between the decoupled antinodal region and the still-coupled nodal region.
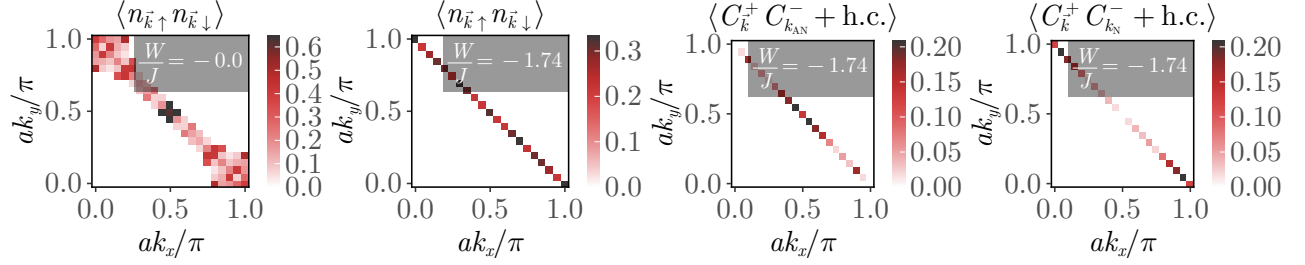
FIG. 9. *Top panels*: Distribution of double occupancy at $W = 0$ and $W = -1.74$ (entry into the pseudogap). While the double occupancy is concentrated near the nodes at $W = 0$, it rises near the antinodes at the start of the pseudogap, signalling its destabilisation. *Bottom panels*: Charge-transfer correlation χ_c (defined in main text) starting from antinode (left) and node (right), at the beginning of the pseudogap phase. Strong node-antinode correlations are clearly visible.

VI. NATURE OF GAPLESS EXCITATIONS IN THE IMPURITY PSEUDOGAP

A. Emergence of a two-channel Kondo Model

As the bath interaction W is tuned through the L-PG phase, the four nodal points in the Brillouin zone are the last to decouple from the impurity. This allows us to write down a simpler Kondo model near the transition, focusing on scattering processes involving the nodal region. Specifically, for the Kondo term $J_{\mathbf{k}_1, \mathbf{k}_2})$, we find that only the following classes of scattering processes survive close to the critical point:

- Both momenta in a neighbourhood around $\mathbf{k}_N$, where $\mathbf{k}_N$ can be any of the four nodal points,

- One momentum from the neighbourhood around $\mathbf{k}_N$, while the other from the neighbourhood around $\mathbf{k}_N + (\pi, \pi)$.

The second class is tied to the first through a symmetry of the Hamiltonian (eq. 20). The crucial feature of these processes is that each node only interacts with the other node directly opposite to it across the origin. That is, $(\pi/2, \pi/2)$ and $(-\pi/2, -\pi/2)$ only interact between themselves, while $(\pi/2, -\pi/2)$ and $(-\pi/2, \pi/2)$ form their own pair of connected regions.

Let $S^\pm$ be the set of momentum states in a small window around nodes along $k_x = \pm k_y$. As discussed immediately above, the Kondo spin-exchange term close to the transition does not lead to scattering of any $k-$state from S^+ to S^-. This is verified by calculating the ratio $\max\left\{J_{k_1^+, k_2^-}\right\}/\max\left\{J_{k_1^+, k_2^+}\right\}$, where the maximum in the numerator is calculated from all the low-energy (fixed point) Kondo scattering processes that connect the two sets $S^\pm$, while the denominator maximum is from within the set S^+. This ratio vanishes (left panel of Fig. 10) within the local pseudogap regime, indicating that no direct Kondo scattering process persists between the two sectors $S^\pm$ at low energies, deep within the pseudogap regime.

The decoupling of the $k-$space regions $S^\pm$ is captured by the following simplified low-energy Hamiltonian:

$$H_{\text{eff}} = H(S^+) + H(S^-); \ H(S) = \sum_{\mathbf{q} \in S, \sigma} \varepsilon_{\mathbf{q}} c_{\mathbf{q}\sigma}^\dagger c_{\mathbf{q}\sigma} + \sum_{\mathbf{q}_1 \in S, \mathbf{q}_2 \in S} \sum_{\alpha, \beta} J^*(\mathbf{q}_1, \mathbf{q}_2) \mathbf{S}_d \cdot \sigma_{\alpha\beta} c_{\mathbf{q}_1 \alpha}^\dagger c_{\mathbf{q}_2 \beta} , \tag{23}$$

where $H(S^\pm)$ represents the dynamics of momentum states residing in regions $S^\pm$. The only source of information transfer between the two regions is the fact that they interact with the same impurity local moment. Eq.23 tells us that the low-energy dynamics of the embedded eSIAM close to the Kondo-breakdown transition is governed by an emergent **two-channel Kondo model**, with the conduction bath states in the sets $S^\pm$ making up the two channels.

FIG. 10. Left: Ratio between the maximum values of the fixed point values of the Kondo couplings for scattering processe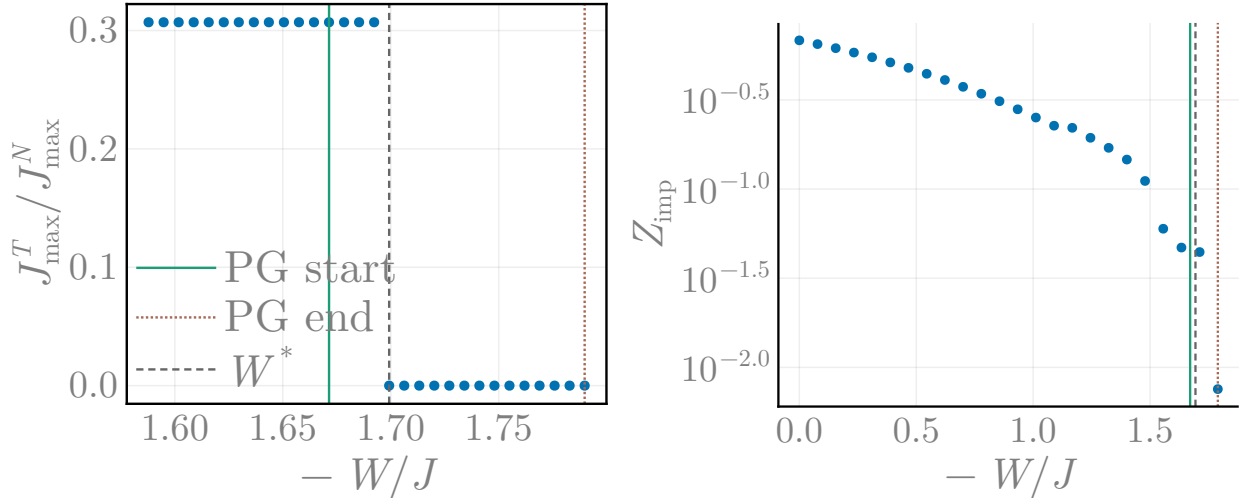s between and within the regions S^+ and S^-. The vanishing of the fixed point ratio indicates that the pseudogap regime features a singular low-energy effective theory, where the Fermi surface neighbourhood splits into two disconnected regions with no explicit term in the Hamiltonian connecting them directly. Right: The quasiparticle residue Z_{imp} of the local gapless excitations in various regions. The vanishingly small values of Z_{imp} lend more support to the two-channel (and hence the non-Fermi liquid) nature of the low-energy physics in the pseudogap regime.

B. Marginal Fermi liquid behaviour in the pseudogap

It is well-known that the two-channel Kondo model hosts non-Fermi liquid excitations at low-energies [20, 21]; that this also happens in the present model is corroborated by our calculations of the quasiparticle residue Z_{imp} for the local gapless excitations. For a single-particle Greens function of an interacting model, the quasiparticle residue Z is defined as the spectral weight of low-energy resonance within the spectral function:

$$G_k = \frac{Z}{\omega - \varepsilon_k - i\Sigma''} + G_{\text{incoh}} \ , \quad 1/Z = 1 - \frac{d\Sigma'}{d\omega} \ , \tag{24}$$

where Σ' and Σ'' are the real and imaginary parts of the self-energy, and G_{incoh} is contribution to the Greens function arising from incoherent short-lived excitations as well as high-energy features that are decoupled from the low-energy excitations [22]. Small values of Z indicate that the excitations cannot be described in terms of a Fermi liquid theory. Indeed, as shown in the right panel of Fig. 10, the quasiparticle residue Z_{imp} of the impurity excitations becomes vanishingly small in the pseudogap region, signalling that the excitations are of a non-Fermi liquid nature. Given that the pseudogap phase is close to a critical point in the impurity model phase diagram (separating the local Fermi liquid and local moment phases), it is not surprising that a quantum critical model emerges at that point.

Coleman and Ioffe have shown that by mapping the two-channel Kondo problem to a "compactified" form where the impurity spin hybridises with the spin and isospin degrees of freedom of a single conduction channel, the impurity self-energy can be shown to display marginal Fermi liquid behaviour [23, 24]:

$$\Sigma \propto \omega \ln \omega \ . \tag{25}$$

As some of us have shown in a previous work [25], this can also be obtained from a renormalisation group calculation of the low-energy excitations of the two-channel overscreened fixed point. For the sake of completeness, we have reproduced the calculation here. By considering minimal hopping into the conduction bath, the low-energy excitations above the 2CK ground state are described by the following Hamiltonian [25]:

$$H_{\text{eff}} = \frac{8t^2}{J} \left[\left(S_{0,1}^z\right)^2 S_{0,2}^+ + \left(S_{0,2}^z\right)^2 S_{0,1}^+ \right] \left(S_{1,1}^- + S_{1,2}^-\right) + \text{h.c.}; \tag{26}$$

where $\boldsymbol{S}_{i,l} = \frac{1}{2}\sum_{\sigma_1,\sigma_2} c_{i,\sigma_1,l}^\dagger \boldsymbol{\sigma}_{\sigma_1,\sigma_2} c_{i,\sigma_2,l}$ are spin operators for the ith site on the lth conduction channel (l can be 1 or 2 for a two-channel model). The labels σ_1 and σ_2 are spin indices that can be ± 1. The site index 0 represents the bath sites connected immediately to the impurity site. The operator $c_{i,\sigma,l}^\dagger$ creates an electron with spin σ on the ith site of the lth conduction channel.

We will Fourier transform this effective Hamiltonian into $k-$space:

$$\frac{2t^2}{J} \sum_{\{k_i, k_i'\}} \sum_{\sigma, l} \left(e^{i(k_1 - k_1')a} c^\dagger_{k\sigma, l} c_{k'\sigma, l} c^\dagger_{k_2\uparrow, \bar{l}} c_{k_2'\downarrow, \bar{l}} c^\dagger_{k_1\downarrow, \bar{l}} c_{k_1'\uparrow, \bar{l}} + \text{h.c.} \right) \ . \tag{27}$$

Such a three particle interaction term was also obtained for the NFL phase of the 2D Hubbard model from a URG treatment (see Appendix B of Ref.[6]). The channel indices in Eq. 27 can be mapped to the normal directions in [6]. The 2 particle-1 hole interaction in Eq. 27 has a diagonal component which can be obtained by setting $k = k', k_1 = k_2'$ and $k_2 = k_1'$:

$$\begin{aligned} H_{\text{MFL}} &= \sum_{\substack{k, k_1, \\ k_2, \sigma, l}} \frac{2t^2 e^{i(k_1 - k_2)a}}{J} \hat{n}_{k\sigma, l} \hat{n}_{k_2\uparrow, \bar{l}} \left(1 - \hat{n}_{k_1\downarrow, \bar{l}} \right) + \text{h.c.} \\ &= \sum_{\substack{k, k_1, \\ k_2, \sigma, l}} \frac{4t^2}{J} \cos a \left(k_1 - k_2 \right) \hat{n}_{k\sigma, l} \hat{n}_{k_2\uparrow, \bar{l}} \left(1 - \hat{n}_{k_1\downarrow, \bar{l}} \right) . \end{aligned} \tag{28}$$

The most dominant contribution comes from $k_1 = k_2 = k'$, revealing the non-Fermi liquid metal [26, 27]:

$$H^*_{\text{MFL}} = \frac{4t^2}{J} \sum_{\sigma, k, k', l} \hat{n}_{k\sigma, l} \hat{n}_{k'\uparrow, \bar{l}} \left(1 - \hat{n}_{k'\downarrow, \bar{l}} \right) \ . \tag{29}$$

A non-local version of this effective Hamiltonian was found to describe the normal phase of the Mott insulator of the 2D Hubbard model, as seen from a URG analysis [6, 7]. Following [6], one can track the RG evolution of the dual coupling $R_j = \frac{4t^2}{J_j}$ at the jth RG step, in the form of the URG equation

$$\Delta R_j = -\frac{R_j^2}{\omega - \epsilon_j/2 - R_j/8} \ . \tag{30}$$

In the RG equation, ϵ_j represents the energy of the jth isoenergetic shell. It is seen from the RG equation that R is relevant in the range of $\omega < \frac{1}{2}\epsilon_j$ that has been used throughout, leading to a fixed-point at $R^*/8 = \omega - \frac{1}{2}\epsilon^*$). The relevance of R is expected because the strong coupling J is irrelevant and $R \sim 1/J$.

The renormalisation in R leads to a renormalisation in the single-particle self-energy [6]. The $k-$space-averaged self-energy renormalisation is

$$\Delta\Sigma(\omega) = \rho R^{*2} \int_0^{\epsilon^*} \frac{d\epsilon_j}{\omega - \epsilon_j/2 + R_j/8} \ . \tag{31}$$

The density of states can be approximated to be N^*/R^*, where N^* is the total number of states over the interval R^*. As suggested by the fixed point value of R_j, we can approximate its behaviour near the fixed point by a linear dependence on the dispersion ϵ_j. The two limits of the integration are the starting and ending points of the RG. We start the RG very close to the Fermi surface and move towards the fixed point ϵ^*. Near the starting point, we substitute $\epsilon = 0$ and $R = \omega$, following the fixed point condition. From the fixed point condition, we also substitute $R^*/8 = \omega - \frac{1}{2}\epsilon^*$. On defining $\bar{\omega} = N^* \left(\omega - \frac{1}{2}\epsilon^* \right)$, we can write

$$\Delta\Sigma(\omega) \sim \bar{\omega} \ln \frac{N^*\omega}{\bar{\omega}} \ . \tag{32}$$

The self-energy also provides the quasiparticle residue for each channel[6]:

$$Z(\bar{\omega}) = \left(2 - \ln \frac{2\bar{\omega}}{N^*\omega} \right)^{-1} \ . \tag{33}$$

As $\omega \to 0$, the Z vanishes, implying that the ground state is *not adiabatically connected* to the Fermi gas in the presence of the NFL terms. This is the orthogonality catastrophe [28–31] in the two-channel Kondo problem, and it is brought about by the presence of the channel-non diagonal terms in Eq. 29.

VII.   THE TILING ALGORITHM

A.   Formal description of the tiling procedure

We will now define the *tiling* procedure by which we can recreate the complete lattice model by using instances of an auxiliary model Hamiltonian. The first step is of course to identify an impurity model that can act as a good

auxiliary model for out lattice model. The local behaviour of this impurity model should reflect the essential local physics of the lattice model. Typically, we will consider impurity model geometries where the real-space bath site connected directly to the impurity also harbours some kind of local interaction. We will henceforth refer to this site as the zeroth site. In the case where multiple sites are connected directly to the impurity, we will choose one of these sites for reference and call that the *bath zeroth site* throughout.

In order to identify a *unit cell* for our tiling procedure, we place the impurity site at a reference site $\mathbf{r}_d$ of our lattice, and the bath zeroth site at a nearest-neighbour site $\mathbf{z}$, and label the corresponding auxiliary model Hamiltonian as $\mathcal{H}_{\mathrm{aux}}(\mathbf{r}_d, \mathbf{z})$. The unit cell at the position $\mathbf{r}_d$ is then obtained by placing the zeroth site on all nearest-neighbours of $\mathbf{r}_d$ and averaging over these configurations:

$$\mathcal{H}_{\mathrm{aux}}(\mathbf{r}_d) = \frac{1}{\mathcal{Z}} \sum_{\mathbf{z} \in \mathrm{NN}(\mathbf{r}_d)} \mathcal{H}_{\mathrm{aux}}(\mathbf{r}_d, \mathbf{z}) \ , \tag{34}$$

where $\mathbf{z}$ is summed over all nearest-neighbours of $\mathbf{r}_d$ and $\mathcal{Z}$ is the number of such nearest-neighbours.

In order to create the bulk model, we now need to translate this auxiliary model over the entire lattice. For this, we define *many-particle global* translation operators $T(\mathbf{a})$ that translate all positions by a vector $\mathbf{a}$. In terms of manybody states and operators, their action is defined as

$$\begin{aligned} T^{\dagger}(\mathbf{a}) |\mathbf{r}_1, \mathbf{r}_2, \ldots\rangle &= |\mathbf{r}_1 + \mathbf{a}\rangle \otimes |\mathbf{r}_2 + \mathbf{a}\rangle \ldots \otimes |\mathbf{r}_n + \mathbf{a}\rangle \\ T^{\dagger}(\mathbf{a})\mathcal{O}(\mathbf{r}_1, \mathbf{r}_2, \ldots) T(\mathbf{a}) &= \mathcal{O}(\mathbf{r}_1 + \mathbf{a}, \mathbf{r}_2 + \mathbf{a}, \ldots) \ , \end{aligned} \tag{35}$$

where $|\mathbf{r}_1, \mathbf{r}_2, \ldots\rangle$ is a state in the manyparticle Fock-space basis with the particles localised at the specified positions. For example, for a local fermionic creation operator $c^{\dagger}(\mathbf{r})$, we have

$$T^{\dagger}(\mathbf{a})c^{\dagger}(\mathbf{r})T(\mathbf{a}) = c^{\dagger}(\mathbf{r} + \mathbf{a}) \ . \tag{36}$$

It acts similarly on the auxiliary model Hamiltonian:

$$T^{\dagger}(\mathbf{a})\mathcal{H}_{\mathrm{aux}}(\mathbf{r}_d)T(\mathbf{a}) = \mathcal{H}_{\mathrm{aux}}(\mathbf{r}_d + \mathbf{a}) \ , \tag{37}$$

translating all sites by the vector $\mathbf{a}$. By introducing the Fourier transform to momentum space,

$$|\mathbf{r}_1, \mathbf{r}_2, \ldots\rangle = \otimes_{j=1}^{N} \int d\mathbf{k}_j e^{-i\mathbf{r}_j \cdot \mathbf{k}_j} |\mathbf{k}_j\rangle \ , \tag{38}$$

it is easy to see that the total momentum states are eigenstates of the global translation operators:

$$\begin{aligned} T^{\dagger}(\mathbf{a}) |\mathbf{k}_1, \mathbf{k}_2, \ldots\rangle &= \otimes_{j=1}^{N} \int d\mathbf{r}_j e^{i\mathbf{r}_j \cdot \mathbf{k}_j} T^{\dagger}(\mathbf{a}) |\mathbf{r}_j\rangle \ , \\ &= \otimes_{j=1}^{N} \int d\mathbf{r}_j e^{i\mathbf{r}_j \cdot \mathbf{k}_j} |\mathbf{r}_j + \mathbf{a}\rangle \\ &= e^{-i\mathbf{a}_j \cdot \mathbf{k}_{\mathrm{tot}}} |\mathbf{k}_1, \mathbf{k}_2, \ldots\rangle , \end{aligned} \tag{39}$$

where $\mathbf{k}_{\mathrm{tot}} = \sum_j \mathbf{k}_j$ is the total momentum.

The auxiliary model, being an impurity model, lacks translation symmetry. The lattice model does remain invariant under global translation operations. In order to reconstruct the full lattice model and restore its translation invariance, we translate the unit cell across all sites of the lattice:

$$\begin{aligned} \mathcal{H}_{\mathrm{tiled}} &= \sum_{\mathbf{r}} \mathcal{H}_{\mathrm{aux}}(\mathbf{r}) \\ &= \sum_{\mathbf{r}} T^{\dagger}(\mathbf{r} - \mathbf{r}_d)\mathcal{H}_{\mathrm{aux}}(\mathbf{r}_d)T(\mathbf{r} - \mathbf{r}_d) \\ &= \frac{1}{\mathcal{Z}} \sum_{\mathbf{r}} \sum_{\mathbf{z} \in \mathrm{NN}(\mathbf{r}_d)} T^{\dagger}(\mathbf{r} - \mathbf{r}_d)\mathcal{H}_{\mathrm{aux}}(\mathbf{r}_d, \mathbf{z})T(\mathbf{r} - \mathbf{r}_d) \end{aligned} \tag{40}$$

where $\mathbf{r}$ sums over all lattice sites.

B. Extending the Anderson impurity model: Identifying the correct auxiliary model

The standard Anderson model consists of a correlated impurity site coupled with a non-interacting conduction bath. The double occupancy cost on the impurity is U, while the single-particle hopping strength between the impurity and the conduction bath is V. Such a model does not exhibit a phase transition; the low-energy phase is one of strong-coupling for all parameter regimes. We have recently studied an extended Anderson impurity model (e-SIAM) where we introduced an explicit Kondo coupling J and a local correlation U_b on the bath zeroth site, which is the site connected to the impurity (see [32] for some recent findings of non-local effective attractive interactions within the Hubbard model). The Hamiltonian of the e-SIAM for a half-filled impurity site is of the form

$$\mathcal{H}_{\text{E-S}} = \mathcal{H}_{\text{cbath}} + \mathcal{H}_{\text{imp}} + \mathcal{H}_{\text{imp-cbath}} \;, \tag{41}$$

where

- $\mathcal{H}_{\text{cbath}} = -\frac{1}{\mathcal{Z}}t\sum_{i=0,1,\dots;\sigma}\left(c_{i,\sigma}^{\dagger}c_{i+1,\sigma} + \text{h.c.}\right) - \frac{1}{2}U_b\left(\hat{n}_{0\uparrow} - \hat{n}_{0\downarrow}\right)^2$ is the Hamiltonian of the conduction bath consisting of a kinetic energy term and some local interaction terms on the zeroth site,

- $\mathcal{H}_{\text{imp}} = -\frac{U}{2}\left(\hat{n}_{d\uparrow} - \hat{n}_{d\downarrow}\right)^2$ is the Hamiltonian for the localised impurity site, and

- $\mathcal{H}_{\text{imp-bath}} = J\mathbf{S}_d \cdot \mathbf{S}_0 - V\sum_{\sigma}\left(c_{0\sigma}^{\dagger}c_{d\sigma} + h.c.\right)$ describes the interaction between the impurity orbitals and the conduction bath.

Here, $c_{d\sigma}$ is the impurity electron operator, $c_{i\sigma}$ is the conduction bath electron operator, $c_{0,\sigma}$ is the bath zeroth site operator, $\mathbf{S}_d$ is the impurity spin operator and $\mathbf{S}_0 = \sum_{\alpha,\beta}\sigma c_{0,\alpha}^{\dagger}c_{0,\beta}$ is the operator for the local spin in the conduction bath. We have found that the e-SIAM has a stable local moment phase for $U_b < -J/4$ with an antiferromagnetic Kondo coupling ($J > 0$). We have also shown that this model captures much of the phenomenology of the infinite dimensional Hubbard model (as discovered via DMFT), such as a second-order phase transition at $T = 0$ and the presence of an optical gap in the local spectral function beyond a certain value of interaction strength. Note that the impurity site and the conduction bath are both at half-filling.

C. Tiling towards a Hubbard-Heisenberg model with an embedded extended SIAM

In this subsection, we provide an explicit example of constructing a lattice model. We will consider a slightly more generalised version of the extended SIAM described in the previous section, where the impurity site coupled to the conduction bath purely through the s-wave channel. We will show that that model leads to a form of a Hubbard-Heisenberg model upon restoring translation invariance via repeated translation operations. The generalisation involve allowing an arbitrary filling on the impurity site and in the conduction bath, through two additional parameter: (i) a particle-hole asymmetry parameter η for the impurity site, (ii) a chemical potential for the conduction bath, and (iii) embedding the impurity into the lattice of the 2D conduction bath. This modified impurity model is shown in Fig. 4. The first term modifies the impurity Hamiltonian $\mathcal{H}_{\text{imp}}$ into

$$\mathcal{H}_{\text{imp}} = -\frac{U}{2}\left(\hat{n}_{\mathbf{r}_d\uparrow} - \hat{n}_{\mathbf{r}_d\downarrow}\right)^2 - \eta\sum_{\sigma}\hat{n}_{\mathbf{r}_d\sigma} \;. \tag{42}$$

where we have placed the impurity site at the position $\mathbf{r}_d$. The second term modifies the conduction bath Hamiltonian $\mathcal{H}_{\text{cbath}}$:

$$\mathcal{H}_{\text{cbath}} = -\frac{1}{\sqrt{\mathcal{Z}}}t\sum_{\langle\mathbf{r}_i,\mathbf{r}_j\rangle\neq\mathbf{r}_d;\sigma}\left(c_{\mathbf{r}_i,\sigma}^{\dagger}c_{\mathbf{r}_j,\sigma} + \text{h.c.}\right)$$
$$-\frac{1}{2\mathcal{Z}}U_b\sum_{\mathbf{z}\in\text{NN}(\mathbf{r}_d)}\left(\hat{n}_{\mathbf{z},\uparrow} - \hat{n}_{\mathbf{z},\downarrow}\right)^2 - \mu\sum_{\mathbf{r}_i\neq\mathbf{r}_d}\hat{n}_{\mathbf{r}_i,\sigma} \;, \tag{43}$$

where $\langle\mathbf{r}_i,\mathbf{r}_j\rangle\neq\mathbf{r}_d$ indicates that the sum is over all nearest-neighbour pairs of sites avoiding the impurity site $\mathbf{r}_d$.

In this notation, the interaction Hamiltonian can be written as

$$\mathcal{H}_{\text{imp-cbath}} = \frac{J}{\mathcal{Z}}\sum_{\sigma,\sigma'}\sum_{\mathbf{z}\in\text{NN}(\mathbf{r}_d)}\mathbf{S}_{\mathbf{r}_d}\cdot\boldsymbol{\tau}_{\sigma,\sigma'}c_{\mathbf{z},\sigma}^{\dagger}c_{\mathbf{z},\sigma'}$$
$$-\frac{V}{\sqrt{\mathcal{Z}}}\sum_{\sigma}\sum_{\mathbf{z}\in\text{NN}(\mathbf{r}_d)}\left(c_{\mathbf{r}_d,\sigma}^{\dagger}c_{\mathbf{z},\sigma} + h.c.\right) \tag{44}$$

where $\boldsymbol{\tau} = (\tau_x, \tau_y, \tau_z)$ is the vector of Pauli matrices. σ and σ' can be ± 1 and represent up and down configurations.

We now follow the prescription laid out in eq. 40. The tiled Hamiltonian can be written as

$$\mathcal{H}_{\text{tiled}} = \sum_{\mathbf{r}} T^{\dagger}(\mathbf{r} - \mathbf{r}_d) \left[\mathcal{H}_{\text{cbath}} + \mathcal{H}_{\text{imp}} \right. \tag{45}$$
$$\left. + \mathcal{H}_{\text{imp-cbath}} \right] T(\mathbf{r} - \mathbf{r}_d) \, .$$

Note that in comparison to eq. 40, we have dropped the sum over the zeroth sites, because our impurity model Hamiltonian (defined using eqs. 42 through 44) already contains a sum over these zeroth sites.

We consider the effect of the translation operations on each part of the Hamiltonian. We first have

$$\sum_{\mathbf{r}} T^{\dagger}(\mathbf{r} - \mathbf{r}_d) \mathcal{H}_{\text{cbath}}(\mathbf{r}_d, \mathbf{z}) T(\mathbf{r} - \mathbf{r}_d)$$
$$= \sum_{\mathbf{r}} T^{\dagger}(\mathbf{r} - \mathbf{r}_d) \left[-\frac{1}{\sqrt{\mathcal{Z}}} t \sum_{\langle \mathbf{r}_i, \mathbf{r}_j \rangle \neq \mathbf{r}_d; \sigma} \left(c^{\dagger}_{\mathbf{r}_i, \sigma} c_{\mathbf{r}_j, \sigma} + \text{h.c.} \right) \right.$$
$$\left. -\frac{U_b}{2\mathcal{Z}} \sum_{\mathbf{z} \in \text{NN}(\mathbf{r}_d)} (\hat{n}_{\mathbf{z},\uparrow} - \hat{n}_{\mathbf{z},\downarrow})^2 - \mu \sum_{\mathbf{r}_i \neq \mathbf{r}_d} \hat{n}_{\mathbf{r}_i, \sigma} \right] T(\mathbf{r} - \mathbf{r}_d)$$
$$= -\frac{1}{\sqrt{\mathcal{Z}}} t \sum_{\langle \mathbf{r}_i, \mathbf{r}_j \rangle; \sigma} \sum_{\mathbf{r} \neq \mathbf{r}_i, \mathbf{r}_j} \left(c^{\dagger}_{\mathbf{r}_i, \sigma} c_{\mathbf{r}_j, \sigma} + \text{h.c.} \right) \tag{46}$$
$$-\frac{U_b}{2\mathcal{Z}} \sum_{\mathbf{r}} \sum_{\mathbf{z} \in \text{NN}(\mathbf{r})} (\hat{n}_{\mathbf{z},\uparrow} - \hat{n}_{\mathbf{z},\downarrow})^2 - \mu \sum_{\mathbf{r}_i} \sum_{\mathbf{r} \neq \mathbf{r}_i} \hat{n}_{\mathbf{r}_i, \sigma}$$
$$= -\frac{1}{\sqrt{\mathcal{Z}}} (N - 2) t \sum_{\langle \mathbf{r}_i, \mathbf{r}_j \rangle; \sigma} \left(c^{\dagger}_{\mathbf{r}_i, \sigma} c_{\mathbf{r}_j, \sigma} + \text{h.c.} \right)$$
$$-\frac{1}{2} U_b \sum_{\mathbf{r}} (\hat{n}_{\mathbf{r},\uparrow} - \hat{n}_{\mathbf{r},\downarrow})^2 - \mu(N - 1) \sum_{\mathbf{r}} \hat{n}_{\mathbf{r}, \sigma}$$

In the first step, the factor of $\mathcal{Z}$ is cancelled out by the trivial sum over $\mathbf{r}_0$ in the first and third terms. At the last step, the three terms simplified for the following reasons. The inequality $\langle \mathbf{r}_i, \mathbf{r}_j \rangle \neq \mathbf{r}$ in the first term ensures that each nearest-neighbour pair appears in $N - 2$ instances of the auxiliary model, N being the total number of lattice sites; the two instances that do not contribute are the ones in which the impurity site itself is at $\mathbf{r}_i$ or $\mathbf{r}_j$. For the second term, the double sum $\sum_{\mathbf{r}} \sum_{\mathbf{z} \in \text{NN}(\mathbf{r})}$ evaluates to $\mathcal{Z} \sum_{\mathbf{r}}$, because each point on the lattice appears $\mathcal{W}$ times in the summation. This factor of $\mathcal{W}$ cancels the one in the denominator. In the third term, the inner summation simply evaluates to $N - 1$, and we finally replace the dummy index $\mathbf{r}_i$ with $\mathbf{r}$.

The next part is

$$\sum_{\mathbf{r}} T^{\dagger}(\mathbf{r} - \mathbf{r}_d) \mathcal{H}_{\text{imp}} T(\mathbf{r} - \mathbf{r}_d)$$
$$= -\frac{U}{2} \sum_{\mathbf{r}} (\hat{n}_{\mathbf{r}\uparrow} - \hat{n}_{\mathbf{r}\downarrow})^2 - \eta \sum_{\mathbf{r}, \sigma} \hat{n}_{\mathbf{r}\sigma} \, . \tag{47}$$

This is obtained simply by replacing the impurity position $\mathbf{r}_d$ with the translated position $\mathbf{r}$, generating a translation-invariant Hubbard term (the first term) and a finite chemical potential (second term).

We now consider the final term:

$$\sum_{\mathbf{r}} T^\dagger(\mathbf{r} - \mathbf{r}_d)\mathcal{H}_{\text{imp-cbath}}T(\mathbf{r} - \mathbf{r}_d)$$

$$= \sum_{\mathbf{r}} T^\dagger(\mathbf{r} - \mathbf{r}_d)\left[\frac{1}{\mathcal{Z}}\sum_{\mathbf{z}\in\text{NN}(\mathbf{r}_d)}\sum_{\sigma,\sigma'}J\mathbf{S}_{\mathbf{r}_d}\cdot\boldsymbol{\tau}_{\sigma,\sigma'}c^\dagger_{\mathbf{z},\sigma}c_{\mathbf{z},\sigma'}\right.$$

$$\left. -\frac{1}{\sqrt{\mathcal{Z}}}\sum_{\mathbf{z}\in\text{NN}(\mathbf{r}_d)}\sum_{\sigma}V\left(c^\dagger_{\mathbf{r}_d,\sigma}c_{\mathbf{z},\sigma}+h.c.\right)\right]T(\mathbf{r}-\mathbf{r}_d)$$

$$= \sum_{\mathbf{r}}\sum_{\mathbf{z}\in\text{NN}(\mathbf{r})}\left[\frac{1}{\mathcal{Z}}\sum_{\sigma,\sigma'}J\mathbf{S}_{\mathbf{r}}\cdot\boldsymbol{\tau}_{\sigma,\sigma'}c^\dagger_{\mathbf{z},\sigma}c_{\mathbf{z},\sigma'}\right.$$

$$\left. -\frac{1}{\sqrt{\mathcal{Z}}}\sum_{\sigma}V\left(c^\dagger_{\mathbf{r}_d,\sigma}c_{\mathbf{z},\sigma}+h.c.\right)\right] \tag{48}$$

$$= \sum_{\langle\mathbf{r}_i,\mathbf{r}_j\rangle}\left[\frac{2}{\mathcal{Z}}J\mathbf{S}_{\mathbf{r}_i}\cdot\mathbf{S}_{\mathbf{r}_j}-\frac{2}{\sqrt{\mathcal{Z}}}V\sum_{\sigma}\left(c^\dagger_{\mathbf{r}_i,\sigma}c_{\mathbf{r}_j,\sigma}+h.c.\right)\right]$$

At the last step, each nearest-neighbour pair of sites $\mathbf{r}_i, \mathbf{r}_j$ appear 2 times in the summation, because any site is a member of two distinct nearest-neighbour pairs. We have also defined $\mathbf{S}_{\mathbf{r}_j} = \sum_{\sigma,\sigma'}\boldsymbol{\tau}_{\sigma,\sigma'}c^\dagger_{\mathbf{z},\sigma}c_{\mathbf{z},\sigma'}$ as the local spin operator.

The total tiled Hamiltonian is therefore

$$\mathcal{H}_{\text{tiled}}$$
$$= -\frac{N-2}{\sqrt{\mathcal{Z}}}t\sum_{\langle\mathbf{r}_i,\mathbf{r}_j\rangle,\sigma}\left(c^\dagger_{\mathbf{r}_i,\sigma}c_{\mathbf{r}_j,\sigma}+h.c.\right)-\mu(N-1)\sum_{\mathbf{r}}\hat{n}_{\mathbf{r},\sigma}$$

$$-\frac{1}{2}U_b\sum_{\mathbf{r}}\left(\hat{n}_{\mathbf{r},\uparrow}-\hat{n}_{\mathbf{r},\downarrow}\right)^2-\frac{U}{2}\sum_{\mathbf{r}}\left(\hat{n}_{\mathbf{r}\uparrow}-\hat{n}_{\mathbf{r}\downarrow}\right)^2-\eta\sum_{\mathbf{r},\sigma}\hat{n}_{\mathbf{r}\sigma} \tag{49}$$

$$+\sum_{\langle\mathbf{r}_i,\mathbf{r}_j\rangle}\left[\frac{2}{\mathcal{Z}}J\mathbf{S}_{\mathbf{r}_i}\cdot\mathbf{S}_{\mathbf{r}_j}-\frac{2}{\sqrt{\mathcal{Z}}}V\sum_{\sigma}\left(c^\dagger_{\mathbf{r}_i,\sigma}c_{\mathbf{r}_j,\sigma}+h.c.\right)\right]$$

While constructing the tiled Hamiltonian, we have added extra copies of the non-interacting Hamiltonian $\mathcal{H}_{\text{cbath-nint}} = -\frac{1}{\sqrt{\mathcal{Z}}}t\sum_{\langle\mathbf{r}_i,\mathbf{r}_j\rangle;\sigma}\left(c^\dagger_{\mathbf{r}_i,\sigma}c_{\mathbf{r}_j,\sigma}+h.c.\right)-\mu\sum_{\mathbf{r}}\hat{n}_{\mathbf{r},\sigma}$ for the conduction bath (this results in the factors of $N-2$ and $N-1$ in front of the first and third terms). Upon removing these repeated terms, the tiled Hamiltonian becomes

$$\mathcal{H}_{\text{tiled}} = \sum_{\mathbf{r}}\mathcal{H}_{\text{aux}}(\mathbf{r})-(N-3)\mathcal{H}_{\text{cbath-nint}}$$

$$= -\frac{1}{\sqrt{\mathcal{Z}}}(t+2V)\sum_{\langle\mathbf{r}_i,\mathbf{r}_j\rangle;\sigma}\left(c^\dagger_{\mathbf{r}_i,\sigma}c_{\mathbf{r}_j,\sigma}+h.c.\right)$$

$$-\frac{1}{2}\left(U+U_b\right)\sum_{\mathbf{r}}\left(\hat{n}_{\mathbf{r},\uparrow}-\hat{n}_{\mathbf{r},\downarrow}\right)^2-(\eta+2\mu)\sum_{\mathbf{r}}\hat{n}_{\mathbf{r},\sigma} \tag{50}$$

$$+\frac{2}{\mathcal{Z}}J\sum_{\langle\mathbf{r}_i,\mathbf{r}_j\rangle}\mathbf{S}_{\mathbf{r}_i}\cdot\mathbf{S}_{\mathbf{r}_j}$$

The result of the tiling operations is a Hubbard-Heisenberg model, of the form

$$\mathcal{H}_{\text{HH}} = -\frac{1}{\sqrt{\mathcal{Z}}}\tilde{t}\sum_{\langle\mathbf{r}_i,\mathbf{r}_j\rangle;\sigma}\left(c^\dagger_{\mathbf{r}_i,\sigma}c_{\mathbf{r}_j,\sigma}+h.c.\right)-\tilde{\mu}\sum_{\mathbf{r}}\hat{n}_{\mathbf{r},\sigma}$$

$$+\frac{1}{\mathcal{Z}}\tilde{J}\sum_{\langle\mathbf{r}_i,\mathbf{r}_j\rangle}\mathbf{S}_{\mathbf{r}_i}\cdot\mathbf{S}_{\mathbf{r}_j}-\frac{1}{2}\tilde{U}\sum_{\mathbf{r}}\left(\hat{n}_{\mathbf{r},\uparrow}-\hat{n}_{\mathbf{r},\downarrow}\right)^2 \ , \tag{51}$$

where the tilde symbol indicates that the parameters are for the lattice model (and not the auxiliary model). By comparing the tiled model and the general lattice model, the lattice model parameters and the auxiliary model parameters can be mapped to each other:

$$\tilde{t} = t + 2V, \quad \tilde{U} = U + U_b, \quad \tilde{\mu} = 2\mu + \eta, \quad \tilde{J} = 2J \ . \tag{52}$$

In summary, the appropriate method for reconstructing the lattice model Hamiltonian is therefore

$$\mathcal{H}_{\text{tiled}} = \sum_{\mathbf{r}} \mathcal{H}_{\text{aux}}(\mathbf{r}) - N\mathcal{H}_{\text{cbath-nint}} \ , \tag{53}$$

where we replaced $N - 3$ with N assuming a large number of sites. Using this, the extended-SIAM gets "expanded" into a Hubbard-Heisenberg model.

D. Translation symmetry and a conserved total momentum

From the form in eq. 53, the tiled Hamiltonian is symmetric under global many-body translations of the kind defined in eq. 35, by arbitrary lattice spacings:

$$T(\mathbf{a})^{\dagger} \sum_{\mathbf{r}} \mathcal{H}_{\text{aux}}(\mathbf{r}) T(\mathbf{a}) = \sum_{\mathbf{r}} \mathcal{H}_{\text{aux}}(\mathbf{r} + \mathbf{a}) = \sum_{\mathbf{r}'} \mathcal{H}_{\text{aux}}(\mathbf{r}')$$

$$T(\mathbf{a})^{\dagger} \sum_{\mathbf{r}} \mathcal{H}_{\text{cbath-nint}} T(\mathbf{a}) = \mathcal{H}_{\text{cbath-nint}} \tag{54}$$

$$\implies T(\mathbf{a})^{\dagger} \mathcal{H}_{\text{tiled}} T(\mathbf{a}) = \mathcal{H}_{\text{tiled}} \ .$$

In the first equation, we used the fact that the translation operator simply translates the auxiliary model at the position $\mathbf{r}$ into another one at the position $\mathbf{r} + \mathbf{a}$. Since both are part of the summation, the summation remains unchanged. The second equation uses the fact that the Hamiltonian $\mathcal{H}_{\text{cbath-nint}}$ is that of a tight-binding model and is therefore translation-invariant. The fact that the Hamiltonian $\mathcal{H}_{\text{tiled}}$ commutes with the many-body translation operator implies that the total crystal momentum $\vec{k}$ is a conserved quantity.

VIII.   FORM OF THE EIGENSTATES: BLOCH'S THEOREM

In the tight-binding approach to lattice problems, the full Hamiltonian is described by adding the localised Hamiltonians at each site, and the full eigenstate $|\Psi\rangle$ is then obtained by constructing liner combinations of the eigenstates $|\psi_i\rangle$ of the local Hamiltonians such that $|\Psi\rangle$ satisfies Bloch's theorem: $|\Psi_{\mathbf{k}}\rangle = \sum_i e^{i\mathbf{k}\cdot\mathbf{r}_i} |\psi_i\rangle$, where $\mathbf{r}_i$ sums over the positions of the local Hamiltonians. Bloch's theorem ensures that eigenstates satisfy the following relation under a translation operation by an arbitrary number of lattice spacings $n\mathbf{a}$:

$$T^{\dagger}(n\mathbf{a}) |\Psi_{\mathbf{k}}\rangle = \sum_i e^{i\mathbf{k}\cdot\mathbf{r}_i} |\psi_{i+n}\rangle = e^{-in\mathbf{k}\cdot\mathbf{a}} |\Psi_{\mathbf{k}}\rangle \tag{55}$$

The definition and some properties of these global translation operations were provided in Appendix C. It was shown there that they share eigenstates with the total momentum operator. In a lattice model, this continuous symmetry gets lowered to its discrete form: the total *crystal* momentum is conserved by any scattering process. As a result, the eigenstates can be labelled using the combined index $s = (\mathbf{k}, n)$ where $\mathbf{k}$ is the total crystal momentum and n is a band index n.

The eigenstates $|\Psi_s\rangle$ ($s = (\mathbf{k}, n)$) of the lattice Hamiltonians obtained using eq. 53 also enjoy a *many-body* Bloch's theorem [33], because the tiling procedure restores the translation symmetry of the Hamiltonian (as shown in eq. 54). This means that the *local* eigenstates $|\psi_n(\mathbf{r}_d)\rangle$ (with the impurity located at an arbitrary position $\mathbf{r}_d$) of the unit cell auxiliary model Hamiltonian $\mathcal{H}_{\text{aux}}(\mathbf{r}_d)$ defined in eq. 34 can be used to construct eigenstates of the lattice Hamiltonian. The index $n(= 0, 1, \ldots)$ in the subscript indicates that it is the nth eigenstate of the auxiliary model.

The state $|\psi_n(\mathbf{r}_d)\rangle$ does not specify the position of the zeroth site, because the unit cell Hamiltonian $\mathcal{H}_{\text{aux}}(\mathbf{r}_d)$ itself has been averaged over $\mathcal{Z}$ zeroth sites. Accordingly, we can express the averaged eigenstate $|\psi_n(\mathbf{r}_d)\rangle$ as

$$|\psi_n(\mathbf{r}_d)\rangle = \frac{1}{\sqrt{\mathcal{Z}}} \sum_{\mathbf{z} \in \text{NN}(\mathbf{r}_d)} |\psi_n(\mathbf{r}_d, \mathbf{z})\rangle \ , \tag{56}$$

where $|\psi_n\left(\mathbf{r}_d,\mathbf{z}\right)\rangle$ is an auxiliary model eigenstate with the impurity and zeroth sites placed at $\mathbf{r}_d$ and $\mathbf{z}$. With this in mind, the following unnormalised combination of the auxiliary model eigenstates satisfies a many-particle equivalent of Bloch's theorem [33]:

$$|\Psi_s\rangle \equiv |\Psi_{\mathbf{k},n}\rangle = \frac{1}{\sqrt{N}}\sum_{\mathbf{r}_d}e^{i\mathbf{k}\cdot\mathbf{r}_d}|\psi_n\left(\mathbf{r}_d\right)\rangle = \frac{1}{\sqrt{\mathcal{Z}N}}\sum_{\mathbf{r}_d}\sum_{\mathbf{z}\in\mathrm{NN}(\mathbf{r}_d)}e^{i\mathbf{k}\cdot\mathbf{r}_d}|\psi_n\left(\mathbf{r}_d,\mathbf{z}\right)\rangle \ , \tag{57}$$

where N is the total number of lattice sites and $\mathbf{r}_d$ is summed over all lattice spacings. The set of $n=0$ states form the lowest band in the spectrum of the lattice, while higher values of n produce the more energetic bands. The ground state $s=s_0$ is obtained by setting $\mathbf{k}$ and n to 0:

$$|\Psi_{\mathrm{gs}}\rangle \equiv |\Psi_{s_0}\rangle = \frac{1}{\sqrt{N}}\sum_{\mathbf{r}_d}e^{i\mathbf{k}\cdot\mathbf{r}_d}|\psi_{\mathrm{gs}}\left(\mathbf{r}_d\right)\rangle = \frac{1}{\sqrt{\mathcal{Z}N}}\sum_{\mathbf{r}_d}\sum_{\mathbf{z}\in\mathrm{NN}(\mathbf{r}_d)}e^{i\mathbf{k}\cdot\mathbf{r}_d}|\psi_{\mathrm{gs}}\left(\mathbf{r}_d,\mathbf{z}\right)\rangle \tag{58}$$

IX. ONE-PARTICLE GREENS FUNCTIONS

A. Momentum-space

In the previous part, we proposed a form for the ground state $|\Psi_{\mathrm{gs}}\rangle$ of the bulk Hamiltonian in terms of the ground-states $|\psi_{\mathrm{gs}}\rangle$ of the auxiliary models. In this section, we will relate one-particle Greens functions of the bulk lattice to those of the auxiliary model. We will assume that the auxiliary model Hilbert space has the same dimensions as that of the bulk lattice model. We define the retarded time-domain lattice $k-$space Greens function at zero temperature as

$$\tilde{G}(\mathbf{K}\sigma;t) = -i\theta(t)\langle\Psi_{\mathrm{gs}}|\left\{c_{\mathbf{K}\sigma}(t),c_{\mathbf{K}\sigma}^\dagger\right\}|\Psi_{\mathrm{gs}}\rangle \ . \tag{59}$$

where the bulk Hamiltonian H_{tiled} leads to the dynamics of the annihilation operators at time t:

$$c_{\mathbf{K}\sigma}(t) = e^{itH_{\mathrm{tiled}}}c_{\mathbf{K}\sigma}e^{-itH_{\mathrm{tiled}}} \ . \tag{60}$$

We now proceed to simplify one of the terms of the anticommutator (for simplicity of notation):

$$\langle\Psi_{\mathrm{gs}}|c_{\mathbf{K}\sigma}(t)c_{\mathbf{K}\sigma}^\dagger|\Psi_{\mathrm{gs}}\rangle = \frac{1}{N^2}\sum_{\vec{r},\vec{\Delta}}e^{-i\mathbf{K}_0\cdot\vec{\Delta}}\langle\psi_0(\vec{r}+\vec{\Delta})|c_{\mathbf{K}\sigma}(t)c_{\mathbf{K}\sigma}^\dagger|\psi_0(\vec{r})\rangle \ . \tag{61}$$

To make further progress, we insert the identity resolution $1 = \sum_s|\Psi_s\rangle\langle\Psi_s|$ in between the two operators, where $s=(\mathbf{k},n)$ sums over all eigenstates (with energies $\tilde{E}_s$). The lattice eigenstates themselves can again be written in terms of those of the auxiliary model, using eq. 57:

$$|\Psi_s\rangle\langle\Psi_s| = \sum_{\vec{r'},\vec{\Delta}'}e^{i\vec{k}\cdot\vec{\Delta}'}|\psi_n(\vec{r'}+\vec{\Delta}')\rangle\langle\psi_n(\vec{r'})| \ . \tag{62}$$

With this, eq. 61 becomes

$$\langle\Psi_{\mathrm{gs}}|c_{\mathbf{K}\sigma}(t)c_{\mathbf{K}\sigma}^\dagger|\Psi_{\mathrm{gs}}\rangle = \frac{1}{N^2}\sum_s\sum_{\vec{r},\vec{\Delta}}\sum_{\vec{r'},\vec{\Delta}'}e^{-i\vec{k}_0\cdot\vec{\Delta}}e^{i\vec{k}\cdot\vec{\Delta}'}\langle\psi_0(\vec{r}+\vec{\Delta})|c_{\mathbf{K}\sigma}(t)|\psi_n(\vec{r'}+\vec{\Delta}')\rangle\langle\psi_n(\vec{r'})|c_{\mathbf{K}\sigma}^\dagger|\psi_0(\vec{r})\rangle \ . \tag{63}$$

In order to bring this expression closer to the form of an auxiliary model Greens function, we would like to transform the initial and final states $|\psi(\vec{r})\rangle$ and $|\psi(\vec{r}+\vec{\Delta})\rangle$ to apply to the same auxiliary model. This is done by using the relation: $|\psi(\vec{r}+\Delta)\rangle = T^\dagger(\vec{\Delta})|\psi(\vec{r})\rangle$, where $T^\dagger(\vec{\Delta})$ translates all lattice sites by the vector $\vec{\Delta}$.

$$\langle\psi_0(\vec{r}+\vec{\Delta})|c_{\mathbf{K}\sigma}(t)|\psi_n(\vec{r'}+\vec{\Delta}')\rangle = \langle\psi_0(\vec{r})|T(\vec{\Delta})c_{\mathbf{K}\sigma}(t)|\psi_n(\vec{r'}+\vec{\Delta}')\rangle = \langle\psi_0(\vec{r})|T(\vec{\Delta})c_{\mathbf{K}\sigma}(t)T^\dagger(\vec{\Delta})|\psi_n(\vec{r'}+\vec{\Delta}'-\vec{\Delta})\rangle \tag{64}$$

The effect of the translation operators on the $k-$space annihilation operator can be easily ascertained by transforming it to real-space, using the Fourier transform definition

$$c(\mathbf{K}) = \frac{1}{\sqrt{N}}\sum_{\mathbf{r}}e^{-i\mathbf{K}\cdot\mathbf{r}}c(\mathbf{r}) \ . \tag{65}$$

Upon applying this, we get

$$T\left(\vec{a}\right)c(\mathbf{K})T^{\dagger}\left(\vec{a}\right) = \frac{1}{N}\sum_{\mathbf{r}}e^{-i\mathbf{K}\cdot\mathbf{r}}T\left(\vec{a}\right)c(\mathbf{r})T^{\dagger}\left(\vec{a}\right) = \frac{1}{N}\sum_{\mathbf{r}}e^{-i\mathbf{K}\cdot\mathbf{r}}c(\mathbf{r}-\vec{a}) = e^{-i\mathbf{K}\cdot\vec{a}}c(\mathbf{K}) . \tag{66}$$

Using this identity on the above expression gives

$$\langle\psi_0(\vec{r}+\vec{\Delta})|c_{\mathbf{K}\sigma}(t)|\psi_n(\vec{r}'+\vec{\Delta}')\rangle = e^{-i\mathbf{K}\cdot\vec{\Delta}}\,\langle\psi_0(\vec{r})|c_{\mathbf{K}\sigma}(t)|\psi_n(\vec{r}'+\vec{\Delta}'-\vec{\Delta})\rangle \tag{67}$$

Finally replacing this all the way back into eq. 63 gives

$$\langle\Psi_{\mathrm{gs}}|c_{\mathbf{K}\sigma}(t)c_{\mathbf{K}\sigma}^{\dagger}|\Psi_{\mathrm{gs}}\rangle = \frac{1}{N^2}\sum_{s}\sum_{\vec{r},\vec{\Delta}}\sum_{\vec{r}',\vec{\Delta}'}e^{-i(\vec{k}_0+\mathbf{K})\cdot\vec{\Delta}}e^{i\vec{k}\cdot\vec{\Delta}'}\,\langle\psi_0(\vec{r})|c_{\mathbf{K}\sigma}(t)\,|\psi_n(\vec{r}'+\vec{\Delta}'-\vec{\Delta})\rangle\,\langle\psi_n(\vec{r}')|\,c_{\mathbf{K}\sigma}^{\dagger}|\psi_0(\vec{r})\rangle . \tag{68}$$

To further unify the operators, we make the substitution $\vec{\Delta}' \to \vec{\Delta}' + \vec{\Delta}$, leading to the expression

$$\langle\Psi_{\mathrm{gs}}|c_{\mathbf{K}\sigma}(t)c_{\mathbf{K}\sigma}^{\dagger}|\Psi_{\mathrm{gs}}\rangle = \frac{1}{N^2}\sum_{s}\sum_{\vec{r},\vec{\Delta}}\sum_{\vec{r}',\vec{\Delta}'}e^{-i(\vec{k}_0+\mathbf{K}-\vec{k})\cdot\vec{\Delta}}e^{i\vec{k}\cdot\vec{\Delta}'}\,\langle\psi_0(\vec{r})|c_{\mathbf{K}\sigma}(t)\,|\psi_n(\vec{r}'+\vec{\Delta}')\rangle\,\langle\psi_n(\vec{r}')|\,c_{\mathbf{K}\sigma}^{\dagger}|\psi_0(\vec{r})\rangle . \tag{69}$$

The sum over $\vec{\Delta}$ can now be carried out, resulting in

$$\langle\Psi_{\mathrm{gs}}|c_{\mathbf{K}\sigma}(t)c_{\mathbf{K}\sigma}^{\dagger}|\Psi_{\mathrm{gs}}\rangle = \frac{1}{N}\sum_{n}\sum_{\vec{r},\vec{r}',\vec{\Delta}'}e^{i(\vec{k}_0+\mathbf{K})\cdot\vec{\Delta}'}\,\langle\psi_0(\vec{r})|c_{\mathbf{K}\sigma}(t)\,|\psi_n(\vec{r}'+\vec{\Delta}')\rangle\,\langle\psi_n(\vec{r}')|\,c_{\mathbf{K}\sigma}^{\dagger}|\psi_0(\vec{r})\rangle , \tag{70}$$

where the sum over $s = (\vec{k}, n)$ has been reduced to a sum over the auxiliary model eigenstate index n because of the Kronecker delta $\delta\left(\vec{k}_0 + \mathbf{K} - \vec{k}\right)$. This can be further simplified by splitting the sum over $\vec{\Delta}'$ into positive and negative parts and then making the transformation $\vec{r}' \to \vec{r}' + \vec{\Delta}'$:

$$\sum_{\vec{r}',\vec{\Delta}'}e^{i(\vec{k}_0+\mathbf{K})\cdot\vec{\Delta}'}\,|\psi_n(\vec{r}'+\vec{\Delta}')\rangle\,\langle\psi_n(\vec{r}')| = \frac{1}{2}\sum_{\vec{r}',\vec{\Delta}'}\left[e^{i(\vec{k}_0+\mathbf{K})\cdot\vec{\Delta}'}\,|\psi_n(\vec{r}'+\vec{\Delta}')\rangle\,\langle\psi_n(\vec{r}')| + e^{-i(\vec{k}_0+\mathbf{K})\cdot\vec{\Delta}'}\,|\psi_n(\vec{r}'-\vec{\Delta}')\rangle\,\langle\psi_n(\vec{r}')|\right]$$
$$= \frac{1}{2}\sum_{\vec{r}',\vec{\Delta}'}\left[e^{i(\vec{k}_0+\mathbf{K})\cdot\vec{\Delta}'}\,|\psi_n(\vec{r}'+\vec{\Delta}')\rangle\,\langle\psi_n(\vec{r}')| + e^{-i(\vec{k}_0+\mathbf{K})\cdot\vec{\Delta}'}\,|\psi_n(\vec{r}')\rangle\,\langle\psi_n(\vec{r}'+\vec{\Delta}')|\right]$$
$$\tag{71}$$

For each pair of $\vec{r}'$ and $\vec{\Delta}'$, the term within the box brackets has the form of a two-level Hamiltonian between the states $|\psi_n(\vec{r}')\rangle$ and $|\psi_n(\vec{r}'+\vec{\Delta}')\rangle$, with a tunnelling amplitude $e^{i(\vec{k}_0+\mathbf{K})\cdot\vec{\Delta}'}$. The term can therefore be written in the eigenbasis of this Hamiltonian:

$$\sum_{\vec{r}',\vec{\Delta}'}e^{i(\vec{k}_0+\mathbf{K})\cdot\vec{\Delta}'}\,|\psi_n(\vec{r}'+\vec{\Delta}')\rangle\,\langle\psi_n(\vec{r}')| = \frac{1}{2}\sum_{\vec{r}',\vec{\Delta}'}\left[|\chi_n^+(\vec{r}',\vec{\Delta}')\rangle\,\langle\chi_n^+(\vec{r}',\vec{\Delta}')| - |\chi_n^-(\vec{r}',\vec{\Delta}')\rangle\,\langle\chi_n^-(\vec{r}',\vec{\Delta}')|\right], \tag{72}$$

where $|\chi_n^{\pm}(\vec{r}',\vec{\Delta}')\rangle = \frac{1}{\sqrt{2}}\left[|\psi_n(\vec{r}')\rangle \pm e^{i(\vec{k}_0+\mathbf{K})\cdot\vec{\Delta}'}\,|\psi_n(\vec{r}'+\vec{\Delta}')\rangle\right]$ are the eigenvectors of the tunnelling Hamiltonian with eigenvalues ± 1 respectively. With this basis transformation, we can rewrite eq. 70 as

$$\langle\Psi_{\mathrm{gs}}|c_{\mathbf{K}\sigma}(t)c_{\mathbf{K}\sigma}^{\dagger}|\Psi_{\mathrm{gs}}\rangle = \frac{1}{2N}\sum_{n}\sum_{\vec{r},\vec{r}',\vec{\Delta}'}\langle\psi_0(\vec{r})|c_{\mathbf{K}\sigma}(t)\left[|\chi_n^+(\vec{r}',\vec{\Delta}')\rangle\,\langle\chi_n^+(\vec{r}',\vec{\Delta}')| - |\chi_n^-(\vec{r}',\vec{\Delta}')\rangle\,\langle\chi_n^-(\vec{r}',\vec{\Delta}')|\right]c_{\mathbf{K}\sigma}^{\dagger}|\psi_0(\vec{r})\rangle . \tag{73}$$

In order to make the expression more transparent, we consider the various components separately:

a. $\vec{r}' = \vec{r}, \vec{\Delta}' = 0$:

$$\langle\Psi_{\mathrm{gs}}|c_{\mathbf{K}\sigma}(t)c_{\mathbf{K}\sigma}^{\dagger}|\Psi_{\mathrm{gs}}\rangle \to \frac{1}{N}\sum_{n}\sum_{\vec{r}}\langle\psi_0(\vec{r})|c_{\mathbf{K}\sigma}(t)\,|\psi_n(\vec{r})\rangle\,\langle\psi_n(\vec{r})|\,c_{\mathbf{K}\sigma}^{\dagger}|\psi_0(\vec{r})\rangle . \tag{74}$$

These terms represent those contributions to the total Greens function that arise from excitations that start and end at a specific auxiliary model (at $\vec{r}$), and also evolve dynamically within the same auxiliary model. These terms are therefore exactly equal to the auxiliary model Greens function at position $\vec{r}$, and are the most dominant contribution due to the localised nature of the impurity model.

b. $\vec{r}' \neq \vec{r}, \vec{\Delta}' = 0$:

$$\langle \Psi_{\text{gs}} | c_{\mathbf{K}\sigma}(t) c_{\mathbf{K}\sigma}^\dagger | \Psi_{\text{gs}} \rangle \rightarrow \frac{1}{N} \sum_n \sum_{\vec{r}, \vec{r}' \neq \vec{r}} \langle \psi_0(\vec{r}) | c_{\mathbf{K}\sigma}(t) | \psi_n(\vec{r}') \rangle \langle \psi_n(\vec{r}') | c_{\mathbf{K}\sigma}^\dagger | \psi_0(\vec{r}) \rangle \ . \tag{75}$$

These are more non-local contributions; they involve excitations whose time evolution is governed by a different auxiliary model than the terminal one. These contributions are highly suppressed in the Kondo screened phase because of the strong entanglement of the singlet ground state.

c. $\vec{r}' \neq \vec{r}, \vec{\Delta}' \neq 0$:

$$\langle \Psi_{\text{gs}} | c_{\mathbf{K}\sigma}(t) c_{\mathbf{K}\sigma}^\dagger | \Psi_{\text{gs}} \rangle \rightarrow \frac{1}{2N} \sum_n \sum_{\vec{r}, \vec{r}' \neq \vec{r}, \vec{\Delta}' \neq 0} \langle \psi_0(\vec{r}) | c_{\mathbf{K}\sigma}(t) \left[|\chi_n^+(\vec{r}', \vec{\Delta}')\rangle \langle \chi_n^+(\vec{r}', \vec{\Delta}')| - |\chi_n^-(\vec{r}', \vec{\Delta}')\rangle \langle \chi_n^-(\vec{r}', \vec{\Delta}')| \right] c_{\mathbf{K}\sigma}^\dagger | \psi_0(\vec{r}) \rangle \ . \tag{76}$$

These are the most non-local contributions; they involve excitations whose time evolution is governed by three different auxiliary models. Accordingly, these contributions are further suppressed.

We now consider each type of contribution in more detail.

B. $\vec{r}' = \vec{r}, \vec{\Delta}' = 0$

Restricting ourselves to just the single auxiliary model contributions gives

$$\langle \Psi_{\text{gs}} | c_{\mathbf{K}\sigma}(t) c_{\mathbf{K}\sigma}^\dagger | \Psi_{\text{gs}} \rangle = \frac{1}{N} \sum_n \sum_{\vec{r}} \langle \psi_0(\vec{r}) | c_{\mathbf{K}\sigma}(t) | \psi_n(\vec{r}) \rangle \langle \psi_n(\vec{r}) | c_{\mathbf{K}\sigma}^\dagger | \psi_0(\vec{r}) \rangle \ . \tag{77}$$

We first consider more carefully the transition operator $\mathcal{T}_{\mathbf{K}\sigma} = c_{\mathbf{K}\sigma}$ for the 1-particle excitation giving rise to the above Greens function. Within our auxiliary model approach, gapless excitations within the lattice model are represented by gapless excitations of the impurity site, specifically those that screen the impurity site and form the local Fermi liquid. As a result, the uncoordinated $\mathcal{T}-$matrix for the lattice model must be replaced by a combined $\mathcal{T}-$matrix within the impurity model that captures those gapless excitations that occur in connection with the impurity, and projects out the uncorrelated excitations that take place even when the impurity site is decoupled from the bath.

In order to construct this auxiliary model $\mathcal{T}-$matrix, we note that the impurity site can have both spin and charge excitations. Considering both excitations, the modified $\mathcal{T}-$matrix that constructs $k-$space excitations in correlation with the impurity site are

$$\mathcal{T}_{\mathbf{K}\sigma} = c_{\mathbf{K}\sigma} \left(\sum_{\sigma'} c_{d\sigma}^\dagger + \text{h.c.} \right) + c_{\mathbf{K}\sigma} \left(S_d^+ + \text{h.c.} \right) \ , \tag{78}$$

leading to the updated expression for the complete Greens function:

$$\tilde{G}(\mathbf{K}\sigma; t) = -i\theta(t) \frac{1}{N} \sum_n \sum_{\vec{r}} \langle \psi_0(\vec{r}) | \left[\mathcal{T}_{\mathbf{K}\sigma}(t) | \psi_n(\vec{r}) \rangle \langle \psi_n(\vec{r}) | \mathcal{T}_{\mathbf{K}\sigma}^\dagger + \mathcal{T}_{\mathbf{K}\sigma}^\dagger | \psi_n(\vec{r}) \rangle \langle \psi_n(\vec{r}) | \mathcal{T}_{\mathbf{K}\sigma}(t) \right] | \psi_0(\vec{r}) \rangle \ . \tag{79}$$

In order to convert this into a more useful form, we use eq. 60:

$$\langle \psi_0(\vec{r}) | \mathcal{T}_{\mathbf{K}\sigma}(t) | \psi_n(\vec{r}) \rangle = \langle \psi_0(\vec{r}) | e^{itH_{\text{tiled}}} \mathcal{T}_{\mathbf{K}\sigma} e^{-itH_{\text{tiled}}} | \psi_n(\vec{r}) \rangle \ . \tag{80}$$

Guided by the relation in eq. 53 $H_{\text{tiled}} = \sum_{\mathbf{r}} \mathcal{H}_{\text{aux}}(\mathbf{r}) - N\mathcal{H}_{\text{cbath-nint}}$ between the tiled Hamiltonian and the auxiliary model, we assume that the operator $e^{-itH_{\text{tiled}}}$ acting on the state $|\psi_n(\vec{r})\rangle$ involves the excitation energy E_n of only a single auxiliary model. Specifically, E_n is the energy of the eigenstate $|\psi_n(\vec{r})\rangle$. This is supported by the fact that this class of contributions to the Greens function is completed within a single auxiliary model. Accordingly, we replace H_{tiled} with $E_n - \varepsilon_{\mathbf{k}}$, where $\varepsilon_{\mathbf{k}}$ are the eigenenergies of the non-interacting conduction bath $\mathcal{H}_{\text{cbath-nint}}$ and $\mathbf{k}$ is the crystal momentum associated with the state $|\psi_n(\vec{r})\rangle$. This momentum was found to be constrained to $\mathbf{k}_0 + \mathbf{K}$ below eq. 70. In the same way, the action of H_{tiled} on the terminal state $|\psi_0(\vec{r})\rangle$ gives $E_0 - \varepsilon_{\mathbf{k}_0}$, where E_0 is the ground state energy of the auxiliary model at $\mathbf{r}$. Applying this to our expression gives

$$\tilde{G}(\mathbf{K}\sigma; t) = -i\theta(t) \frac{1}{N} \sum_n \sum_{\vec{r}} \langle \psi_0(\vec{r}) | \left[e^{-it\omega_p} \mathcal{T}_{\mathbf{K}\sigma}(t) | \psi_n(\vec{r}) \rangle \langle \psi_n(\vec{r}) | \mathcal{T}_{\mathbf{K}\sigma}^\dagger + e^{-it\omega_h} \mathcal{T}_{\mathbf{K}\sigma}^\dagger | \psi_n(\vec{r}) \rangle \langle \psi_n(\vec{r}) | \mathcal{T}_{\mathbf{K}\sigma}(t) \right] | \psi_0(\vec{r}) \rangle \ , \tag{81}$$

where $\omega_p = (E_n - \varepsilon_{\mathbf{k_0}+\mathbf{K}}) - (E_0 - \varepsilon_{\mathbf{k_0}})$ is the particle-excitation cost and $\omega_h = -\omega_p$ is the hole-excitation cost. We now introduce the Fourier transform $g(\omega) = \int dt\, e^{i\omega T} f(t)$ to obtain the frequency-domain Greens function in its spectral representation:

$$\tilde{G}(\mathbf{K}\sigma;\omega) = \frac{1}{N} \sum_{\vec{r}} \sum_{n} \langle \psi_0(\vec{r})| \left[\frac{1}{\omega - \omega_p} \mathcal{T}_{\mathbf{K}\sigma}(t) |\psi_n(\vec{r})\rangle \langle \psi_n(\vec{r})| \mathcal{T}_{\mathbf{K}\sigma}^\dagger + \frac{1}{\omega - \omega_h} \mathcal{T}_{\mathbf{K}\sigma}^\dagger |\psi_n(\vec{r})\rangle \langle \psi_n(\vec{r})| \mathcal{T}_{\mathbf{K}\sigma}(t) \right] |\psi_0(\vec{r})\rangle .$$
(82)

For each value of $\vec{r}$, the term within that summation is simply the Greens function (for the excitation $\mathcal{T}_{\mathbf{K}\sigma}$) of the auxiliary model with the impurity site at $\vec{r}$. Since all these impurity models are physically equivalent (because of translation invariance), we can replace the average over $\mathbf{r}$ with the value obtained from any one auxiliary model.

$$\tilde{G}(\mathbf{K}\sigma;\omega) = \sum_{n} \langle \psi_0| \left[\frac{1}{\omega - \omega_p} \mathcal{T}_{\mathbf{K}\sigma}(t) |\psi_n\rangle \langle \psi_n| \mathcal{T}_{\mathbf{K}\sigma}^\dagger + \frac{1}{\omega - \omega_h} \mathcal{T}_{\mathbf{K}\sigma}^\dagger |\psi_n\rangle \langle \psi_n| \mathcal{T}_{\mathbf{K}\sigma}(t) \right] |\psi_0\rangle .$$
(83)

C. $\vec{r}' \neq \vec{r}, \; \vec{\Delta}' = 0$

Allowing for more non-local contributions, and updating the $\mathcal{T}-$matrix similar to the previous section gives the following Greens function:

$$\tilde{G}(\mathbf{K}\sigma;t) = -i\theta(t) \frac{1}{N} \sum_{n} \sum_{\vec{r},\vec{r}'} \langle \psi_0(\vec{r})| \left[\mathcal{T}_{\mathbf{K}\sigma}(t) |\psi_n(\vec{r}')\rangle \langle \psi_n(\vec{r}')| \mathcal{T}_{\mathbf{K}\sigma}^\dagger + \mathcal{T}_{\mathbf{K}\sigma}^\dagger |\psi_n(\vec{r}')\rangle \langle \psi_n(\vec{r}')| \mathcal{T}_{\mathbf{K}\sigma}(t) \right] |\psi_0(\vec{r})\rangle .$$
(84)

In order to allow computations within a single auxiliary model, we replace the translated state $|\psi_n(\vec{r}')\rangle$ with $T^\dagger(\vec{r} \to \vec{r}') |\psi_n(\vec{r})\rangle$, where $T^\dagger(\vec{r} - \vec{r}')$ translates all sites by the vector $\vec{r}' - \vec{r}$. This leads to a modified correlation function but within a single auxiliary model:

$$\tilde{G}(\mathbf{K}\sigma;t) = -i\theta(t) \frac{1}{N} \sum_{n,\vec{r},\vec{r}'} \langle \psi_0(\vec{r})| \left[\mathcal{T}_{\mathbf{K}\sigma}(t) T^\dagger(\vec{r} - \vec{r}') |\psi_n(\vec{r})\rangle \langle \psi_n(\vec{r})| T(\vec{r} - \vec{r}') \mathcal{T}_{\mathbf{K}\sigma}^\dagger + \right.$$
$$\left. \mathcal{T}_{\mathbf{K}\sigma}^\dagger T^\dagger(\vec{r} - \vec{r}') |\psi_n(\vec{r})\rangle \langle \psi_n(\vec{r})| T(\vec{r} - \vec{r}') \mathcal{T}_{\mathbf{K}\sigma}(t) \right] |\psi_0(\vec{r})\rangle .$$
(85)

In fact, by the same arguments as in the previous section, we can obtain a frequency-resolved Greens function:

$$\tilde{G}(\mathbf{K}\sigma;\omega) = \sum_{n} \langle \psi_0| \left[\frac{1}{\omega - \omega_p} \mathcal{T}_{\mathbf{K}\sigma}(t) T^\dagger(\vec{r} - \vec{r}') |\psi_n\rangle \langle \psi_n| T(\vec{r} - \vec{r}') \mathcal{T}_{\mathbf{K}\sigma}^\dagger + \right.$$
$$\left. \frac{1}{\omega - \omega_h} \mathcal{T}_{\mathbf{K}\sigma}^\dagger T^\dagger(\vec{r} - \vec{r}') |\psi_n\rangle \langle \psi_n| T(\vec{r} - \vec{r}') \mathcal{T}_{\mathbf{K}\sigma}(t) \right] |\psi_0\rangle .$$
(86)

To obtain the above, we used the fact that H_{tiled} commutes with the translation operator.

X. EQUAL-TIME GROUND STATE CORRELATORS

Properties of the ground state can be probed using static correlation functions that are expectation values of operators that propagate excitations. We will consider general correlations, in real and momentum space.

A. Real-space correlation functions

We first consider a real-space operator $\mathcal{O}(\mathbf{r} + \boldsymbol{\Delta})\mathcal{O}^\dagger(\mathbf{r})$ that quantifies the presence of correlations over a distance $\boldsymbol{\Delta}$. The correlation function itself is given by the expectation value of this operator in the ground state:

$$C_\mathcal{O}(\boldsymbol{\Delta}) = \langle \Psi_{\text{gs}}| \mathcal{O}(\mathbf{r} + \boldsymbol{\Delta})\mathcal{O}^\dagger(\mathbf{r}) |\Psi_{\text{gs}}\rangle .$$
(87)

To obtain a tractable expression for this, we first replace the full ground state with its expression in terms of the auxiliary model ground states (eq. 58):

$$C_\mathcal{O}(\boldsymbol{\Delta}) = \frac{1}{N} \sum_{\mathbf{r}_1,\mathbf{r}'} \langle \psi_{\text{gs}} (\mathbf{r}_1 + \mathbf{r}' + \mathbf{r}_c + \mathbf{r}) | \mathcal{O}(\mathbf{r} + \boldsymbol{\Delta})\mathcal{O}^\dagger(\mathbf{r}) |\psi_{\text{gs}} (\mathbf{r}_1 + \mathbf{r}_c + \mathbf{r})\rangle e^{-i\mathbf{k}_0 \cdot (\mathbf{r}_1 - \mathbf{r}_2)} ,$$
(88)

where $\mathbf{r}_1$ and $\mathbf{r}_1 + \mathbf{r}'$ are the positions of the incoming and outgoing auxiliary model states, relative to $\mathbf{r}_c + \mathbf{r}$, and $\mathbf{k}_0$ is the crystal momentum of the ground state (which we will immediately set to zero). In order to convert the incoming and outgoing states into the same auxiliary mode at a reference location $\mathbf{r}_c$ (which would then allow computations purely within a single auxiliary model), we use the relation: $|\psi_{\mathrm{gs}}(\mathbf{x})\rangle = T^\dagger(\mathbf{x} - \mathbf{r}_c)\psi_{\mathrm{gs}}|\psi(\mathbf{r}_c)\rangle$. Substituting this appropriately for both the auxiliary model states gives:

$$
\begin{aligned}
C_{\mathcal{O}}(\boldsymbol{\Delta}) &= \frac{1}{N}\sum_{\mathbf{r}_1,\mathbf{r}'}\langle\psi_{\mathrm{gs}}(\mathbf{r}_c)|T(\mathbf{r}_1 + \mathbf{r}' + \mathbf{r})\mathcal{O}(\mathbf{r} + \boldsymbol{\Delta})\mathcal{O}^\dagger(\mathbf{r})T^\dagger(\mathbf{r}_1 + \mathbf{r})|\psi_{\mathrm{gs}}(\mathbf{r}_c)\rangle \\
&= \frac{1}{N}\sum_{\mathbf{r}_1,\mathbf{r}'}\langle\psi_{\mathrm{gs}}(\mathbf{r}_c)|T(\mathbf{r}')\mathcal{O}(\boldsymbol{\Delta} - \mathbf{r}_1)\mathcal{O}^\dagger(-\mathbf{r}_1)|\psi_{\mathrm{gs}}(\mathbf{r}_c)\rangle \\
&= \frac{1}{N}\sum_{\mathbf{r}_1,\mathbf{r}'}\langle\psi_{\mathrm{gs}}(\mathbf{r}_c + \mathbf{r}')|\mathcal{O}(\boldsymbol{\Delta} - \mathbf{r}_1)\mathcal{O}^\dagger(-\mathbf{r}_1)|\psi_{\mathrm{gs}}(\mathbf{r}_c)\rangle \ .
\end{aligned}
\tag{89}
$$

As a final cosmetic change, we transform $\mathbf{r}_1 \to -\mathbf{r}$:

$$
C_{\mathcal{O}}(\boldsymbol{\Delta}) = \frac{1}{N}\sum_{\mathbf{r},\mathbf{r}'}\langle\psi_{\mathrm{gs}}(\mathbf{r}_c + \mathbf{r}')|\mathcal{O}(\boldsymbol{\Delta} + \mathbf{r})\mathcal{O}^\dagger(\mathbf{r})|\psi_{\mathrm{gs}}(\mathbf{r}_c)\rangle \ .
\tag{90}
$$

Like in the Greens function calculation, we now consider the various kinds of contributions separately.

1. Intra-auxiliary model contributions: $\mathbf{r}' = 0$

These terms describe excitations that start and propagate within the same auxiliary model, upto a distance $\boldsymbol{\Delta}$:

$$
C_{\mathcal{O}}(\boldsymbol{\Delta}) \to \frac{1}{N}\sum_{\mathbf{r}}\langle\psi_{\mathrm{gs}}(\mathbf{r}_c)|\mathcal{O}(\boldsymbol{\Delta} + \mathbf{r})\mathcal{O}^\dagger(\mathbf{r})|\psi_{\mathrm{gs}}(\mathbf{r}_c)\rangle \ .
\tag{91}
$$

With an eye towards introducing the impurity operators into the correlations, we insert a complete basis defined by the eigenstates $\{|\psi_n(\mathbf{r}_c)\rangle\}$ of the auxiliary model into the expression:

$$
C_{\mathcal{O}}(\boldsymbol{\Delta}) \to \frac{1}{N}\sum_{\mathbf{r}}\sum_{n}\langle\psi_{\mathrm{gs}}(\mathbf{r}_c)|\mathcal{O}(\boldsymbol{\Delta} + \mathbf{r})|\psi_n(\mathbf{r}_c)\rangle\langle\psi_n(\mathbf{r}_c)|\mathcal{O}^\dagger(\mathbf{r})|\psi_{\mathrm{gs}}(\mathbf{r}_c)\rangle \ .
\tag{92}
$$

For the excitations that exist purely in the conduction bath ($\mathbf{r} \neq \mathbf{r}_c$), the excitation operators must be suitably modified (see the arguments around eq. 78) in order to incorporate Kondo screening. The modified excitation operators are generally defined as

$$
\tilde{\mathcal{O}}(\mathbf{r}) = \mathcal{O}(\mathbf{r})\mathcal{O}^\dagger(d)\mathcal{P}_{\mathrm{gs}} \ ,
\tag{93}
$$

where $\mathcal{O}^\dagger(d)$ is the hermitian conjugate of the correlation operator $\mathcal{O}$, but applied on the impurity sites. This therefore constitutes a time-reversed scattering process on the impurity site relative to the process in the bath. The operator $\mathcal{P}_{\mathrm{gs}}$ projects onto the ground state of the auxiliary model, since we are interested in ground state correlations. The operator multiplying the old correlation operator represents all possible excitations of the impurity site, and ensure that the bath and impurity excitation processes take place in correlation. The projector ensures that only tripartite correlations between the impurity site and the two momentum states are captured by the correlation, which is what's desired within the tiling method.

With this modified operator, this class of correlation functions can be written as

$$
C_{\mathcal{O}}(\boldsymbol{\Delta}) \to \frac{1}{N}\sum_{\mathbf{r}}\langle\psi_{\mathrm{gs}}(\mathbf{r}_c)|\tilde{\mathcal{O}}(\boldsymbol{\Delta} + \mathbf{r})|\psi_{\mathrm{gs}}(\mathbf{r}_c)\rangle\langle\psi_{\mathrm{gs}}(\mathbf{r}_c)|\tilde{\mathcal{O}}^\dagger(\mathbf{r})|\psi_{\mathrm{gs}}(\mathbf{r}_c)\rangle \ .
\tag{94}
$$

This can be interpreted as the fact that within our auxiliary model formalism, the correlation between the sites $\mathbf{r}$ and $\boldsymbol{\Delta} + \mathbf{r}$ can only occur through a transition process that connect one of the sites with the impurity site and then a return process that connects the impurity site with the other site.

These are the most non-local contributions, and involve excitations that connect different auxiliary models:

$$C_{\mathcal{O}}(\boldsymbol{\Delta}) \to \frac{1}{N} \sum_{\mathbf{r}' \neq 0} \langle \psi_{\text{gs}}\left(\mathbf{r}_c + \mathbf{r}'\right) | \tilde{\mathcal{O}}(\boldsymbol{\Delta} + \mathbf{r}) | \psi_{\text{gs}}\left(\mathbf{r}_c\right) \rangle \langle \psi_{\text{gs}}\left(\mathbf{r}_c\right) | \tilde{\mathcal{O}}^{\dagger}(\mathbf{r}) | \psi_{\text{gs}}\left(\mathbf{r}_c\right) \rangle \ . \tag{95}$$

B. Momentum-space correlation functions

We now consider momentum space correlations, through a general operator $\mathcal{O}(\mathbf{k}_2)\mathcal{O}^{\dagger}(\mathbf{k}_1)$:

$$C_{\mathcal{O}}(\mathbf{k}_1, \mathbf{k}_2) = \langle \Psi_{\text{gs}} | \mathcal{O}(\mathbf{k}_2) \mathcal{O}^{\dagger}(\mathbf{k}_1) | \Psi_{\text{gs}} \rangle \ . \tag{96}$$

Note that $\mathcal{O}$ itself is a two-particle operator. To obtain a tractable expression for this, we first replace the full ground state with its expression in terms of the auxiliary model ground states (eq. 58):

$$C_{\mathcal{O}}(\mathbf{k}_1, \mathbf{k}_2) = \frac{1}{N} \sum_{\mathbf{r}_1, \mathbf{r}_2} \langle \psi_{\text{gs}}\left(\mathbf{r}_2\right) | \mathcal{O}(\mathbf{k}_2) \mathcal{O}^{\dagger}(\mathbf{k}_1) | \psi_{\text{gs}}\left(\mathbf{r}_1\right) \rangle \ , \tag{97}$$

where $\mathbf{r}_1$ and $\mathbf{r}_2$ are the positions of the incoming and outgoing auxiliary model states. In order to convert the incoming and outgoing states into the same auxiliary mode at a reference location $\mathbf{r}_c$ (which would then allow computations purely within a single auxiliary model), we use the relation: $|\psi_{\text{gs}}\left(\mathbf{x}\right)\rangle = T^{\dagger}\left(\mathbf{x} - \mathbf{r}_c\right) \psi_{\text{gs}} |\psi\left(\mathbf{r}_c\right)\rangle$. Substituting this appropriately for both the auxiliary model states gives:

$$C_{\mathcal{O}}(\mathbf{k}_1, \mathbf{k}_2) = \frac{1}{N} \sum_{\mathbf{r}_1, \mathbf{r}_2} \langle \psi_{\text{gs}}\left(\mathbf{r}_c\right) | T\left(\mathbf{r}_2 - \mathbf{r}_c\right) \mathcal{O}(\mathbf{k}_2) \mathcal{O}^{\dagger}(\mathbf{k}_1) T^{\dagger}\left(\mathbf{r}_1 - \mathbf{r}_c\right) | \psi_{\text{gs}}\left(\mathbf{r}_c\right) \rangle \ . \tag{98}$$

In order to simplify the translation operators, we can use eq. 66. For that, we would need to know whether the operator $\mathcal{O}$ involves the net transfer of momentum. If $\mathcal{O}(\mathbf{k})$ commutes with the total number operator $n_{\mathbf{k}} = \sum_{\sigma} n_{\mathbf{k},\sigma}$, there is no momentum transfer. Examples of such operators are spin operators, $S_{\alpha\beta}(\mathbf{k}) \equiv c_{\mathbf{k}\alpha}^{\dagger} c_{\mathbf{k}\beta}$, and density operators $n_{\mathbf{k}\alpha}$. If $\mathcal{O}(\mathbf{k})$ does not commute with $n_{\mathbf{k}}$, there is a net transfer of momentum, and one such operator would be the charge isospin operator $C^{+}(\mathbf{k}) = c_{\mathbf{k}\uparrow}^{\dagger} c_{\mathbf{k}\downarrow}^{\dagger}$. For the first kind of operators, we have $T(\mathbf{a})\mathcal{O}(\mathbf{k})T^{\dagger}(\mathbf{a}) = \mathcal{O}(\mathbf{k})$, while the for the latter, we get $T(\mathbf{a})\mathcal{O}(\mathbf{k})T^{\dagger}(\mathbf{a}) = e^{-\mathbf{a} \cdot 2\mathbf{k}} \mathcal{O}(\mathbf{k})$, where $2\mathbf{k}$ represents the momentum being transferred by the operator. We consider the two cases separately.

1. Momentum-conserving operators: $[\mathcal{O}(\mathbf{k}), n_{\mathbf{k}}] = 0$

For these operators, the expression for the correlation gives

$$\begin{aligned} C_{\mathcal{O}}(\mathbf{k}_1, \mathbf{k}_2) &= \frac{1}{N} \sum_{\mathbf{r}_1, \mathbf{r}_2} \langle \psi_{\text{gs}}\left(\mathbf{r}_c\right) | T\left(\mathbf{r}_2 - \mathbf{r}_1\right) \mathcal{O}(\mathbf{k}_2) \mathcal{O}^{\dagger}(\mathbf{k}_1) | \psi_{\text{gs}}\left(\mathbf{r}_c\right) \rangle \\ &= \sum_{\mathbf{r}, \boldsymbol{\Delta}} \langle \psi_{\text{gs}}\left(\mathbf{r}_c + \boldsymbol{\Delta}\right) | \mathcal{O}(\mathbf{k}_2) \mathcal{O}^{\dagger}(\mathbf{k}_1) | \psi_{\text{gs}}\left(\mathbf{r}_c\right) \rangle \ . \end{aligned} \tag{99}$$

To obtain the last form, we defined $\boldsymbol{\Delta} = \mathbf{r}_2 - \mathbf{r}_1$ as the distance between the incoming and outgoing auxiliary model states, and preformed the sum over the free variable $\mathbf{r}_1$ to cancel out the factor of $1/N$. Just like before, this expression can be decomposed into a term that involves a single auxiliary model and other terms that involve two distinct auxiliary models.

2. Non-momentum-conserving operators: $[\mathcal{O}(\mathbf{k}), n_{\mathbf{k}}] \neq 0$

This class of operators incur an additional phase factor of $e^{-\mathbf{a}\cdot 2\mathbf{k}}$ when the translation operators are translated across them:

$$
\begin{aligned}
C_{\mathcal{O}}(\mathbf{k}_1, \mathbf{k}_2) &= \frac{1}{N} \sum_{\mathbf{r}_1, \mathbf{r}_2} \langle \psi_{\mathrm{gs}}(\mathbf{r}_c) | T(\mathbf{r}_2 - \mathbf{r}_1) \mathcal{O}(\mathbf{k}_2)\mathcal{O}^\dagger(\mathbf{k}_1)|\psi_{\mathrm{gs}}(\mathbf{r}_c)\rangle \, e^{2i(\mathbf{r}_1 - \mathbf{r}_c)\cdot(\mathbf{k}_1 - \mathbf{k}_2)} \\
&= \delta_{\mathbf{k}_1, \mathbf{k}_2} \sum_{\boldsymbol{\Delta}} \langle \psi_{\mathrm{gs}}(\mathbf{r}_c + \boldsymbol{\Delta}) | \mathcal{O}(\mathbf{k}_2)\mathcal{O}^\dagger(\mathbf{k}_1)|\psi_{\mathrm{gs}}(\mathbf{r}_c)\rangle \; .
\end{aligned}
\tag{100}
$$

For this expression, we again defined $\boldsymbol{\Delta}$ similar to before, and carried out the sum of $\mathbf{r}_1$ involving the exponential to obtain a factor of $N\delta_{\mathbf{k}_1, \mathbf{k}_2}$. The Kronecker delta factor is a manifestation of translational invariance and the associated total momentum conservation.

As it stands, operators like $\mathcal{O}(\mathbf{k}_1)$ act purely on the conduction bath degrees of freedom. In order to incorporate impurity-bath correlation effects, we modify these operators using the appropriate $T-$matrices, by employing eq. 93. The final computations are carried out using these modified operators.

XI. ENTANGLEMENT

We will now describe the prescription of calculating entanglement measures of the lattice model from within our auxiliary model treatment. In this section, we are interested mainly in two such measures, the entanglement entropy and the mutual information. Given a pure state $|\Psi\rangle$ describing the complete system, the entanglement entropy $S_{\mathrm{EE}}(\nu)$ of a subsystem ν quantifies the entanglement of ν with the rest of the subsystem, and is defined as

$$
S_{\mathrm{EE}}(\nu) = -\mathrm{Tr}\left[\rho(\nu)\log\rho(\nu)\right], \quad \rho(\nu) = \mathrm{Tr}_\nu\left[|\Psi\rangle\langle\Psi|\right]
\tag{101}
$$

where $\mathrm{Tr}\left[\cdot\right]$ is the trace operator, and $\rho(\nu)$ is the reduced density matrix for the subsystem ν obtained by taking the partial trace Tr_ν (over the states of ν) of the full density matrix $\rho = |\Psi\rangle\langle\Psi|$. If the subsystem ν describes local regions in real space (or states in $k-$space), we might be interested in the entanglement between two such subsystems ν_1 and ν_2. The correct measure to quantify such entanglement is the mutual information:

$$
I_2(\nu_1, \nu_2) = S_{\mathrm{EE}}(\nu_1) + S_{\mathrm{EE}}(\nu_2) - S_{\mathrm{EE}}(\nu_1 \cup \nu_2) \;,
\tag{102}
$$

where $\nu_1 \cup \nu_2$ is a larger subsystem formed by combining ν_1 and ν_2.

A. Real-space entanglement

Real-space entanglement measures can be used to probe delocalisation-localisation transitions. The simplest such measure is the entanglement of a local mode. Since the local entanglement entropy will be uniform at each lattice site for a system with translation invariance, it suffices to calculate the real-space averaged entanglement entropy $S_{\mathrm{EE}}^{\mathrm{loc}} = \frac{1}{N}\sum_{\mathbf{r}} S_{\mathrm{EE}}(\mathbf{r})$. By visualising the lattice model as a superposition of auxiliary models placed at various sites (eq. 53), the real space average of the lattice model can be thought of as an average over sites of a particular impurity model, and then a second average over all the impurity models. But since all all impurity models are equivalent to each other, the second average is redundant. Secondly, all correlations must derive from the impurity site, which can be formally encoded by subtracting, from this average, the corresponding contribution obtained in the absence of the impurity site. In total, the lattice-auxiliary model relation for the local entanglement entropy can be written as

$$
S_{\mathrm{EE}}^{\mathrm{loc}} = \frac{1}{N}\sum_{\mathbf{r}}\left[S_{\mathrm{EE}}(\mathbf{r}_d + \mathbf{r}) - S_{\mathrm{EE}}^{(0)}(\mathbf{r}_d + \mathbf{r})\right] \;,
\tag{103}
$$

where $\mathbf{r}_d$ is the impurity site position, $\mathbf{r}$ is the distance of a conduction bath site from the impurity site (can be zero), and $S_{\mathrm{EE}}(\mathbf{r}_d + \mathbf{r})$ is the entanglement entropy, calculated within the impurity model, at the locatiom $\mathbf{r}_d + \mathbf{r}$. $S_{\mathrm{EE}}^{(0)}(\mathbf{r}_d + \mathbf{r})$ is the same entanglement entropy, but calculated for an impurity model but with vanishing impurity-bath hybridisation and bath interaction.

B. Momentum-space entanglement

Entanglement measures in $k-$space can provide valuable information regarding the Fermi surface structure and the nature of gapless excitations proximate to it. The most elementary measure is the entanglement entropy $S_{\mathrm{EE}}(\mathbf{q})$ of a single excitation carrying momentum $\mathbf{q}$. Unlike $S_{\mathrm{EE}}^{\mathrm{loc}}$, this does not involve an average, and involves a single computation:

$$S_{\mathrm{EE}}^{\mathrm{loc}} = S_{\mathrm{EE}}(\mathbf{q}) - S_{\mathrm{EE}}^{(0)}(\mathbf{q}) \ . \tag{104}$$

It is possible to improve this by considering inter-auxiliary model contributions in the reduced density matrix $\rho(\mathbf{q})$. On the lattice model, $\rho(\mathbf{q})$ is defined as

$$\rho(\mathbf{q}) = \mathrm{Tr}_{\mathbf{q}} \left[|\Psi_{\mathrm{gs}}\rangle \langle \Psi_{\mathrm{gs}}| \right] \ , \tag{105}$$

where $\mathrm{Tr}_{\mathbf{q}} [\cdot]$ is the partial trace over the Hilbert space of $\mathbf{q}$, and $|\Psi_{\mathrm{gs}}\rangle$ is the tiled ground state. Using eq. 58, we can write the ground state in terms of those of the auxiliary model. These leads to two classes of terms, one purely within a single auxiliary model ground state $|\psi_{\mathrm{gs}}\rangle$, and the other involving transitions across auxiliary models:

$$\rho(\mathbf{q}) = \mathrm{Tr}_{\mathbf{q}} \left[|\psi_{\mathrm{gs}}(\mathbf{r}_d)\rangle \langle \psi_{\mathrm{gs}}(\mathbf{r}_d)| \right] + \frac{1}{N} \mathrm{Tr}_{\mathbf{q}} \sum_{\mathbf{r}} \left[|\psi_{\mathrm{gs}}(\mathbf{r}_d)\rangle \langle \psi_{\mathrm{gs}}(\mathbf{r}_d + \mathbf{r})| \right] \ , \tag{106}$$

where $|\psi_{\mathrm{gs}}(\mathbf{r}_d)\rangle$ is a reference auxiliary model ground state, and $|\psi_{\mathrm{gs}}(\mathbf{r}_d + \mathbf{r})\rangle$ sums over other auxiliary models at increasing distances from this reference model. The first term leads to the expression in eq. 105, while the second term can be used to improve this estimate. Away from any quantum critical points, the localised nature of the impurity-bath hybridisation ensures that impurity correlations decay exponentially away from the transition. This ensures that the second term is very small away from a critical point. We therefore restrict ourselves to just the first term in the present work.

XII. JOURNEY THROUGH THE PSEUDOGAP ON THE LATTICE MODEL

We have already seen from the lattice-embedded impurity model that the impurity phase transition is anisotropic in $k-$space. This has consequences for the metal-insulator transition of the lattice model. We now describe, in terms of correlations, how the Fermi surface of the lattice model is destabilised when the system is tuned through the pseudogap. For this, we employ the relations we derived between correlations on the impurity model and those on the lattice model.

A. $k-$space spectral function and self-energy

The primary indicator of the pseudogapping nature of the transition is of course the $k-$space density of states or the spectral function, shown in Fig. 11. For $W = 0$, all points on the Fermi surface are gapless. As we enter the pseudogap, the region around the antinodes lose all spectral weight and become gapped. Increasing the value of W further leads to the enlargement of the gapped region; exactly at the transition, we end up with a singular Fermi surface composed of just the nodal points.

This is also supported by our computations of the $k-$space self-energy. We show the zero frequency value of the $k-$space self-energy in Fig. 12. This is computed from using Dyson's equation $\Sigma_k = 1/G_k^{(0)} - 1/G_k$, where G_k is the interacting $k-$space Greens function while $G_k^{(0)}$ is the non-interacting $W = 0$ Greens function. We find that the beginning of the pseudogap is marked by poles in the self-energy at the antinodal points; at the transition, only the nodes display vanishing self-energy at zero frequency.

B. Momentum-space spin-correlations

We first look at static spin correlations $\chi_s(k_1, k_2) = \frac{1}{2} \left\langle S_{k_1}^+ S_{k_2}^- + \mathrm{h.c.} \right\rangle$. These processes correspond to the gapless excitations of the Fermi liquid phase. We find that
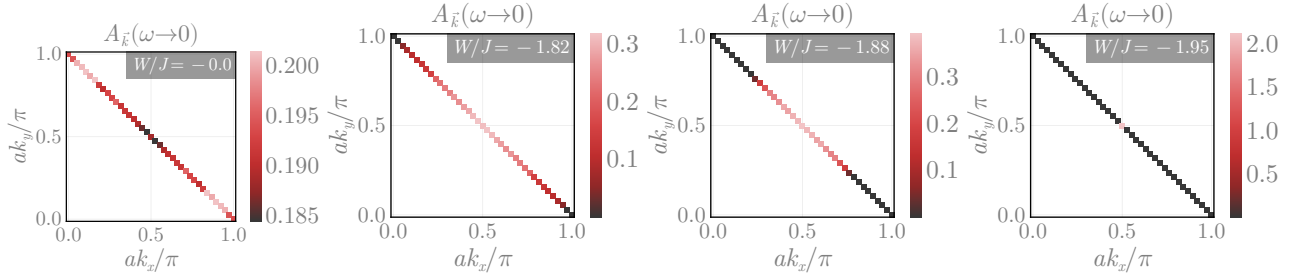
FIG. 11. One-particle $k-$space spectral function. In the absence of bath interactions, all points on Fermi surface are gapless (first panel). Proceeding through the pseudogap results in the gapping out of Fermi surface points starting from the antinode (second panel) and approaching the node (third panel), until finally only the node remains at the critical point (fourth panel).
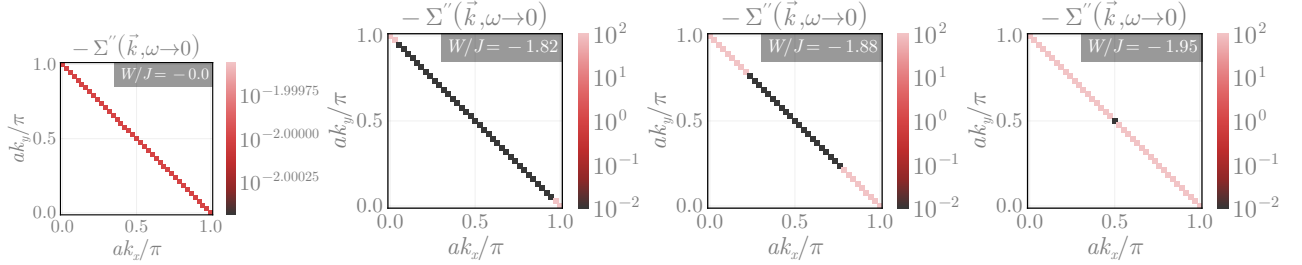

FIG. 12. $k-$space self-energy. For $W = 0$, the self-energy is vanishingly small, leading to a Fermi liquid phase described by well-defined quasiparticles. Inside the pseudogap, the self-energy diverges near the antinodes, leading to their gapping. The coexistence of gapped and gapless points on the Fermi surface in the pseudogapped region leads to non-Fermi liquid behaviour of the gapless excitations, as captured by the emergent two-channel behaviour within the impurity model. The metal at the transition is supported only the four nodal points.
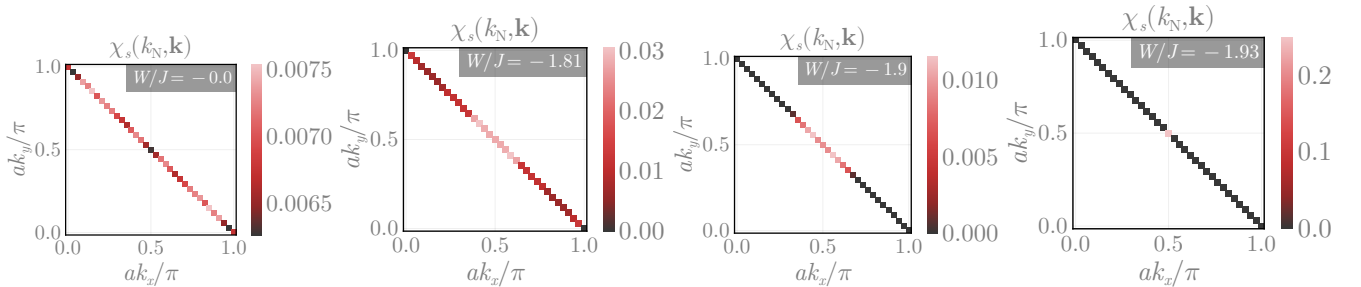
FIG. 13. Spin-flip correlations $\left\langle S(k_N)^+, S(\mathbf{k})^- \right\rangle$ between the nodal point $k_N = (-\pi/2, -\pi/2)$ and an arbitrary $k-$point on the Fermi surface. In the absence of bath interaction (first panel), the correlations are somewhat uniformly distributed along the Fermi surface. As we enter the pseudogap (second panel), the spin-correlations near the antinode vanish, indicating that they have been removed from the metallic excitations. Passing through the pseudogap involves in the extensions of the gapped region (third panel), until finally only the node remains (fourth panel).
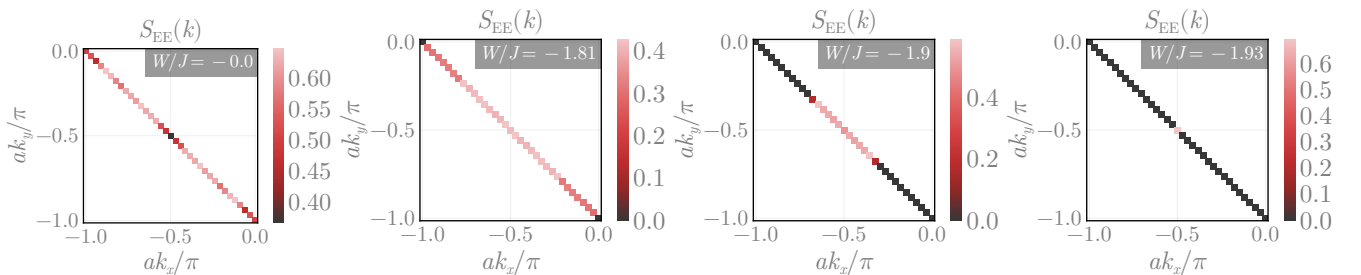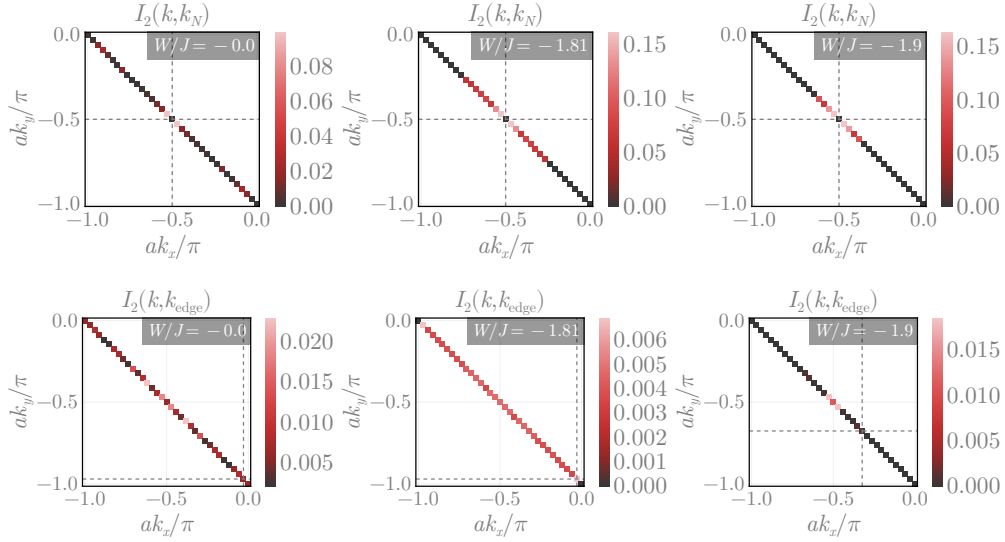
C. Entanglement entropy and Mutual information

D. Heisenberg model as a low-energy description of the insulator

In the insulating phase, the ground state of each auxiliary model hosts a decoupled local moment. Upon applying the tiling procedure, the lattice model ground state becomes that of the Hubbard model in the atomic limit. In order to lift the extensive degeneracy of the state, we will now take into consideration inter-auxiliary model virtual scattering processes that were subdominant in the metallic phase and were hence ignored. These one-particle scattering processes lead to the emergence of a nearest-neighbour superexchange interaction.

For simplicity, we consider two impurity sites labelled 1 and 2 associated with two nearest-neighbour auxiliary models. The ground state subspace is four-fold degenerate:

$$|\Psi_L\rangle = \{|\sigma_1, \sigma_2\rangle\} \ , \quad \sigma_i = \pm 1 \tag{107}$$

where σ_i is the spin state of site i. This ground state is derived from the following "zeroth order" Hamiltonian that emerges in the local moment phase of the auxiliary models when all scattering processes between the impurity and conduction bath are RG-irrelevant:

$$H_0 = -\frac{U}{2} \sum_{i=1,2} \left(n_{i\uparrow} - n_{i\downarrow}\right)^2 \ ; \tag{108}$$

the local correlation on the impurity site becomes the largest scale in the problem in this phase and pushes the $|n_i = 2\rangle$ and $|n_i = 0\rangle$ states to high energies. This then defines the high-energy subspace for our calculation:

$$|\Psi_H\rangle = |C_1, C_2\rangle \ , \tag{109}$$

where C_i can take values 0 or 2, indicating that the state i is either empty or full, respectively. Both the double and hole states exist at a charge gap of the order of $U/2$ above the low-energy singly-occupied subspace defined by the states $|\Psi_L\rangle$.

In order to allow virtual fluctuations that can lift the large ground state degeneracy and lower the energy, we consider (perturbatively) the effects of an irrelevant single-particle hybridisation that connects the nearest-neighbour sites. This perturbation Hamiltonian is therefore of the form

$$H_t = \sum_{\omega} V(\omega)\mathcal{P}(\omega) \sum_{\sigma} \left(c_{1\sigma}^\dagger c_{2\sigma} + \text{h.c.}\right) \ , \tag{110}$$

where $V(\omega)$ only acts on states at the energy scale ω; the renormalisation of V is encoded in the fact that $V(\omega)$ is largest for the excited states and vanishes at low-energies: $V(\omega \to 0) = 0$.

In order to obtain a low-energy effective Hamiltonian for the impurity sites arising from this hybridisation, we integrate out H_t via a Schrieffer-Wolff transformation. This leads to the following second-order Hamiltonian:

$$H_{\text{eff}} = \mathcal{P}_L H_t G \mathcal{H}_t \mathcal{P}_L \ . \tag{111}$$

The operator $\mathcal{P}_L$ projects onto the low-energy subspace $|\Psi_L\rangle$ - this ensures that we remain in the low-energy subspace at the beginning and at the end of the total process. The Greens function $G = (E_L - H_0)^{-1}$ incorporates the excitation energy to go from the low-energy subspace $|\Psi\rangle_L$ (of energy E_L) to the excited subspace $|\Psi\rangle_H$ of energy $E_L + U/2$. Substituting the form of the perturbation Hamiltonian and the excitation energy into the above expression gives

$$H_{\text{eff}} = \frac{V_H^2}{-U/2} \sum_{\sigma,\sigma'} \left[c_{1\sigma}^\dagger c_{2\sigma} c_{2\sigma'}^\dagger c_{1\sigma'} + c_{2\sigma}^\dagger c_{1\sigma} c_{1\sigma'}^\dagger c_{2\sigma'} \right] . \tag{112}$$

where $V_H \equiv V(\omega \to U/2)$ is the impurity-bath hybridisation at energy scales of the order of the Mott gap, in the sense of an RG flow. Terms with consecutive creation or annihilation operators on the same site are prohibited because each site is singly-occupied in the ground state. It is now easy to cast this Hamiltonian into a more recognizable form. For $\sigma' = \sigma$, we get

$$\sum_\sigma \delta_{\sigma,\sigma'} c_{1\sigma}^\dagger c_{2\sigma} c_{2\sigma'}^\dagger c_{1\sigma'} = \sum_\sigma \left(n_{1\sigma} - n_{1\sigma} n_{2\sigma} \right) , \tag{113}$$

while $\sigma = -\sigma' = \pm 1$ gives

$$\sum_\sigma \delta_{\sigma,-\sigma'} c_{1\sigma}^\dagger c_{2\sigma} c_{2\sigma'}^\dagger c_{1\sigma'} = - \left(S_1^+ S_2^- + \text{h.c.} \right) . \tag{114}$$

For the latter expression, we introduced the local spin-flip operators $S_i^\pm$. The expression above it can also be cast into spin variables, using the equations

$$\frac{1}{2} \sum_\sigma n_{i\sigma} = \frac{1}{2},$$
$$\frac{1}{2} \sum_\sigma \sigma n_{i\sigma} = S_i^z, \tag{115}$$

where the first equation is simply the condition of half-filling at each site, and the second equation is the definition of the local spin operator in z−direction. Adding and subtracting the equations gives $n_{i\sigma} = \frac{1}{2} + \sigma S_i^z$.

Substituting everything back into eq. 112 and dropping constant terms gives

$$H_{\text{eff}} = 2 \frac{V_H^2}{U/2} \left(2 S_1^z S_2^z + S_1^+ S_2^- + S_1^- S_2^+ \right) = J_{\text{eff}} \mathbf{S}_1 \cdot \mathbf{S}_2 , \tag{116}$$

where the effective antiferromagnetic Heisenberg coupling is $J_{\text{eff}} = \frac{8 V_H^2}{U}$.

XIII.   TOPOLOGICAL NATURE OF THE TRANSITION

Since the impurity charge hybridising with the bath contributes to the total Luttinger volume of the system [34], decoupling of the impurity from the conduction bath leads to a difference in the value of the Luttinger volume between the local moment (LM) and the strong-coupling (SC) fixed points. If we define $\mathcal{N}_L$ as the Luttinger volume with the spin-degeneracy accounted for, we can write

$$\mathcal{N}_L^{\text{lm}} - \mathcal{N}_L^{\text{sc}} = 1 \tag{117}$$

where $\mathcal{N}_L^{\text{lm}}, \mathcal{N}_L^{\text{sc}}$ are the Luttinger volumes at the local moment and strong-coupling fixed points respectively. This equation expresses the fact that the Luttinger volume of the bath increases by 1 when the system is tuned from LM to SC, and this happens because the single-particle impurity excitation in the lower-Hubbard at the atomic limit gets transferred to the bath Greens function in the process. The quantity which tracks this transfer is therefore $\mathcal{N}_{\text{imp}}$, the number of poles minus the number of zeros in the impurity Greens function at and below the Fermi surface:

$$\mathcal{N}_{\text{imp}} = \begin{cases} 1 & \text{at LM} \\ 0 & \text{at SC} \end{cases} \implies \Delta \mathcal{N}_{\text{imp}} = 1 \tag{118}$$

The Luttinger volume $\mathcal{N}_L$ is related to this impurity count by the equation

$$\mathcal{N}_L = \mathcal{N} - \mathcal{N}_{\text{imp}} \tag{119}$$

where $\mathcal{N}$ is the total number of electrons in the system, accounting for the spin degeneracy. If we keep this total number fixed (isolated system), the changes in the impurity count and Luttinger volume become constrained:

$$\Delta\mathcal{N}_L = -\Delta\mathcal{N}_{\mathrm{imp}} . \tag{120}$$

Eq. 118 then readily implies eq. 117.

In order to connect this impurity topological change with the bulk model, we write the total number of particles in the bulk system in the following manner:

$$\mathcal{N} = \mathcal{N}_{\mathrm{loc}} + \mathcal{N}_{\mathrm{deloc}} \tag{121}$$

$\mathcal{N}_{\mathrm{loc}}$ is the number of real poles minus the number of zeros of the local Greens function. $\mathcal{N}_{\mathrm{deloc}}$ is the number of real poles minus the number of zeros of the $k-$space Greens functions. The former (latter) contributes only in the insulating (metallic) phase, because in the metallic (insulating) phase, the local ($k-$space) Greens function develop imaginary self-energy and the real poles in these Greens functions get replaced by imaginary poles. Together, these two terms accurately count the total number of particles in both these phases. These two terms are defined as

$$\mathcal{N}_{\mathrm{loc}} = \sum_i \mathcal{N}_i = \oint \frac{dz}{2\pi i} n_F(z) \mathrm{Tr}\left[G_i(z)\right], \quad \mathcal{N}_{\mathrm{deloc}} = \sum_k \mathcal{N}_k = \oint \frac{dz}{2\pi i} n_F(z) \mathrm{Tr}\left[G_k(z)\right] = \mathcal{N}_L \tag{122}$$

$G_i(z)$ is the local Greens function at site i of the bulk model, and $G_k(z)$ is the $k-$space Greens function in the bulk model. N_{deloc} is just the Luttinger volume $\mathcal{N}_L$ of the bulk system. With this, the total number of particles in the bulk can be expressed as

$$\mathcal{N} = \sum_i \mathcal{N}_i + \mathcal{N}_{\mathrm{L}} \tag{123}$$

From eq. **??**, we know that the bulk local Greens function is proportional to that of the auxiliary model, and that gives $\sum_i \mathcal{N}_i = \mathcal{N}_{\mathrm{imp}} \sum_i = \mathcal{N} \mathcal{N}_{\mathrm{imp}}$. There we used the fact that for a half-filled system, the total number of sites is equal to the total number of particles in the system. Substituting this into eq. 123 and again using $\Delta\mathcal{N} = 0$ gives

$$\mathcal{N} = \mathcal{N}\mathcal{N}_{\mathrm{imp}} + \mathcal{N}_{\mathrm{L}} \implies \Delta\mathcal{N}_{\mathrm{L}} = -\mathcal{N}\Delta\mathcal{N}_{\mathrm{imp}} \tag{124}$$

We already know that $\Delta\mathcal{N}_{\mathrm{imp}} = 1$ across the transition, so we get

$$\mathcal{N}_L^{\mathrm{metal}} - \mathcal{N}_L^{\mathrm{insulator}} = \mathcal{N}\left(\mathcal{N}_{\mathrm{imp}}^{\mathrm{sc}} - \mathcal{N}_{\mathrm{imp}}^{\mathrm{lm}}\right) = \mathcal{N} \tag{125}$$

The metal-insulator transition is therefore characterised by a change in the topological quantity $\mathcal{N}_L$. The topological nature arises from the fact that it can be expressed in terms of winding numbers related to the corresponding Greens functions. $\mathcal{N}_{\mathrm{imp}}$, which derives from the impurity Greens function G_d, is related to the winding numbers of the curves $\mathrm{Det}[G_d^{-1}(\Gamma^<)]$ and $\mathrm{Det}[G_d^{-1}(\Gamma^0)]$. The winding number is simply the number of times this function encircles the origin when traced on the curves $\Gamma^<$ and Γ^0 that enclose all poles inside and on the Fermi surface respectively. An example of such a winding number is shown in fig. 14.
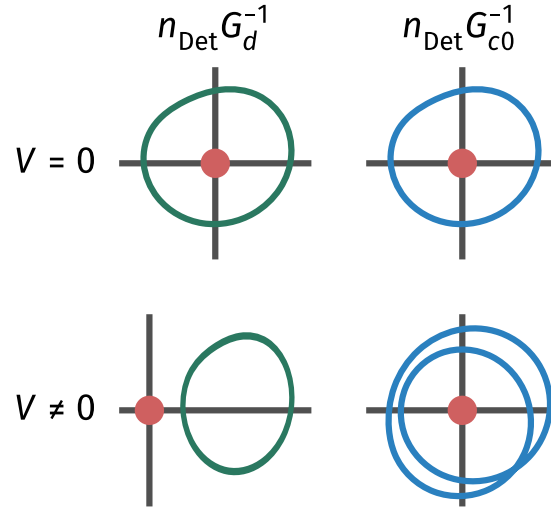
FIG. 14. The green lines describe the winding number related to the impurity Greens function, while the blue lines do it for the bath. At the local moment fixed point $V = 0$, the impurity has a winding number of 1 because the curve encircles the origin once. At the strong-coupling fixed point, this winding number becomes zero, indicated by the fact that the curve does not encircle the origin even once. The reduction in the winding number on the part of the impurity is directly linked to the increase in the winding number of the bath - it encircles the origin once at the local moment fixed point but twice at strong-coupling.

APPENDICES

Appendix A: Effective action for the Hubbard-Heisenberg model and the eSIAM

In order to better understand the similarities and differences between the tiling approach outlined here and the approach adopted in dynamical mean-field approximations, we compute the effective action for the local impurity as well as the impurity-zeroth site system, in both the auxiliary and bulk models. This will be done in the limit of infinite coordination number, in order to create a tractable effective theory.

1. Local theory for the Hubbard-Heisenberg model

We will first work with the Hubbard-Heisenberg model. Let us recall that within the eSIAM, most of the dynamics is governed by the physics of the impurity site and the bath site coupled to the impurity. Accordingly, we will first obtain an effective action within the Hubbard-Heisenberg model for the small system consisting of a local site and all its nearest-neighbours.

We choose a certain local site that we call 0, whose nearest-neighbours will be denoted as $\{\bar{0}\}$. The action for the full Hubbard-Heisenberg model can be formally separated into three parts:

$$S_{\text{H-H}} = S_{0,\bar{0}} + S^{(0,\bar{0})} + S_{\text{int}} \ , \tag{A1}$$

where $S_{0,\bar{0}}$ represents the part of the action that involves only the sites 0 and $\{\bar{0}\}$, $S^{(0,\bar{0})}$ represents the part that has all the sites apart from 0 and $\{\bar{0}\}$, while S_{int} contains all terms that connect these two parts. These three parts have the forms

$$
\begin{aligned}
S_{0,\bar{0}} = & \sum_{i=0,\bar{0}} \sum_{\sigma} \int_0^{\beta} \mathrm{d}\tau \ c_{i\sigma}^{\dagger}(\tau)\partial_{\tau}c_{i\sigma}(\tau) - t \sum_{\bar{0},\sigma} \int_0^{\beta} \mathrm{d}\tau \ \left[c_{0\sigma}^{\dagger}(\tau)c_{\bar{0}\sigma}(\tau) + \text{h.c.} \right] \\
& - \frac{U}{2} \sum_{i=0,\bar{0}} \int_0^{\beta} \mathrm{d}\tau \ (n_{i\uparrow}(\tau) - n_{i\downarrow}(\tau))^2 + J \sum_{\bar{0}} \int_0^{\beta} \mathrm{d}\tau \vec{S}_0(\tau) \cdot \vec{S}_{\bar{0}}(\tau) \ ,
\end{aligned}
\tag{A2}
$$

$$
\begin{aligned}
S^{(0,\bar{0})} = & \sum_{j \neq (0,\bar{0})} \sum_{\sigma} \int_0^{\beta} \mathrm{d}\tau \ c_{j\sigma}^{\dagger}(\tau)\partial_{\tau}c_{j\sigma}(\tau) - t \sum_{\langle j,l \rangle \neq (0,\bar{0}),\sigma} \int_0^{\beta} \mathrm{d}\tau \ \left[c_{j\sigma}^{\dagger}(\tau)c_{l\sigma}(\tau) + \text{h.c.} \right] \\
& - \frac{U}{2} \sum_{j \neq (0,\bar{0})} \int_0^{\beta} \mathrm{d}\tau \ (n_{j\uparrow}(\tau) - n_{j\downarrow}(\tau))^2 + J \sum_{\langle j,l \rangle \neq (0,\bar{0})} \int_0^{\beta} \mathrm{d}\tau \vec{S}_l(\tau) \cdot \vec{S}_j(\tau) \ ,
\end{aligned}
\tag{A3}
$$

$$S_{\text{int}} = -t \sum_{i \in \bar{0}} \sum_{j \in \text{NN of } i} \sum_{\sigma} \int_0^{\beta} \mathrm{d}\tau \ \left(c_{i\sigma}^{\dagger}(\tau)c_{j\sigma}(\tau) + \text{h.c.} \right) + J \sum_{i \in \bar{0}} \sum_{j \in \text{NN of } i} \int_0^{\beta} \mathrm{d}\tau \vec{S}_i(\tau) \cdot \vec{S}_j(\tau) = S_{\text{int}}^{\text{hop}} + S_{\text{int}}^{\text{spin}} \tag{A4}$$

In order to obtain an effective theory $S_{\text{eff}}^{0,\bar{0}}$ purely for the local system $(0,\bar{0})$, we need to trace over all the other degrees of freedom. This partial trace will be carried out over the states of the so-called "cavity" system $S^{(0,\bar{0})}$. The effective action can be constructed by tracing over scattering processes of all orders that leave the final action diagonal in the system $(0,\bar{0})$. The formal expression can be written as

$$S_{\text{eff}}^{0,\bar{0}} = S_{0,\bar{0}} + \sum_{n=1}^{\infty} \left\langle \left(S_{\text{int}}^{\text{hop}} \right)^{2n} \right\rangle_{(0,\bar{0})} + \sum_{n=1}^{\infty} \left\langle \left(S_{\text{int}}^{\text{spin}} \right)^{2n} \right\rangle_{(0,\bar{0})} \tag{A5}$$

where, as mentioned before, the average is carried out in the cavity system $S^{(0,\bar{0})}$. Each hopping term in the expansion

is of the form

$$
\left(S_{\text{int}}^{\text{hop}}\right)^{2n} = t^{2n} \sum_{\sigma} \sum_{(i_1,i_1')\ldots,(i_n,i_n')} \sum_{(j_1,j_1')\ldots,(j_n,j_n')} \int_0^\beta d\tau_1 \ldots d\tau_n d\tau_1' \ldots d\tau_{j_n}'
$$

$$
c_{i_1\sigma}^\dagger(\tau_{i_1}) c_{i_2\sigma}^\dagger(\tau_2) \ldots c_{i_n\sigma}^\dagger(\tau_n) c_{i_1'\sigma}(\tau_1') c_{i_2'\sigma}(\tau_2') \ldots c_{i_n'\sigma}(\tau_n') \left\langle c_{j_1\sigma}(\tau_1) c_{j_2\sigma}(\tau_2) \ldots c_{j_n\sigma} \; c_{j_1'\sigma}^\dagger(\tau_1') \ldots c_{j_n'\sigma}^\dagger(\tau_n') \right\rangle_{(0,\bar{0})}
$$

$$
= t^{2n} \sum_{\sigma} \sum_{(i_1,i_1')\ldots,(i_n,i_n')} \sum_{(j_1,j_1')\ldots,(j_n,j_n')} \int_0^\beta d\tau_1 \ldots d\tau_{j_n}' c_{i_1\sigma}^\dagger(\tau_{i_1}) \ldots c_{i_n\sigma}^\dagger(\tau_n) \; c_{i_1'\sigma}(\tau_1') \ldots c_{i_n'\sigma}(\tau_n')
$$

$$
G_n^{(0,\bar{0})}\left(\tau_1 \ldots \tau_n; \tau_1' \ldots \tau_n'\right) \; ,
$$

(A6)

where the indices i_1 through i_n and their primed counterparts run through $\bar{0}$, while j_l ($\in \{j_1,\ldots,j_n'\}$) runs through the nearest-neighbours of the corresponding i_l index. The $n-$particle Greens function $G_n^{(0,\bar{0})}\left(\tau_1 \ldots \tau_n; \tau_1' \ldots \tau_n'\right)$ for the cavity system is defined in the usual fashion

$$
G_n^{(0,\bar{0})}\left(\tau_1 \ldots \tau_n; \tau_1' \ldots \tau_n'\right) = \left\langle c_{j_1\sigma}(\tau_1) c_{j_2\sigma}(\tau_2) \ldots c_{j_n\sigma} \; c_{j_1'\sigma}^\dagger(\tau_1') \ldots c_{j_n'\sigma}^\dagger(\tau_n') \right\rangle_{(0,\bar{0})}
$$

(A7)

In the limit of infinite coordination number, only the $n=1$ term survives:

$$
\lim_{\mathcal{Z}\to\infty} \sum_{n=1}^\infty \langle \left(S_{\text{int}}^{\text{hop}}\right)^{2n} \rangle_{(0,\bar{0})} = t^2 \sum_\sigma \sum_{i,i'} \int_0^\beta d\tau d\tau' c_{i\sigma}^\dagger(\tau) c_{i'\sigma}(\tau') \sum_{j,j'} G_1^{(0,\bar{0})}\left(j\tau; j'\tau'\right)
$$

$$
= \sum_\sigma \sum_{i,i'} \int_0^\beta d\tau d\tau' \; \Delta_{ii',\sigma}(\tau-\tau') c_{i\sigma}^\dagger(\tau) c_{i'\sigma}(\tau') \; ,
$$

(A8)

where we have defined the bath hybridisation function $\Delta_{ii',\sigma}(\tau-\tau')$ as

$$
\Delta_{ii',\sigma}(\tau-\tau') = t^2 \sum_{j \in \text{NN of } i} \sum_{j' \in \text{NN of } i'} G_1^{(0,\bar{0})}\left(j\sigma\tau; j'\sigma\tau'\right) \; .
$$

(A9)

Under similar approximations, the spin term in the action reduces to

$$
\lim_{\mathcal{Z}\to\infty} \sum_{n=1}^\infty \langle \left(S_{\text{int}}^{\text{spin}}\right)^{2n} \rangle_{(0,\bar{0})} = \sum_{i,i'} \int_0^\beta d\tau d\tau' \; \chi(\tau-\tau') \vec{S}_i(\tau) \cdot \vec{S}_{i'}(\tau') \; ,
$$

(A10)

where the susceptibility $\chi_{ii'}(\tau-\tau')$ is defined as

$$
\chi_{ii'}(\tau-\tau') = J^2 \sum_{j \in \text{NN of } i} \sum_{j' \in \text{NN of } i'} \vec{S}_j(\tau) \cdot \vec{S}_{j'}(\tau') \; .
$$

(A11)

The effective action for the $0,\bar{0}$ system, in the limit of large coordination number, simplifies to

$$
S_{\text{eff}}^{0,\bar{0}} = \sum_{i=0,\bar{0}} \sum_\sigma \int_0^\beta d\tau \; c_{i\sigma}^\dagger(\tau) \partial_\tau c_{i\sigma}(\tau) - t \sum_{\bar{0},\sigma} \int_0^\beta d\tau \; \left[c_{0\sigma}^\dagger(\tau) c_{\bar{0}\sigma}(\tau) + \text{h.c.}\right] - \frac{U}{2} \sum_{i=0,\bar{0}} \int_0^\beta d\tau \; \left(n_{i\uparrow}(\tau) - n_{i\downarrow}(\tau)\right)^2
$$

$$
+ J \sum_{\bar{0}} \int_0^\beta d\tau \vec{S}_0(\tau) \cdot \vec{S}_{\bar{0}}(\tau) + \sum_{i,i'} \int_0^\beta d\tau d\tau' \left[\sum_\sigma \Delta_{ii',\sigma}(\tau-\tau') c_{i\sigma}^\dagger(\tau) c_{i'\sigma}(\tau') + \chi_{ii'}(\tau-\tau') \vec{S}_i(\tau) \cdot \vec{S}_{i'}(\tau')\right]
$$

(A12)

One can also write down an effective action purely for the local site 0. The sites $\bar{0}$ will now be a part of the environment action $S^{(0)}$ instead of the system action, but since the system is thermodynamically large, the cavity action can be assumed to remain the same, such the expectation values are calculated in the same system. As a result, the hybridisation and susceptibility functions remain unchanged. S_{int} is now made of terms that connect 0 and $\bar{0}$, so the transformation from $S^{(0,\bar{0})}$ can be made by replacing the set $\{j\}$ with the set $\bar{0}$, and the set $\bar{0}$ itself will be replaced by the local site 0. We quote the final form of the local effective action:

$$
S_{\text{eff}}^0 = \sum_\sigma \int_0^\beta d\tau \; c_{0\sigma}^\dagger(\tau) \partial_\tau c_{0\sigma}(\tau) - \frac{U}{2} \int_0^\beta d\tau \; \left(n_{0\uparrow}(\tau) - n_{0\downarrow}(\tau)\right)^2
$$

$$
+ \int_0^\beta d\tau d\tau' \left[\sum_\sigma \Delta_{00,\sigma}(\tau-\tau') c_{i\sigma}^\dagger(\tau) c_{i'\sigma}(\tau') + \chi_{00}(\tau-\tau') \vec{S}_i(\tau) \cdot \vec{S}_{i'}(\tau')\right]
$$

(A13)

2. Local theory for the extended SIAM

The Hamiltonian for the extended SIAM model is shown in eq. 41. We will denote the impurity with the label d and the bath sites with the label c. Among the bath sites, we will represent the site coupled to the impurity with z. The full action has the form

$$S_{\mathrm{ES}} = \sum_{d,c}\sum_\sigma \int_0^\beta \mathrm{d}\tau\; c_{i\sigma}^\dagger(\tau)\partial_\tau c_{i\sigma}(\tau) - t\sum_{\langle i,j\rangle\in c,\sigma}\int_0^\beta \mathrm{d}\tau\; \left[c_{i\sigma}^\dagger(\tau)c_{j\sigma}(\tau) + \mathrm{h.c.}\right] - V\sum_\sigma \int_0^\beta \mathrm{d}\tau\; \left[c_{d\sigma}^\dagger(\tau)c_{z\sigma}(\tau) + \mathrm{h.c.}\right]$$

$$+ J\int_0^\beta \mathrm{d}\tau \vec{S}_d(\tau)\cdot \vec{S}_z(\tau) - \frac{U}{2}\int_0^\beta \mathrm{d}\tau\; (n_{d\uparrow}(\tau) - n_{d\downarrow}(\tau))^2 - \frac{U_b}{2}\int_0^\beta \mathrm{d}\tau\; (n_{z\uparrow}(\tau) - n_{z\downarrow}(\tau))^2\;,$$

$$\tag{A14}$$

As in the Hubbard-Heisenberg model, we first obtain an effective action for the pair of sites (d,z). As in the previous calculation, this will again generate a hybridisation function $\Delta_{zz,\sigma}$ for the bath site nearest to the zeroth site. No susceptibility will be generated however, because there is no spin-exchange coupling within the bath. The net result is

$$S_{\mathrm{eff}}^{d,z} = \sum_{d,c}\sum_\sigma \int_0^\beta \mathrm{d}\tau\; c_{i\sigma}^\dagger(\tau)\partial_\tau c_{i\sigma}(\tau) - V\sum_\sigma \int_0^\beta \mathrm{d}\tau\; \left[c_{d\sigma}^\dagger(\tau)c_{z\sigma}(\tau) + \mathrm{h.c.}\right] + J\int_0^\beta \mathrm{d}\tau \vec{S}_d(\tau)\cdot \vec{S}_z(\tau)$$

$$- \frac{U}{2}\int_0^\beta \mathrm{d}\tau\; (n_{d\uparrow}(\tau) - n_{d\downarrow}(\tau))^2 - \frac{U_b}{2}\int_0^\beta \mathrm{d}\tau\; (n_{z\uparrow}(\tau) - n_{z\downarrow}(\tau))^2 \tag{A15}$$

$$+ \int_0^\beta \mathrm{d}\tau\mathrm{d}\tau'\; \sum_\sigma \Delta_{zz,\sigma}(\tau - \tau')c_{z\sigma}^\dagger(\tau)c_{z\sigma}(\tau')$$

This hybridisation $\Delta_{zz,\sigma}$ is calculated in the cavity model of the eSIAM, obtained by removing the impurity and the zeroth site from the full model; it is a completely non-interacting system.

One can go one step further and also remove the zeroth site in order to obtain a theory for the impurity site. With this choice, the cavity model now also includes the zeroth site, and hence contains the correlation term associated with U_b. The one-particle connection V will lead to a modified hybridisation $\mathcal{F}$ for this effective theory; the Kondo terms will generate a susceptibility. The resultant action is

$$S_{\mathrm{eff}}^d = \sum_\sigma \int_0^\beta \mathrm{d}\tau\; c_{d\sigma}^\dagger(\tau)\partial_\tau c_{d\sigma}(\tau) - \frac{U}{2}\int_0^\beta \mathrm{d}\tau\; (n_{d\uparrow}(\tau) - n_{d\downarrow}(\tau))^2$$

$$+ \int_0^\beta \mathrm{d}\tau\mathrm{d}\tau'\; \left[\sum_\sigma \mathcal{F}_\sigma(\tau - \tau')c_{i\sigma}^\dagger(\tau)c_{i'\sigma}(\tau') + \chi_d(\tau - \tau')\vec{S}_i(\tau)\cdot \vec{S}_{i'}(\tau')\right] \tag{A16}$$

where $\mathcal{F}$ is defined in terms of the local correlator of the zeroth site

$$\mathcal{F}_\sigma(\tau - \tau') = V^2 G_1^{(d)}\left(z\sigma\tau; z\sigma\tau'\right) = V^2 \left\langle c_{z\sigma}(\tau)c_{z\sigma}^\dagger(\tau')\right\rangle_{(d)} \tag{A17}$$

with the average computed in the interacting cavity model that has the impurity site removed. The interaction arises from the U_b-term. The susceptibility is also calculated in this interacting cavity model, and follows the same definition as in the bulk model:

$$\chi_d(\tau - \tau') = J^2 \vec{S}_z(\tau)\cdot \vec{S}_z(\tau')\;. \tag{A18}$$

Appendix B: Zero temperature Greens function in frequency domain

1. Spectral representation of Greens function

The impurity retarded Green's function is defined as

$$G_{d\sigma}(t) = -i\theta(t)\left\langle \left\{\mathcal{O}_\sigma(t), \mathcal{O}_\sigma^\dagger\right\}\right\rangle \tag{B1}$$

where the average $\langle\rangle$ is over a canonical ensemble at temperature T, and $\mathcal{O}_\sigma$ is the excitation whose spectral function we are interested in. What follows is a standard calculation where we write the Green's function in the spectral

representation. The ensemble average for the operator $\mathcal{O}_\sigma$ can be written in terms of the exact eigenstates of the Hamiltonian:

$$H \left| n \right\rangle = E_n \left| n \right\rangle, \quad \left\langle \mathcal{O}_\sigma \right\rangle \equiv \frac{1}{Z} \sum_n \left\langle n | \mathcal{O}_\sigma | n \right\rangle e^{-\beta E_n} \tag{B2}$$

where $Z = \sum_n e^{-\beta E_n}$ is the partition function and $\{\left| n \right\rangle\}$ is the set of eigenfunctions of the Hamiltonian. We can therefore write

$$
\begin{aligned}
&\left\langle \left\{ \mathcal{O}_\sigma(t), \mathcal{O}_\sigma^\dagger \right\} \right\rangle \\
&= \frac{1}{Z} \sum_m e^{-\beta E_m} \left\langle m \right| \left\{ \mathcal{O}_\sigma(t), \mathcal{O}_\sigma^\dagger \right\} \left| m \right\rangle \\
&= \frac{1}{Z} \sum_{m,n} e^{-\beta E_m} \left\langle m \right| \left(\mathcal{O}_\sigma(t) \left| n \right\rangle \left\langle n \right| \mathcal{O}_\sigma^\dagger + \mathcal{O}_\sigma^\dagger \left| n \right\rangle \left\langle n \right| \mathcal{O}_\sigma(t) \right) \left| m \right\rangle \qquad \left[\sum_n \left| n \right\rangle \left\langle n \right| = 1 \right] \\
&= \frac{1}{Z} \sum_{m,n} e^{-\beta E_m} \left\langle m \right| \left(e^{iH^*t} \mathcal{O}_\sigma e^{-iH^*t} \left| n \right\rangle \left\langle n \right| \mathcal{O}_\sigma^\dagger + \mathcal{O}_\sigma^\dagger \left| n \right\rangle \left\langle n \right| e^{iH^*t} \mathcal{O}_\sigma e^{-iH^*t} \right) \left| m \right\rangle \\
&= \frac{1}{Z} \sum_{m,n} e^{-\beta E_m} \left(e^{i(E_m - E_n)t} \left\langle m \right| \mathcal{O}_\sigma \left| n \right\rangle \left\langle n \right| \mathcal{O}_\sigma^\dagger \left| m \right\rangle + e^{i(E_n - E_m)t} \left\langle m \right| \mathcal{O}_\sigma^\dagger \left| n \right\rangle \left\langle n \right| \mathcal{O}_\sigma \left| m \right\rangle \right) \\
&= \frac{1}{Z} \sum_{m,n} e^{i(E_m - E_n)t} || \left\langle m \right| \mathcal{O}_\sigma \left| n \right\rangle ||^2 \left(e^{-\beta E_m} + e^{-\beta E_n} \right)
\end{aligned}
\tag{B3}
$$

The time-domain impurity Green's function can thus be written as (this is the so-called Lehmann-Kallen representation)

$$G_{d\sigma} = -i\theta(t) \frac{1}{Z} \sum_{m,n} e^{i(E_m - E_n)t} || \left\langle m \right| \mathcal{O}_\sigma \left| n \right\rangle ||^2 \left(e^{-\beta E_m} + e^{-\beta E_n} \right) \tag{B4}$$

We are interested in the frequency domain form.

$$
\begin{aligned}
G_{dd}^\sigma(\omega) &= \int_{-\infty}^\infty dt\, e^{i(\omega)t} G_{dd}^\sigma(t) \\
&= \frac{1}{Z} \sum_{m,n} || \left\langle m \right| \mathcal{O}_\sigma \left| n \right\rangle ||^2 \left(e^{-\beta E_m} + e^{-\beta E_n} \right) (-i) \int_{-\infty}^\infty dt\, \theta(t) e^{i(\omega + E_m - E_n)t}
\end{aligned}
\tag{B5}
$$

To evaluate the time-integral, we will use the integral representation of the Heaviside function:

$$\theta(t) = -\frac{1}{2\pi i} \lim_{\eta \to 0^+} \int_{-\infty}^\infty \frac{1}{x + i\eta} e^{-ixt} dx \tag{B6}$$

With this definition, the integral in $G_{d\sigma}(\omega)$ becomes

$$
\begin{aligned}
(-i) \int_{-\infty}^\infty dt\, \theta(t) e^{i(\omega + i0^+ + E_m - E_n)t} &= (-i) \frac{-1}{2\pi i} \lim_{\eta \to 0^+} \int_{-\infty}^\infty dx \frac{1}{x + i\eta} \int_{-\infty}^\infty dt\, e^{i(\omega + i0^+ + E_m - E_n - x)t} \\
&= \frac{1}{2\pi} \lim_{\eta \to 0^+} \int_{-\infty}^\infty dx \frac{1}{x + i\eta} 2\pi \delta\left(\omega + i0^+ + E_m - E_n - x \right) \\
&= \frac{1}{\omega + E_m - E_n + i0^+} \, .
\end{aligned}
\tag{B7}
$$

The frequency-domain Green's function is thus

$$G_{dd}^\sigma(\omega) = \frac{1}{Z} \sum_{m,n} || \left\langle m \right| \mathcal{O}_\sigma \left| n \right\rangle ||^2 \left(e^{-\beta E_m} + e^{-\beta E_n} \right) \frac{1}{\omega + E_m - E_n + i0^+} \tag{B8}$$

The infinitesimally positive imaginary part in the denominator shifts the poles onto the lower half of the complex plane, leaving it analytic in the upper half: this is necessary to make the retarded Greens function causal.

2. Real and imaginary parts - The Sokhotski-Plemelj theorem

In order to write down the real and imaginary parts of the Greens function, we first prove the *Sokhotski-Plemelj* formula:

$$\lim_{\eta \to 0^+} \frac{1}{x + i\eta} = P\left(\frac{1}{x}\right) - i\pi\delta(x) \ . \tag{B9}$$

where $P(f(x))$ is the Cauchy principal value, defined as

$$P\left[\int_{-\infty}^{\infty} \frac{dx}{x}\right] = \int_{-\infty}^{0^-} \frac{dx}{x} + \int_{0^+}^{\infty} \frac{dx}{x} \ . \tag{B10}$$

To prove the above identity, we integrate the left-hand side using a test function $f(x)$:

$$\begin{aligned}
\lim_{\eta \to 0^+} \int_{-\infty}^{\infty} dx \, \frac{f(x)}{x + i\eta} &= \lim_{\eta \to 0^+} \int_{-\infty}^{\infty} dx \, \frac{f(x)\,(x - i\eta)}{x^2 + \eta^2} \\
&= \lim_{\eta \to 0^+} \int_{-\infty}^{\infty} dx \, f(x) \left[\frac{x}{x^2 + \eta^2} - i\eta \frac{1}{x^2 + \eta^2}\right]
\end{aligned} \tag{B11}$$

The first integral can be split into three parts:

$$\lim_{\eta \to 0^+} \int_{-\infty}^{\infty} dx \, f(x) \frac{x}{x^2 + \eta^2} = \lim_{\eta \to 0^+} \lim_{\varepsilon \to 0^+} \left[\int_{-\infty}^{-\varepsilon} dx \, \frac{f(x)x}{x^2 + \eta^2} + \int_{\varepsilon}^{\infty} dx \, \frac{f(x)x}{x^2 + \eta^2} + \int_{-\varepsilon}^{\varepsilon} dx \, \frac{f(x)x}{x^2 + \eta^2}\right] \tag{B12}$$

For the first two parts, it is safe to take the limit of η, because x is always non-vanishing there. For the third part, we can approximate $f(x)$ as $f(0)$ in the neighbourhood $x \in [-\varepsilon, \varepsilon], \varepsilon \to 0$. This leaves an odd function $x/(x^2 + \eta^2)$ as the integrand, being integrated over a symmetric range. The third term therefore vanishes. In total, we get

$$\lim_{\eta \to 0^+} \int_{-\infty}^{\infty} dx \, f(x) \frac{x}{x^2 + \eta^2} = \int_{-\infty}^{-\varepsilon} dx \, \frac{f(x)}{x} + \int_{\varepsilon}^{\infty} dx \, \frac{f(x)}{x} = P\left(\int_{-\infty}^{\infty} dx \, \frac{f(x)}{x}\right) \ . \tag{B13}$$

To evaluate the second integral of eq. B11, we note that the only region in which the integrand is non-zero is when $|x| \simeq 0$; there, we again approximate $f(x)$ as $f(0)$. The remaining integral can then be evaluated easily:

$$-i \lim_{\eta \to 0^+} \eta \int_{-\infty}^{\infty} dx \, \frac{f(x)}{x^2 + \eta^2} = -i \lim_{\eta \to 0^+} \eta f(0) \int_{-\infty}^{\infty} \frac{dx}{x^2 + \eta^2} = -i\pi f(0), \tag{B14}$$

where we used $\int \frac{dx}{x^2 + \eta^2} = \frac{1}{\eta} \arctan(x/\eta)$. Combining eqs. B11, B13 and B14, we get

$$\lim_{\eta \to 0^+} \int_{-\infty}^{\infty} dx \, \frac{f(x)}{x + i\eta} = P\left(\int_{-\infty}^{\infty} dx \, \frac{f(x)}{x}\right) - i\pi \int_{-\infty}^{\infty} dx \, f(x)\delta(x) \ . \tag{B15}$$

This proves eq. B9.

The Sokhotski-Plemelj formula allows us to split the spectral representation into a real and an imaginary part:

$$\begin{aligned}
G'_{d\sigma} &= \frac{1}{Z} \sum_{m,n} || \langle m| \mathcal{O}_\sigma |n \rangle ||^2 \left(e^{-\beta E_m} + e^{-\beta E_n}\right) P\left(\frac{1}{\omega + E_m - E_n}\right) \\
G''_{d\sigma} &= -\pi \frac{1}{Z} \sum_{m,n} || \langle m| \mathcal{O}_\sigma |n \rangle ||^2 \left(e^{-\beta E_m} + e^{-\beta E_n}\right) \delta\left(\omega + E_m - E_n\right) \ .
\end{aligned} \tag{B16}$$

The spectral function, specifically, is defined as follows:

$$A_{d\sigma}(\omega) = -\frac{1}{\pi} G'_{d\sigma} = \frac{1}{Z} \sum_{m,n} || \langle m| \mathcal{O}_\sigma |n \rangle ||^2 \left(e^{-\beta E_m} + e^{-\beta E_n}\right) \delta\left(\omega + E_m - E_n\right) \tag{B17}$$

3. Zero temperature spectral function

We specialise to zero temperature by taking the limit of $\beta \to \infty$. In both the partition function as well as inside the summation, the only term that will survive is the exponential of the ground state energy E_{GS}.

$$Z \equiv \sum_m e^{-\beta E_m} \implies \lim_{\beta \to \infty} Z = d_{\mathrm{GS}} e^{-\beta E_{\mathrm{GS}}}, \quad E_{\mathrm{GS}} \equiv \min\{E_n\}$$

where d_{GS} is the degeneracy of the ground state. The spectral function then simplifies to

$$
\begin{aligned}
A_{d\sigma} &= \frac{1}{d_{\mathrm{GS}} e^{-\beta E_{\mathrm{GS}}}} \sum_{m,n} || \langle m | \mathcal{O}_\sigma | n \rangle ||^2 \left[e^{-\beta E_m} \delta_{E_m, E_{\mathrm{GS}}} + e^{-\beta E_n} \delta_{E_n, E_{\mathrm{GS}}} \right] \delta\left(\omega + E_m - E_n\right) \\
&= \frac{1}{d_{\mathrm{GS}}} \sum_{n, n_{\mathrm{GS}}} \left[|| \langle n_{\mathrm{GS}} | \mathcal{O}_\sigma | n \rangle ||^2 \delta\left(\omega + E_{\mathrm{GS}} - E_n\right) + || \langle n | \mathcal{O}_\sigma | n_{\mathrm{GS}} \rangle ||^2 \delta\left(\omega - E_{\mathrm{GS}} + E_n\right) \right]
\end{aligned}
\tag{B18}
$$

The label n_{GS} sums over all states $|n_{\mathrm{GS}}\rangle$ with energy E_{GS}. In practise, we evaluate this expression by replacing the formal Dirac delta functions with "nascent" ones, such as a Lorentzian function with a sufficiently sharp peak.

4. Reconstructing full Green function from spectral function: Kramers-Kronig relations

As mentioned earlier, the retarded Greens function $G_R(\omega + i0^+)$ has a complex pole in the lower half of the complex plane. In the following, the frequency ω is assumed to be complex. Consider the integral

$$I(\omega) = \oint_C d\omega' \frac{G_R(\omega')}{\omega' - \omega}, \quad \omega \in \mathbb{R}. \tag{B19}$$

The contour C encloses the entirety of the upper half of the complex plane as well as almost all points of the real line but avoids the pole at $\omega' = \omega$ by forming a semicircle about that point that extends into the upper half of the plane. Since the integrand is completely analytic in the region enclosed by the contour (recall again that G_R is analytic in the upper half), the integral evaluates to zero (by Cauchy's theorem):

$$I(\omega) = 0. \tag{B20}$$

One can also evaluate the integral along each part of the contour. The semicircular part contributes zero: this is because while the length of the semicircular arc goes as $|\omega'|$, the integrand vanishes faster than $1/|\omega'|$ as $|\omega'| \to \infty$ (this assumes that the Green function vanishes in the limit of $\omega \to \infty$). The part of the contour along the real axis can now be evaluated. The two parts of the contour on either side of the pole contribute

$$\int_{-\infty}^{\omega - 0^+} d\omega' \frac{G_R(\omega')}{\omega' - \omega} + \int_{\omega + 0^+}^{\infty} d\omega' \frac{G_R(\omega')}{\omega' - \omega} = P \int_{-\infty}^{\infty} d\omega' \frac{G_R(\omega')}{\omega' - \omega} \tag{B21}$$

To evaluate the part of the integral along the small semicircular around $\omega' = \omega$ (that extends into the upper half), we argue that this contribution should be equal to that obtained by taking the semicircle that goes instead into the lower half but circulates in the opposite direction. Each of these contributions should, in turn, be equal to that obtained from joining these two contours. But joining these contours leads to a closed integral about the pole at $\omega' = \omega$, which is equal to $2\pi G_R(\omega)$.

$$\int_{\mathrm{upper}} d\omega' \frac{G_R(\omega')}{\omega' - \omega} = \int_{\mathrm{lower}} d\omega' \frac{G_R(\omega')}{\omega' - \omega} = \frac{1}{2} \oint_{C(\omega)} d\omega' \frac{G_R(\omega')}{\omega' - \omega} = i\pi G_R(\omega). \tag{B22}$$

Combining the last two equations, we get

$$I(\omega) = P \int_{-\infty}^{\infty} d\omega' \frac{G_R(\omega')}{\omega' - \omega} + i\pi G_R(\omega). \tag{B23}$$

Comparing with eq. B20 and separating into real part G_R' and imaginary part G_R'' gives

$$P \int_{-\infty}^{\infty} d\omega' \frac{[G_R'(\omega') + iG_R''(\omega')]}{\omega' - \omega} + \pi \left[-G_R''(\omega) + iG_R'(\omega)\right] = 0. \tag{B24}$$

Comparing the imaginary parts gives

$$G'_R(\omega) = \frac{1}{\pi} P \int_{-\infty}^{\infty} d\omega' \frac{G''_R(\omega')}{\omega' - \omega} = -\mathcal{H}[G''_R(\omega)] , \tag{B25}$$

where $\mathcal{H}[g(\omega)] = \frac{1}{\pi} P \int_{-\infty}^{\infty} d\omega' \frac{g(\omega')}{\omega - \omega'}$ is the Hilbert transform of the function $g(\omega)$. The spectral function was defined above as $-1/\pi$ times the imaginary part of the Greens function. Exchanging G''_R for A gives

$$G'_R(\omega) = \pi \mathcal{H}[A(\omega)] . \tag{B26}$$

This provides a method for calculating the real part of a Greens function if the spectral function is already known.

Appendix C: Properties of the Bloch states

1. Translation invariance

It is easy to verify that $\Psi_{\vec{k}}(\{\mathbf{r}_k\})$ transforms like Bloch functions under translation by a displacement $\mathbf{r}$:

$$\Psi_{\vec{k}}(\{\mathbf{r}_k + \mathbf{r}\}) = \frac{1}{\lambda_{|\vec{k}\rangle} \mathcal{Z}N} \sum_{\mathbf{r}_i, \mathbf{a}} e^{i\vec{k}\cdot\vec{R}_i} \psi_{\text{aux}}(\mathbf{r}_i - \mathbf{r}, \mathbf{a}) = \frac{1}{\lambda_{|\vec{k}\rangle} \mathcal{Z}N} \sum_{\mathbf{r}_j, \mathbf{a}} e^{i\vec{k}\cdot(\vec{R}_j + \mathbf{r})} \psi_{\text{aux}}(\mathbf{r}_j, \mathbf{a}) = e^{i\vec{k}\cdot\vec{R}} \Psi_{\vec{k}}(\{\mathbf{r}_k\}) \tag{C1}$$

In the last equation, we transformed $\mathbf{r}_i \to \mathbf{r}_j = \mathbf{r}_i - \mathbf{r}$. Note that the argument $\mathbf{a}$ does not change under a translation of the system, because that vector always represents the difference between the impurity lattice position and its nearest neighbours, irrespective of the absolute position of the impurity.

The wavefunction can be even brought into the familiar Bloch function form:

$$\Psi_{\vec{k}}^n(\{\mathbf{r}_k\}) = \sum_{\mathbf{r}_i, \mathbf{a}} \frac{e^{i\vec{k}\cdot\vec{R}_i}}{\lambda_{|\vec{k}\rangle} \mathcal{Z}N} \psi_{\text{aux}}(\{\mathbf{r}_d - \mathbf{r}_i, \mathbf{r}_0 - \mathbf{r}_i - \mathbf{a}\}) = \frac{e^{i\vec{k}\cdot\frac{1}{N}\sum_k \vec{r}_k}}{\lambda_{|\vec{k}\rangle} \mathcal{Z}N} \sum_{\mathbf{r}_i, \mathbf{a}} e^{-i\vec{k}\cdot(\frac{1}{N}\sum_k \mathbf{r}_k - \vec{R}_i)} \psi_{\text{aux}}(\{\mathbf{r}_d - \mathbf{r}_i, \mathbf{r}_0 - \mathbf{r}_i - \mathbf{a}\})$$

$$= e^{i\vec{k}\cdot\vec{r}_{\text{COM}}} \eta_{\vec{k}}(\{\mathbf{r}_k\}) \tag{C2}$$

where $\mathbf{r}_{\text{COM}} = \frac{1}{N}\sum_k \mathbf{r}_k$ is the center-of-mass coordinate and $\eta_{\vec{k}}(\{\mathbf{r}_k\}) = \frac{1}{\lambda_{|\vec{k}\rangle} \mathcal{Z}N} \sum_{\mathbf{r}_i} e^{-i\vec{k}\cdot(\frac{1}{N}\sum_k \mathbf{r}_k - \vec{R}_i)} \psi_{\text{aux}}^n(\{\mathbf{r}_k - \mathbf{r}_i\})$ is the translation symmetric function. This form of the eigenstate allows the interpretation that tuning the Bloch momentum $\vec{k}$ corresponds to a translation of the center of mass of the system (or in this case, of the auxiliary models that comprise the system).

2. Orthonormality

It is straightforward to show that these states form an orthonormal basis. We start by writing down the inner product of two distinct such states:

$$\langle \Psi_{\vec{k}'} | \Psi_{\vec{k}} \rangle = \frac{1}{\lambda_{|\vec{k}'\rangle}^* \lambda_{|\vec{k}\rangle} \mathcal{Z}^2 N^2} \sum_{\mathbf{r}_i, \mathbf{r}_j, \mathbf{a}, \mathbf{a}'} e^{i(\vec{k}\cdot\vec{R}_i - \vec{k}'\cdot\vec{R}_j)} \langle \psi_{\text{aux}}(\mathbf{r}_j, \mathbf{a}') | \psi_{\text{aux}}(\mathbf{r}_i, \mathbf{a}) \rangle$$

$$= \frac{1}{\lambda_{|\vec{k}'\rangle}^* \lambda_{|\vec{k}\rangle} \mathcal{Z}^2 N^2} \sum_{\mathbf{r}_i, \mathbf{r}_j, \mathbf{a}, \mathbf{a}'} e^{i(\vec{k}\cdot\vec{R}_i - \vec{k}'\cdot\vec{R}_j)} \langle \psi_{\text{aux}}(\mathbf{r_0}, \mathbf{a}') T^\dagger(\mathbf{r_0} - \mathbf{r}_j) T(\mathbf{r_0} - \mathbf{r}_i) | \psi_{\text{aux}}(\mathbf{r_0}, \mathbf{a}) \rangle \tag{C3}$$

At this point, we insert a complete basis of momentum eigenkets $1 = \sum_{\vec{q}} |\vec{q}\rangle \langle\vec{q}|$ to resolve the translation operators:

$$\langle \Psi_{\vec{k}'} | \Psi_{\vec{k}} \rangle = \frac{1}{\lambda_{|\vec{k}'\rangle}^* \lambda_{|\vec{k}\rangle} \mathcal{Z}^2 N^2} \sum_{\mathbf{r}_i, \mathbf{r}_j, \mathbf{a}, \mathbf{a}', \vec{q}} e^{i(\vec{k}\cdot\vec{R}_i - \vec{k}'\cdot\vec{R}_j)} \langle \psi_{\text{aux}}(\mathbf{r_0}, \mathbf{a}') T(\mathbf{r}_j - \mathbf{r}_i) | \vec{q}\rangle \langle\vec{q}| \psi_{\text{aux}}(\mathbf{r_0}, \mathbf{a}) \rangle$$

$$= \frac{1}{\lambda_{|\vec{k}'\rangle}^* \lambda_{|\vec{k}\rangle} \mathcal{Z}^2 N^2} \sum_{\mathbf{r}_i, \mathbf{r}_j, \mathbf{a}, \mathbf{a}', \vec{q}} e^{i(\vec{k}\cdot\vec{R}_i - \vec{k}'\cdot\vec{R}_j)} \langle \psi_{\text{aux}}(\mathbf{r_0}, \mathbf{a}') e^{i\vec{q}\cdot(\mathbf{r}_j - \mathbf{r}_i)} | \vec{q}\rangle \langle\vec{q}| \psi_{\text{aux}}(\mathbf{r_0}, \mathbf{a}) \rangle \tag{C4}$$

$$= \frac{1}{|\lambda_{|\vec{k}\rangle}|^2 \mathcal{Z}^2} \delta_{\vec{k}, \vec{k}'} \sum_{\mathbf{a}, \mathbf{a}'} \langle \psi_{\text{aux}}(\mathbf{r_0}, \mathbf{a}') | \vec{k}\rangle \langle\vec{k}| \psi_{\text{aux}}(\mathbf{r_0}, \mathbf{a}) \rangle$$

At the last step, we used the summation form of the Kronecker delta function: $\sum_{\mathbf{r}_i} e^{i\mathbf{r}_i(\vec{k}-\vec{q})} \sum_{\mathbf{r}_j} e^{i\mathbf{r}_j(\vec{q}-\vec{k}')} = N\delta_{\vec{k},\vec{q}}N\delta_{\vec{k}',\vec{q}}$. The final remaining step is to identify that the inner products inside the summation are actually independent of the direction $\mathbf{a}, \mathbf{a}'$ of the connecting vector, and both are equal to the normalisation factor $\lambda_{|\vec{k}\rangle}$:

$$\langle \Psi_{\vec{k}'} | \Psi_{\vec{k}} \rangle = \frac{1}{|\lambda_{|\vec{k}\rangle}|^2 \mathcal{Z}^2} \delta_{\vec{k},\vec{k}'} \sum_{\mathbf{a},\mathbf{a}'} |\lambda_{|\vec{k}\rangle}|^2 = \frac{1}{|\lambda_{|\vec{k}\rangle}|^2 \mathcal{Z}^2} \delta_{\vec{k},\vec{k}'} w^2 |\lambda_{|\vec{k}\rangle}|^2 = \delta_{\vec{k},\vec{k}'} \tag{C5}$$

This concludes the proof of orthonormality.

3. Eigenstates

To demonstrate that these are indeed eigenstates of the bulk Hamiltonian, we will calculate the matrix elements of the full Hamiltonian between these states:

$$\langle \Psi_{\vec{k}'} | H_{\text{H-H}} | \Psi_{\vec{k}} \rangle = \frac{1}{\lambda_{|\vec{k}'\rangle}^* \lambda_{|\vec{k}\rangle} \mathcal{Z}^2 N^2} \sum_{\mathbf{r}_i,\mathbf{r}_j,\mathbf{r}_k,\mathbf{a},\mathbf{a}'} e^{i(\vec{k}\cdot\vec{R}_i - \vec{k}'\cdot\vec{R}_j)} \langle \psi_{\text{aux}}(\mathbf{r}_j,\mathbf{a}') | H_{\text{aux}}(\mathbf{r}_k) | \psi_{\text{aux}}(\mathbf{r}_i,\mathbf{a}) \rangle$$

$$= \frac{1}{\lambda_{|\vec{k}'\rangle}^* \lambda_{|\vec{k}\rangle} \mathcal{Z}^2 N^2} \sum_{\mathbf{r}_i,\mathbf{r}_j,\mathbf{r}_k,\mathbf{a},\mathbf{a}'} e^{i(\vec{k}\cdot\vec{R}_i - \vec{k}'\cdot\vec{R}_j)} \langle \psi_{\text{aux}}(\mathbf{r_0},\mathbf{a}') | T_{\mathbf{r_0}-\mathbf{r}_j}^\dagger T_{\mathbf{r_0}-\mathbf{r}_k} H_{\text{aux}}(\mathbf{r_0}) T_{\mathbf{r_0}-\mathbf{r}_k}^\dagger T_{\mathbf{r_0}-\mathbf{r}_i} | \psi_{\text{aux}}(\mathbf{r_0},\mathbf{a}) \rangle \tag{C6}$$

$$= \frac{1}{\lambda_{|\vec{k}'\rangle}^* \lambda_{|\vec{k}\rangle} \mathcal{Z}^2 N^2} \sum_{\mathbf{r}_i,\mathbf{r}_j,\mathbf{r}_k,\mathbf{a},\mathbf{a}'} e^{i(\vec{k}\cdot\vec{R}_i - \vec{k}'\cdot\vec{R}_j)} \langle \psi_{\text{aux}}(\mathbf{r_0},\mathbf{a}') | T_{\mathbf{r}_k-\mathbf{r}_j}^\dagger H_{\text{aux}}(\mathbf{r_0}) T_{\mathbf{r}_k-\mathbf{r}_i} | \psi_{\text{aux}}(\mathbf{r_0},\mathbf{a}) \rangle$$

To resolve the translation operators, we will now insert the momentum eigenstates $|\vec{k}\rangle$ of the full model: $1 = \sum_{\vec{q}} |\vec{q}\rangle \langle \vec{q}|$ in between the operators.

$$\langle \Psi_{\vec{k}'} | H_{\text{H-H}} | \Psi_{\vec{k}} \rangle = \sum_{\substack{\mathbf{r}_i,\mathbf{r}_j,\mathbf{r}_k, \\ \mathbf{a},\mathbf{a}',\vec{q},\vec{q}'}} \frac{e^{i(\vec{k}\cdot\vec{R}_i - \vec{k}'\cdot\vec{R}_j)}}{\lambda_{|\vec{k}'\rangle}^* \lambda_{|\vec{k}\rangle} \mathcal{Z}^2 N^2} \langle \psi_{\text{aux}}(\mathbf{r_0},\mathbf{a}') | \vec{q}'\rangle \langle \vec{q}' | T_{\mathbf{r}_k-\mathbf{r}_j}^\dagger H_{\text{aux}}(\mathbf{r_0}) T_{\mathbf{r}_k-\mathbf{r}_i} | \vec{q}\rangle \langle \vec{q} | \psi_{\text{aux}}(\mathbf{r_0},\mathbf{a}) \rangle$$

$$= \sum_{\substack{\mathbf{r}_i,\mathbf{r}_j,\mathbf{r}_k, \\ \mathbf{a},\mathbf{a}',\vec{q},\vec{q}'}} \frac{e^{i(\vec{k}\cdot\vec{R}_i - \vec{k}'\cdot\vec{R}_j)}}{\lambda_{|\vec{k}'\rangle}^* \lambda_{|\vec{k}\rangle} \mathcal{Z}^2 N^2} \langle \psi_{\text{aux}}(\mathbf{r_0},\mathbf{a}') | \vec{q}'\rangle e^{-i\vec{q}'\cdot(\mathbf{r}_k-\mathbf{r}_j)} e^{i\vec{q}\cdot(\mathbf{r}_k-\mathbf{r}_i)} \langle \vec{q}' | H_{\text{aux}}(\mathbf{r_0}) | \vec{q}\rangle \langle \vec{q} | \psi_{\text{aux}}(\mathbf{r_0},\mathbf{a}) \rangle$$

$$= \frac{N}{\lambda_{|\vec{k}'\rangle}^* \lambda_{|\vec{k}\rangle} \mathcal{Z}^2} \sum_{\mathbf{a},\mathbf{a}',\vec{q},\vec{q}'} \delta_{\vec{k},\vec{q}} \delta_{\vec{q},\vec{q}'} \delta_{\vec{q}',\vec{k}} \langle \psi_{\text{aux}}(\mathbf{r_0},\mathbf{a}') | \vec{q}'\rangle \langle \vec{q}' | H_{\text{aux}}(\mathbf{r_0}) | \vec{q}\rangle \langle \vec{q} | \psi_{\text{aux}}(\mathbf{r_0},\mathbf{a}) \rangle$$

$$= \frac{N}{|\lambda_{|\vec{k}\rangle}|^2 \mathcal{Z}^2} \delta_{kk'} \sum_{\mathbf{a},\mathbf{a}'} \langle \psi_{\text{aux}}(\mathbf{r_0},\mathbf{a}') | \vec{k}\rangle \langle \vec{k} | H_{\text{aux}}(\mathbf{r_0}) | \vec{k}\rangle \langle \vec{k} | \psi_{\text{aux}}(\mathbf{r_0},\mathbf{a}) \rangle$$

$$= \frac{N}{|\lambda_{|\vec{k}\rangle}|^2 \mathcal{Z}^2} \delta_{kk'} \langle \vec{k} | H_{\text{aux}}(\mathbf{r_0}) | \vec{k}\rangle \underbrace{\sum_{\mathbf{a},\mathbf{a}'} \langle \psi_{\text{aux}}(\mathbf{r_0},\mathbf{a}') | \vec{k}\rangle \langle \vec{k} | \psi_{\text{aux}}(\mathbf{r_0},\mathbf{a}) \rangle}_{w^2 |\lambda_{|\vec{k}\rangle}|^2}$$

$$= N\delta_{kk'} \langle \vec{k} | H_{\text{aux}}(\mathbf{r_0}) | \vec{k}\rangle \tag{C7}$$

The momentum eigenket $|\vec{k}\rangle$ can be expressed as a sum over position eigenkets at varying distances from $\mathbf{r_0}$. This form allows a systematic method of improving the energy eigenvalue estimate, because the interacting in the impurity model is extremely localised, so the overlap between two auxiliary models decreases rapidly with distance. The majority of the contribution will come from the state at $\mathbf{r_0}$, and improvements are then made by considering auxiliary models at further distances.

Appendix D: Greens function in the insulating phase: the Hubbard bands and mottness

In the insulating state, the cluster becomes a local moment and the bulk system reduces to the atomic limit $H = -\frac{U}{2} \sum_i (\hat{n}_{i\uparrow} - \hat{n}_{i\downarrow})^2$. The Greens function in this limit is that of the atomic limit of the Hubbard model:

$$G_i(\omega) = \sum_\sigma G_{i,\sigma}(\omega) = \frac{1 + \langle \tau_i \rangle}{\omega - \frac{U}{2}} + \frac{1 - \langle \tau_i \rangle}{\omega + \frac{U}{2}} \tag{D1}$$

where $\tau_i = \sum_\sigma \hat{n}_{i,\sigma} - 1$. At half-filling $\langle \tau_i \rangle = 0$, the low and high-energy poles have equal spectral weights. *This is different from the situation in a band insulator, where the valence band has all the spectral weight in the ground state while the conduction band is empty.* On doping holes into the system such that $\langle \tau_i \rangle = -x < 0$, spectral weight is transferred from the upper Hubbard band at $\omega = U/2$ to the lower one at $\omega = -U/2$:

$$G_i(\omega) = \sum_\sigma G_{i,\sigma}(\omega) = \frac{1 - x}{\omega - \frac{U}{2}} + \frac{1 + x}{\omega + \frac{U}{2}} \tag{D2}$$

This transfer of spectral weight across energy scales of the order of U, as well as the lack of poles at zero energies, is referred to as mottness [35].
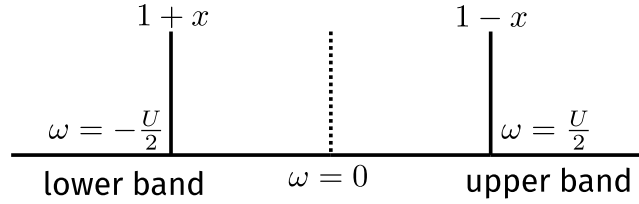

FIG. 15. Structure of the Greens function in the atomic limit. The two poles at $\omega = \pm\frac{U}{2}$ form the two Hubbard bands. Doping the system leads to transfer of spectral weight between the bands.

Appendix E: Nature of propagation: metal vs insulator

In the metallic state, the impurity in the auxiliary model hybridises with the bath through both 1-particle and 2-particle interactions. For any two auxiliary models differing by the locations i_1, i_2 of the impurity, the baths will always overlap. This means that an electron that starts out from the impurity site at i_1 can hop into the bath, and eventually reach i_2 by hopping out of the other bath and into the other impurity. Such processes connect all sites of the lattice and *allow spectral flow*.

In the insulating state, each auxiliary model separates into an impurity and a bath that decoupled from each other. This means that the impurity cannot hybridise into the bath, and hence cannot tunnel into any other impurity. This leads to the atomic limit of the system, where each site develops a local moment configuration because of the repulsive local correlation, but these local moments cannot communicate with each other, either through spin-exchange processes or by breaking into holons and doublons. Any attempt at spectral flow fails because the boundaries of the system become disconnected from each other.

A more accurate picture of the insulating and metallic phases can be obtained by working with a more complicated choice of the cluster. For instance, instead of a single impurity, one can take two correlated impurities interacting with each other through a single-particle hopping, and this cluster then interacts with the bath through the usual interactions. The ground state of such a cluster is actually a quantum liquid, consisting of the entangled spin and charge degrees of freedom. In the metallic state, various members of this liquid such as the holons, doublons and the spinons are free to propagate across the system through the baths. In the insulating state, it is this cluster that then gets decoupled from the other clusters. The composite degrees of freedom are then unable to propagate outside the cluster, and *the holons and the doublons are bound to each other* [1] within the confines of the cluster.
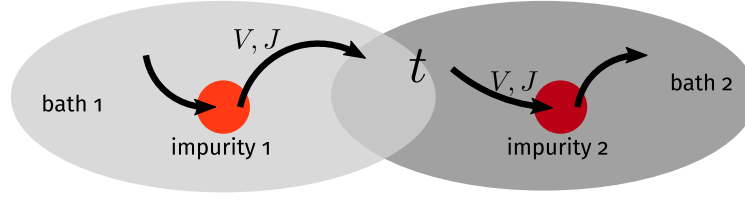
FIG. 16. Propagation of electrons from one cluster to another through the bath, in the metallic state
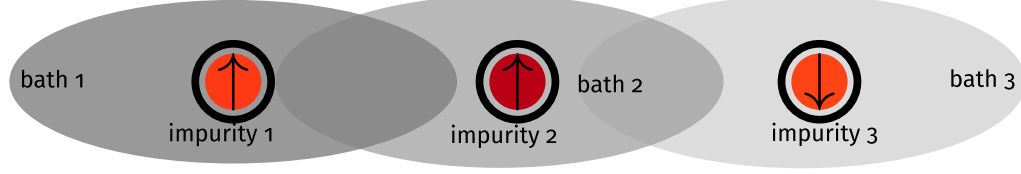

FIG. 17. The clusters get isolated from each other in the insulator, because they get decoupled from their baths.
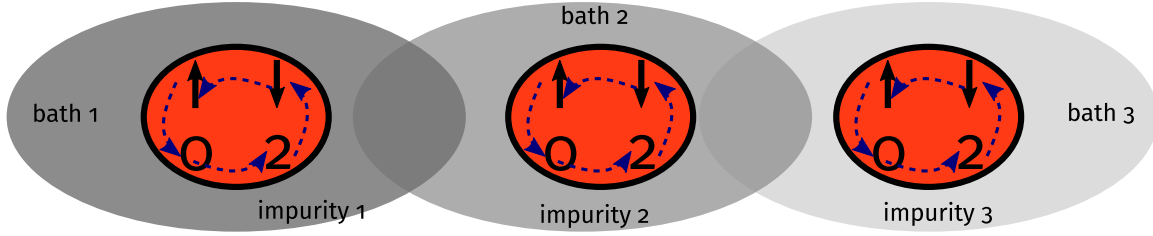

FIG. 18. Each cluster is a quantum liquid composed of spin $(\uparrow, \downarrow)$ and charge $(0, 2)$ degrees of freedom. In the insulating state, these degrees of freedom get bound within the cluster and are unable to propagate outside.

Appendix F: Presence of two self-energies under symmetry-breaking

The effective Hamiltonian that describes either the metallic or the insulating phase has SU(2) symmetry in both the spin and charge sectors. Since the repulsive correlation on the impurity picks out the spin sector, we focus on that for now. Applying a small magnetic field on the impurity breaks this spin-rotation symmetry and picks out either the up or the down state on the impurity, leading to two kinds of self-energies, one for each spin state [36, 37]. The Hamiltonian has the form $H(h)_i = -\frac{U}{2} \left(\hat{n}_{i\uparrow} - \hat{n}_{i\downarrow} \right)^2 - h \left(\hat{n}_{i\uparrow} - \hat{n}_{i\downarrow} \right)$. The unique ground-state is $|\hat{n}_{i,\sigma=\text{sgn}(h)} = 1, \hat{n}_{i,\sigma=-\text{sgn}(h)} = 0\rangle$, with an energy of $E_{\text{gs}} = -\frac{U}{2} - h$. The Greens function is easiest to obtain from the Lehmann-Kallen representation (eq. B18):

$$G_{i,\sigma} = \sum_n \left[|| \langle \text{GS} | c_{i\sigma} | n \rangle ||^2 \frac{1}{\omega + E_{\text{GS}} - E_n} + || \langle n | c_{i\sigma} | \text{GS} \rangle ||^2 \frac{1}{\omega - E_{\text{GS}} + E_n} \right] \tag{F1}$$

We have $c_{i,\sigma} | \text{GS} \rangle = | \hat{n}_i = 0 \rangle \delta_{\sigma, \text{sgn}(h)}$ and $c_{i,\sigma}^\dagger | \text{GS} \rangle = | \hat{n}_i = 2 \rangle \delta_{\sigma, -\text{sgn}(h)}$, so that the only excited states that give non-zero inner product is $|n\rangle = | \hat{n}_i = 0 \rangle$ for the second term and $|n\rangle = | \hat{n}_i = 2 \rangle$ for the first term, with energies $E_n = 0$. Substituting these, we get

$$G_{i,\sigma}(h) = \frac{\delta_{\sigma, -\text{sgn}(h)}}{\omega - \frac{U}{2} - h} + \frac{\delta_{\sigma, \text{sgn}(h)}}{\omega + \frac{U}{2} + h} = \frac{1}{\omega + \left(\frac{U}{2} + h \right) \sigma \times \text{sgn}(h)} \tag{F2}$$

Taking the limit of $h \to 0^\pm$ then gives

$$G_{i,\sigma}(h = 0^\pm) = \frac{1}{\omega \pm \frac{U}{2} \sigma} \tag{F3}$$

The self-energies arising from the correlation U can also be obtained using Dyson's equation $\Sigma = G^{-1} - G_0^{-1}$, where $G_0^{-1} = \omega$ is the Greens function at $U = 0$. Using Dyson's equation, we get

$$\Sigma_{i,\sigma} = \pm \frac{U}{2} \sigma \tag{F4}$$

Appendix G: Derivation of RG equations for the embedded e-SIAM

1. RG scheme

At any given step j of the RG procedure, we decouple the states $\{\mathbf{q}\}$ on the isoenergetic surface of energy ε_j. The diagonal Hamiltonian H_D for this step consists of all terms that do not change the occupancy of the states $\{\mathbf{q}\}$:

$$H_D^{(j)} = \varepsilon_j \sum_{q,\sigma} \tau_{q,\sigma} + \frac{1}{2} \sum_{\mathbf{q}} J_{\mathbf{q},\mathbf{q}} S_d^z \left(\hat{n}_{\mathbf{q},\uparrow} - \hat{n}_{\mathbf{q},\downarrow}\right) - \frac{1}{2} \sum_{\mathbf{q}} W_{\mathbf{q}} \left(\hat{n}_{\mathbf{q},\uparrow} - \hat{n}_{\mathbf{q},\downarrow}\right)^2 , \tag{G1}$$

where $\tau = \hat{n} - 1/2$ and $W_{\mathbf{q}}$ is a shorthand for $W_{\mathbf{q},\mathbf{q},\mathbf{q},\mathbf{q}}$. The three terms, respectively, are the kinetic energy of the momentum states on the isoenergetic shell that we are decoupling, the spin-correlation energy between the impurity spin and the spins formed by these momentum states and, finally, the local correlation energy associated with these states arising from the W term. The off-diagonal part of the Hamiltonian on the other hand leads to scattering in the states $\{\mathbf{q}\}$. We now list these terms, classified by the coupling they originate from.

Arising from the Kondo spin-exchange term

$$T_{KZ1}^\dagger + T_{KZ1} = \frac{1}{2} \sum_{\mathbf{k},\mathbf{q},\sigma} \sigma J_{\mathbf{k},\mathbf{q}} S_d^z \left[c_{\mathbf{q}\sigma}^\dagger c_{\mathbf{k},\sigma} + \text{h.c.} \right],$$

$$T_{KZ2}^\dagger + T_{KZ2} = \frac{1}{2} \sum_{\mathbf{q},\sigma} \sigma J_{\mathbf{q},\bar{\mathbf{q}}} S_d^z \left[c_{\mathbf{q}\sigma}^\dagger c_{\bar{\mathbf{q}},\sigma} + \text{h.c.} \right],$$

$$T_{KT1}^\dagger + T_{KT1} = \frac{1}{2} \sum_{\mathbf{k},\mathbf{q}} J_{\mathbf{k},\mathbf{q}} \left[S_d^+ \left(c_{\mathbf{q}\downarrow}^\dagger c_{\mathbf{k}\uparrow} + c_{\mathbf{k}\downarrow}^\dagger c_{\mathbf{q}\uparrow} \right) + \text{h.c.} \right],$$

$$T_{KT2}^\dagger + T_{KT2} = \frac{1}{2} \sum_{\mathbf{q}} J_{\mathbf{q},\bar{\mathbf{q}}} \left[S_d^+ \left(c_{\mathbf{q}\downarrow}^\dagger c_{\bar{\mathbf{q}}\uparrow} + c_{\bar{\mathbf{q}}\downarrow}^\dagger c_{\mathbf{q}\uparrow} \right) + \text{h.c.} \right],$$

$$\tag{G2}$$

Arising from spin-preserving scattering within conduction bath

$$T_{P1}^\dagger + T_{P1} = -\sum_{\mathbf{q}\in\varepsilon_j} \sum_{\mathbf{k}_2,\mathbf{k}_3,\mathbf{k}_4<\varepsilon_j} \sum_{\sigma} \left[W_{\mathbf{q},\mathbf{k}_2,\mathbf{k}_3,\mathbf{k}_4} c_{\mathbf{q},\sigma}^\dagger c_{\mathbf{k}_2,\sigma} c_{\mathbf{k}_3,\sigma}^\dagger c_{\mathbf{k}_4,\sigma} + \text{h.c.} \right]$$

$$T_{P2}^\dagger + T_{P3} = -\sum_{\mathbf{q}\in\varepsilon_j} \sum_{\mathbf{k}_2<\varepsilon_j} \sum_{\sigma} W_{\mathbf{q},\mathbf{k}_2,\bar{\mathbf{q}},\bar{\mathbf{q}}} c_{\mathbf{q},\sigma}^\dagger c_{\mathbf{k}_2,\sigma} n_{\bar{\mathbf{q}},\sigma} - \sum_{\mathbf{q}\in\varepsilon_j} \sum_{\mathbf{k}_1<\varepsilon_j} \sum_{\sigma} W_{\mathbf{k}_1,\mathbf{q},\mathbf{q},\mathbf{q}} c_{\mathbf{k}_1,\sigma}^\dagger c_{\mathbf{q},\sigma} n_{\mathbf{q},\sigma}$$

$$T_{P4} = -\sum_{\mathbf{q}\in\varepsilon_j} \sum_{\mathbf{k}_2,\mathbf{k}_3<\varepsilon_j} \sum_{\sigma} W_{\mathbf{q},\bar{\mathbf{q}},\mathbf{k}_2,\mathbf{k}_3} c_{\mathbf{q},\sigma}^\dagger c_{\bar{\mathbf{q}},\sigma} c_{\mathbf{k}_2,\sigma}^\dagger c_{\mathbf{k}_3,\sigma}$$

$$T_{P5} = -\sum_{\mathbf{q}\in\varepsilon_j} \sum_{\mathbf{k}_2,\mathbf{k}_3<\varepsilon_j} \sum_{\sigma} W_{\mathbf{q},\mathbf{k}_2,\mathbf{k}_3,\bar{\mathbf{q}}} c_{\mathbf{q},\sigma}^\dagger c_{\mathbf{k}_2,\sigma} c_{\mathbf{k}_3,\sigma}^\dagger c_{\bar{\mathbf{q}},\sigma}$$

$$\tag{G3}$$

$$= +\sum_{\mathbf{q}\in\varepsilon_j} \sum_{\mathbf{k}_2,\mathbf{k}_3<\varepsilon_j} \sum_{\sigma} W_{\mathbf{q},\mathbf{k}_3,\mathbf{k}_2,\bar{\mathbf{q}}} c_{\mathbf{q},\sigma}^\dagger c_{\bar{\mathbf{q}},\sigma} c_{\mathbf{k}_2,\sigma}^\dagger c_{\mathbf{k}_3,\sigma}$$

$$= -T_{P4}$$

Arising from spin-flip scattering within conduction bath

$$T_{F1}^\dagger + T_{F1} = \sum_{\mathbf{q}\in\varepsilon_j} \sum_{\mathbf{k}_2,\mathbf{k}_3,\mathbf{k}_4<\varepsilon_j} \sum_\sigma \left[W_{\mathbf{q},\mathbf{k}_2,\mathbf{k}_3,\mathbf{k}_4} c_{\mathbf{q},\sigma}^\dagger c_{\mathbf{k}_2,\sigma} c_{\mathbf{k}_3,\bar\sigma}^\dagger c_{\mathbf{k}_4,\bar\sigma} + \text{h.c.} \right]$$

$$T_{F2} = \sum_{\mathbf{q},\mathbf{q}'\in\varepsilon_j} \sum_{\mathbf{k}_2,\mathbf{k}_3<\varepsilon_j} \sum_\sigma W_{\mathbf{q},\mathbf{q}',\mathbf{k}_2,\mathbf{k}_3} c_{\mathbf{q},\sigma}^\dagger c_{\mathbf{q}',\sigma} c_{\mathbf{k}_2,\bar\sigma}^\dagger c_{\mathbf{k}_3,\bar\sigma}$$

$$T_{F3} = \sum_{\mathbf{q},\mathbf{q}'\in\varepsilon_j} \sum_{\mathbf{k}_2,\mathbf{k}_3<\varepsilon_j} \sum_\sigma W_{\mathbf{q},\mathbf{k}_2,\mathbf{k}_3,\mathbf{q}'} c_{\mathbf{q},\sigma}^\dagger c_{\mathbf{k}_2,\sigma} c_{\mathbf{k}_3,\bar\sigma}^\dagger c_{\mathbf{q}',\bar\sigma}$$

$$T_{F4}^\dagger + T_{F4} = \sum_{\mathbf{q},\mathbf{q}',\in\varepsilon_j} \sum_{\mathbf{k}_1<\varepsilon_j} \sum_\sigma \left[W_{\mathbf{q},\mathbf{q},\mathbf{q}',\mathbf{k}_1} n_{\mathbf{q},\sigma} c_{\mathbf{q}',\bar\sigma}^\dagger c_{\mathbf{k}_1,\bar\sigma} + \text{h.c.} \right]$$

$$(\text{G4})$$

In all of the terms $T_{P[i]}$ and $T_{F[i]}$, the factor of $1/2$ in front has been cancelled out by a factor of 2 coming from the multiple possibilities of arranging the momentum labels. We will henceforth ignore T_{P4} and T_{P5} because they cancel each other out.

The renormalisation of the Hamiltonian is constructed from the general expression

$$\Delta H^{(j)} = H_X \frac{1}{\omega - H_D} H_X \ . \tag{G5}$$

The states on the isoenergetic shell $\pm|\varepsilon_j|$ come in particle-hole pairs $(\mathbf{q},\bar{\mathbf{q}})$ with energies of opposite signs (relative to the Fermi energy). If $\mathbf{q}$ is defined as the hole state (unoccupied in the absence of quantum fluctuations), it will have positive energy, while the particle state $\bar{\mathbf{q}}$ will be of negative energy and hence below the Fermi surface. To be more specific, given a state $\mathbf{q}$ with energy $\pm|\varepsilon_j|$, we define its particle-hole transformed counterpart as the state $\bar{\mathbf{q}} = \boldsymbol{\pi} + \mathbf{q}$, having energy $\mp|\varepsilon_j|$ and residing in the opposite quadrant of the Brillouin zone. Given this definition, we have the important property that

$$J_{\mathbf{k},\bar{\mathbf{q}}} = -J_{\mathbf{k},\mathbf{q}},$$
$$W_{\{\mathbf{k}\},\bar{\mathbf{q}}} = -W_{\{\mathbf{k}\},\mathbf{q}} \ . \tag{G6}$$
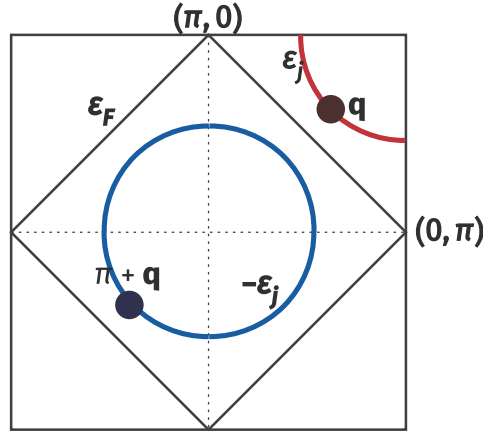

FIG. 19. Particle and hole states.

2. Renormalisation of the bath correlation term W

The bath correlation term W can undergo renormalisation only via scattering processes arising from itself. Irrespective of whether the state $\mathbf{q}$ being decoupled is in a particle or hole configuration in the initial many-body state, the propagator $G = 1/(\omega - H_D)$ of the intermediate excited state is uniform, and equal to

$$G_W = 1/\left(\omega - |\varepsilon_j|/2 + W_\mathbf{q}/2\right) \ , \tag{G7}$$

where $W_\mathbf{q}$ is the same whether $\mathbf{q}$ is above or below the Fermi surface. The $|\varepsilon_j|/2$ in H_D arises from the excited nature of the state after the initial scattering process.

Scattering arising purely from spin-preserving processes

In this subsection, we calculate the renormalisation to W arising from the terms T_{P1}, T_{P2} and T_{P3}. The first term is

$$
\begin{aligned}
T_{P1}^\dagger G_W T_{P3} &= \sum_\sigma \sum_{\mathbf{k}_1,\mathbf{k}_2,\mathbf{k}_3,\mathbf{k}_4} \sum_{\mathbf{q}} W_{\mathbf{q},\mathbf{k}_2,\mathbf{k}_3,\mathbf{k}_4} c_{\mathbf{q},\sigma}^\dagger c_{\mathbf{k}_2,\sigma} c_{\mathbf{k}_3,\sigma}^\dagger c_{\mathbf{k}_4,\sigma} G_W W_{\mathbf{k}_1,\mathbf{q},\mathbf{q},\mathbf{q}} c_{\mathbf{k}_1,\sigma}^\dagger c_{\mathbf{q},\sigma} n_{\mathbf{q},\sigma} \\
&= -\sum_\sigma \sum_{\mathbf{k}_1,\mathbf{k}_2,\mathbf{k}_3,\mathbf{k}_4} c_{\mathbf{k}_1,\sigma}^\dagger c_{\mathbf{k}_2,\sigma} c_{\mathbf{k}_3,\sigma}^\dagger c_{\mathbf{k}_4,\sigma} \sum_{\mathbf{q}\in\mathrm{PS}} W_{\mathbf{q},\mathbf{k}_2,\mathbf{k}_3,\mathbf{k}_4} G_W W_{\mathbf{k}_1,\mathbf{q},\mathbf{q},\mathbf{q}} \ .
\end{aligned}
\tag{G8}
$$

The operators acting on the states being decoupled contract to form a number operator $n_{\mathbf{q},\sigma}$ which projects the sum over $\mathbf{q}$ into the states that are initial occupied (particle sector, PS).

The second such contribution is obtained by flipping the sequence of scattering processes:

$$
\begin{aligned}
T_{P3} G_W T_{P1}^\dagger &= \sum_\sigma \sum_{\mathbf{k}_1,\mathbf{k}_2,\mathbf{k}_3,\mathbf{k}_4} \sum_{\mathbf{q}} W_{\mathbf{k}_1,\mathbf{q},\mathbf{q},\mathbf{q}} c_{\mathbf{k}_1,\sigma}^\dagger c_{\mathbf{q},\sigma} n_{\mathbf{q},\sigma} G_W W_{\mathbf{q},\mathbf{k}_2,\mathbf{k}_3,\mathbf{k}_4} c_{\mathbf{q},\sigma}^\dagger c_{\mathbf{k}_2,\sigma} c_{\mathbf{k}_3,\sigma}^\dagger c_{\mathbf{k}_4,\sigma} \\
&= \sum_\sigma \sum_{\mathbf{k}_1,\mathbf{k}_2,\mathbf{k}_3,\mathbf{k}_4} c_{\mathbf{k}_1,\sigma}^\dagger c_{\mathbf{k}_2,\sigma} c_{\mathbf{k}_3,\sigma}^\dagger c_{\mathbf{k}_4,\sigma} \sum_{\mathbf{q}\in\mathrm{HS}} W_{\mathbf{q},\mathbf{k}_2,\mathbf{k}_3,\mathbf{k}_4} G_W W_{\mathbf{k}_1,\mathbf{q},\mathbf{q},\mathbf{q}} \ .
\end{aligned}
\tag{G9}
$$

By virtue of eq. G6, the product of couplings $W_{\mathbf{q},\mathbf{k}_2,\mathbf{k}_3,\mathbf{k}_4} G_W W_{\mathbf{k}_1,\mathbf{q},\mathbf{q},\mathbf{q}}$ is the same irrespective of whether $\mathbf{q}$ belongs to the particle or hole sector. The two contributions therefore cancel each other. Moreover, the remaining contributions $T_{P3}^\dagger G_W T_{P1}$ and $T_{P1} G_W T_{P2}^\dagger$ are effectively hermitian conjugates of the two contributions considered above, and therefore also cancel each other.

Scattering arising from spin-flip processes

We now come to the processes that involve spin-flips. Considering T_{F1} and T_{F4} first, we get

$$
\begin{aligned}
T_{F1}^\dagger G_W T_{F4} &= \sum_\sigma \sum_{\mathbf{k}_1,\mathbf{k}_2,\mathbf{k}_3,\mathbf{k}_4} \sum_{\mathbf{q}} W_{\mathbf{q},\mathbf{k}_2,\mathbf{k}_3,\mathbf{k}_4} c_{\mathbf{q},\sigma}^\dagger c_{\mathbf{k}_2,\sigma} c_{\mathbf{k}_3,\bar\sigma}^\dagger c_{\mathbf{k}_4,\bar\sigma} G_W W_{\mathbf{k}_1,\mathbf{q},\mathbf{q},\mathbf{q}} c_{\mathbf{k}_1\sigma}^\dagger c_{\mathbf{q}\sigma} n_{\mathbf{q}\bar\sigma} \\
&= -\sum_{1,2,3,4}\sum_\sigma c_{\mathbf{k}_1\sigma}^\dagger c_{\mathbf{k}_2\sigma} c_{\mathbf{k}_3\bar\sigma}^\dagger c_{\mathbf{k}_4\bar\sigma} \sum_{\mathbf{q}\in\mathrm{PS}} W_{\mathbf{q},\mathbf{k}_2,\mathbf{k}_4,\mathbf{k}_4} G_W W_{\mathbf{k}_1,\mathbf{q},\mathbf{q},\mathbf{q}} \ , \\
T_{F4} G_W T_{F1}^\dagger &= \sum_\sigma \sum_{\mathbf{k}_1,\mathbf{k}_2,\mathbf{k}_3,\mathbf{k}_4} \sum_{\mathbf{q}} W_{\mathbf{k}_1,\mathbf{q},\mathbf{q},\mathbf{q}} c_{\mathbf{k}_1\sigma}^\dagger c_{\mathbf{q}\sigma} n_{\mathbf{q}\bar\sigma} G_W W_{\mathbf{q},\mathbf{k}_2,\mathbf{k}_3,\mathbf{k}_4} c_{\mathbf{q},\sigma}^\dagger c_{\mathbf{k}_2,\sigma} c_{\mathbf{k}_3,\bar\sigma}^\dagger c_{\mathbf{k}_4,\bar\sigma} \\
&= \sum_{1,2,3,4}\sum_\sigma c_{\mathbf{k}_1\sigma}^\dagger c_{\mathbf{k}_2\sigma} c_{\mathbf{k}_3\bar\sigma}^\dagger c_{\mathbf{k}_4\bar\sigma} \sum_{\mathbf{q}\in\mathrm{HS}} W_{\mathbf{q},\mathbf{k}_2,\mathbf{k}_4,\mathbf{k}_4} G_W W_{\mathbf{k}_1,\mathbf{q},\mathbf{q},\mathbf{q}} \ .
\end{aligned}
\tag{G10}
$$

By the same arguments as in the previous subsection, these terms cancel each other out. Their hermitian conjugate contributions $T_{F1} G_W T_{F4}^\dagger$ and $T_{F4}^\dagger G_W T_{F1}$ also cancel out. The other two terms are T_{F2} and T_{F3}, and their contributions also cancel out for the same reason:

$$
\begin{aligned}
T_{F2} G_W T_{F2} &= \sum_\sigma \sum_{\mathbf{k}_1,\mathbf{k}_2,\mathbf{k}_3,\mathbf{k}_4} \sum_{\mathbf{q}} W_{\mathbf{q},\bar{\mathbf{q}},\mathbf{k}_3,\mathbf{k}_4} c_{\mathbf{q},\sigma}^\dagger c_{\bar{\mathbf{q}},\sigma} c_{\mathbf{k}_3,\bar\sigma}^\dagger c_{\mathbf{k}_4,\bar\sigma} G_W W_{\bar{\mathbf{q}},\mathbf{q},\mathbf{k}_1,\mathbf{k}_2} c_{\bar{\mathbf{q}},\sigma}^\dagger c_{\mathbf{q},\sigma} c_{\mathbf{k}_1,\bar\sigma}^\dagger c_{\mathbf{k}_2,\bar\sigma} \\
&= \sum_{1,2,3,4}\sum_\sigma c_{\mathbf{k}_1\sigma}^\dagger c_{\mathbf{k}_2\sigma} c_{\mathbf{k}_3\bar\sigma}^\dagger c_{\mathbf{k}_4\bar\sigma} \sum_{\mathbf{q}\in\mathrm{PS}} W_{\mathbf{q},\bar{\mathbf{q}},\mathbf{k}_3,\mathbf{k}_4} G_W W_{\bar{\mathbf{q}},\mathbf{q},\mathbf{k}_1,\mathbf{k}_2} \ , \\
T_{F3} G_W T_{F3} &= \sum_\sigma \sum_{\mathbf{k}_1,\mathbf{k}_2,\mathbf{k}_3,\mathbf{k}_4} \sum_{\mathbf{q}} W_{\mathbf{q},\mathbf{k}_2,\mathbf{k}_3,\bar{\mathbf{q}}} c_{\mathbf{q},\sigma}^\dagger c_{\mathbf{k}_2,\sigma} c_{\mathbf{k}_3,\bar\sigma}^\dagger c_{\bar{\mathbf{q}},\sigma} G_W W_{\bar{\mathbf{q}},\mathbf{k}_4,\mathbf{k}_1,\mathbf{q}} c_{\bar{\mathbf{q}},\bar\sigma}^\dagger c_{\mathbf{k}_4,\bar\sigma} c_{\mathbf{k}_1,\sigma}^\dagger c_{\mathbf{q},\sigma} \\
&= -\sum_{1,2,3,4}\sum_\sigma c_{\mathbf{k}_1\sigma}^\dagger c_{\mathbf{k}_2\sigma} c_{\mathbf{k}_3\bar\sigma}^\dagger c_{\mathbf{k}_4\bar\sigma} \sum_{\mathbf{q}\in\mathrm{PS}} W_{\mathbf{q},\mathbf{k}_2,\mathbf{k}_3,\bar{\mathbf{q}}} G_W W_{\bar{\mathbf{q}},\mathbf{k}_4,\mathbf{k}_1,\mathbf{q}} \ ,
\end{aligned}
\tag{G11}
$$

Scattering involving both spin-flip and spin-preserving processes

These processes involve the combination of terms like T_{P1} with T_{F4}, and T_{P2} with T_{F1}. These again cancel each other out for the same reasons as outline above.

Net renormalisation for the bath correlation term

Since all the contributions cancel out in pairs, the bath correlation term W is *marginal*.

3. Renormalisation of the Kondo scattering term J

We focus on the renormalisation of the spin-flip part of the Kondo interaction. For these processes, the intermediate many-body state always involves the impurity spin being anti-correlated with the conduction electron spin, such that the propagator for that state is $G_J = 1/\left(\omega - |\varepsilon_j|/2 + J_{\mathbf{q}}/4 + W_{\mathbf{q}}/2\right)$.

Impurity-mediated spin-flip scattering purely through Kondo-like processes

The following processes arising from the Kondo term renormalise the spin-flip interaction:

$$
\begin{aligned}
T_{KT1}^\dagger G_J \left(T_{KZ1} + T_{KZ1}^\dagger\right) &= \frac{1}{4} \sum_{\mathbf{k}_1, \mathbf{k}_1, \mathbf{q}} J_{\mathbf{q}, \mathbf{k}_2} S_d^+ \left[-c_{\mathbf{q}\downarrow}^\dagger c_{\mathbf{k}_2\uparrow} G_J c_{\mathbf{k}_1\downarrow}^\dagger c_{\mathbf{q}\downarrow} + c_{\mathbf{k}_2\downarrow}^\dagger c_{\mathbf{q}\uparrow} G_J c_{\mathbf{q}\uparrow}^\dagger c_{\mathbf{k}_1\uparrow} \right] J_{\mathbf{k}_1, \mathbf{q}} S_d^z \\
&= -\frac{1}{8} \sum_{\mathbf{k}_1, \mathbf{k}_1, \mathbf{q}} J_{\mathbf{q}, \mathbf{k}_2} S_d^+ \left[c_{\mathbf{k}_1\downarrow}^\dagger c_{\mathbf{k}_2\uparrow} G_J n_{\mathbf{q}\downarrow} + c_{\mathbf{k}_2\downarrow}^\dagger c_{\mathbf{k}_1\uparrow} (1 - n_{\mathbf{q}\uparrow}) G_J \right] J_{\mathbf{k}_1, \mathbf{q}} \\
&= -\frac{1}{8} \sum_{\mathbf{k}_1, \mathbf{k}_1} S_d^+ c_{\mathbf{k}_1\downarrow}^\dagger c_{\mathbf{k}_2\uparrow} \sum_{\mathbf{q}\in \mathrm{PS}} \left[J_{\mathbf{q}, \mathbf{k}_2} J_{\mathbf{k}_1, \mathbf{q}} + J_{\bar{\mathbf{q}}, \mathbf{k}_1} J_{\mathbf{k}_2, \bar{\mathbf{q}}} \right] G_J \ .
\end{aligned}
\tag{G12}
$$

In getting the final expression, we used the sigma matrix relation $S_d^+ S_d^z = -\frac{1}{2} S_d^+$, and absorbed the projector $1 - n_{\mathbf{q}\uparrow}$ into the sum over the particle sector by replacing q with its particle-hole transformed counterpart $\bar{q}$. An identical contribution is obtained by switching the sequence of processes:

$$
\begin{aligned}
\left(T_{KZ1} + T_{KZ1}^\dagger\right) G_J T_{KT1}^\dagger &= \frac{1}{4} \sum_{\mathbf{k}_1, \mathbf{k}_1, \mathbf{q}} J_{\mathbf{k}_1, \mathbf{q}} S_d^z \left[-c_{\mathbf{k}_1\downarrow}^\dagger c_{\mathbf{q}\downarrow} G_J c_{\mathbf{q}\downarrow}^\dagger c_{\mathbf{k}_2\uparrow} + c_{\mathbf{q}\uparrow}^\dagger c_{\mathbf{k}_1\uparrow} G_J c_{\mathbf{k}_2\downarrow}^\dagger c_{\mathbf{q}\uparrow} \right] J_{\mathbf{q}, \mathbf{k}_2} S_d^+ \\
&= -\frac{1}{8} \sum_{\mathbf{k}_1, \mathbf{k}_1} S_d^+ c_{\mathbf{k}_1\downarrow}^\dagger c_{\mathbf{k}_2\uparrow} \sum_{\mathbf{q}\in \mathrm{PS}} \left[J_{\bar{\mathbf{q}}, \mathbf{k}_2} J_{\mathbf{k}_1, \bar{\mathbf{q}}} + J_{\mathbf{q}, \mathbf{k}_1} J_{\mathbf{k}_2, \mathbf{q}} \right] G_J \ .
\end{aligned}
\tag{G13}
$$

Scattering processes involving interplay between the Kondo interaction and conduction bath interaction

Looking at $T_{KT1}^\dagger$ first, we have

$$
T_{KT1}^\dagger G_J \left(T_{F4} + T_{F4}^\dagger\right) = \frac{1}{2} \sum_{\mathbf{k}_1, \mathbf{k}_2, \mathbf{q}} J_{\mathbf{k}_2, \mathbf{q}} S_d^+ \left(c_{\mathbf{q}\downarrow}^\dagger c_{\mathbf{k}_2\uparrow} G_J W_{\mathbf{q}, \mathbf{q}, \mathbf{k}_1, \mathbf{q}} n_{q\uparrow} c_{\mathbf{k}_1\downarrow}^\dagger c_{\mathbf{q}\downarrow} + c_{\mathbf{k}_2\downarrow}^\dagger c_{\mathbf{q}\uparrow} G_J W_{\bar{\mathbf{q}}, \bar{\mathbf{q}}, \mathbf{q}, \mathbf{k}_1} n_{\bar{q}\downarrow} c_{\mathbf{q}\uparrow}^\dagger c_{\mathbf{k}_1\uparrow} \right) \ .
\tag{G14}
$$

For either of the two choices of the functional form of W, it is easy to show that $W_{\mathbf{q}, \mathbf{q}, \mathbf{k}_1, \mathbf{q}} = W_{\bar{\mathbf{q}}, \bar{\mathbf{q}}, \mathbf{q}, \mathbf{k}_1}$.

$$
T_{KT1}^\dagger G_J \left(T_{F4} + T_{F4}^\dagger\right) = \frac{1}{2} \sum_{\mathbf{k}_1, \mathbf{k}_2, \mathbf{q}} J_{\mathbf{k}_2, \mathbf{q}} W_{\mathbf{q}, \mathbf{q}, \mathbf{k}_1, \mathbf{q}} G_J S_d^+ \left[-c_{\mathbf{k}_1\downarrow}^\dagger c_{\mathbf{k}_2\uparrow} n_{\mathbf{q}\downarrow} n_{q\uparrow} + c_{\mathbf{k}_2\downarrow}^\dagger c_{\mathbf{k}_1\uparrow} (1 - n_{\mathbf{q}\uparrow}) n_{\bar{q}\downarrow} \right] \ .
\tag{G15}
$$

Another contribution is obtained by switching the sequence of the scattering processes:

$$
\begin{aligned}
\left(T_{F4} + T_{F4}^\dagger\right) G_J T_{KT1}^\dagger &= \frac{1}{2} \sum_{\mathbf{k}_1, \mathbf{k}_2, \mathbf{q}} \left(W_{\mathbf{q}, \mathbf{q}, \mathbf{k}_1, \mathbf{q}} n_{\bar{q}\uparrow} c_{\mathbf{k}_1\downarrow}^\dagger c_{\mathbf{q}\downarrow} G_J c_{\mathbf{q}\downarrow}^\dagger c_{\mathbf{k}_2\uparrow} + W_{\bar{\mathbf{q}}, \bar{\mathbf{q}}, \mathbf{q}, \mathbf{k}_1} n_{q\downarrow} c_{\mathbf{q}\uparrow}^\dagger c_{\mathbf{k}_1\uparrow} G_J c_{\mathbf{k}_2\downarrow}^\dagger c_{\mathbf{q}\uparrow} \right) J_{\mathbf{k}_2, \mathbf{q}} S_d^+ \\
&= \frac{1}{2} \sum_{\mathbf{k}_1, \mathbf{k}_2, \mathbf{q}} \left(c_{\mathbf{k}_1\downarrow}^\dagger c_{\mathbf{k}_2\uparrow} n_{\bar{q}\uparrow} (1 - n_{\mathbf{q}\downarrow}) - c_{\mathbf{k}_2\downarrow}^\dagger c_{\mathbf{k}_1\uparrow} n_{q\downarrow} n_{\mathbf{q}\uparrow} \right) W_{\mathbf{q}, \mathbf{q}, \mathbf{k}_1, \mathbf{q}} G_J J_{\mathbf{k}_2, \mathbf{q}} S_d^+
\end{aligned}
\tag{G16}
$$

The two contributions (eqs. G15 and G16) arising from T_{KT1} cancel each other.

We now consider the other spin-exchange process $T_{KT2}^\dagger$. One such contribution is

$$T_{KT2}^\dagger G_J T_{F3} = \frac{1}{2} \sum_{\mathbf{k}_1,\mathbf{k}_2,\mathbf{q}} J_{\mathbf{q},\bar{\mathbf{q}}} S_d^+ \left(c_{\mathbf{q}\downarrow}^\dagger c_{\bar{\mathbf{q}}\uparrow} G_J c_{\bar{\mathbf{q}}\uparrow}^\dagger c_{\mathbf{k}_2\uparrow} c_{\mathbf{k}_1\downarrow}^\dagger c_{\mathbf{q}\downarrow} + c_{\bar{\mathbf{q}}\downarrow}^\dagger c_{\mathbf{q}\uparrow} G_J c_{\mathbf{q}\uparrow}^\dagger c_{\mathbf{k}_2\uparrow} c_{\mathbf{k}_1\downarrow}^\dagger c_{\bar{\mathbf{q}}\downarrow} \right) W_{\bar{\mathbf{q}},\mathbf{k}_2,\mathbf{k}_1,\mathbf{q}}$$

$$= -\frac{1}{2} \sum_{\mathbf{k}_1,\mathbf{k}_2,\mathbf{q}} S_d^+ c_{\mathbf{k}_1\downarrow}^\dagger c_{\mathbf{k}_2\uparrow} \left[n_{\mathbf{q}\downarrow}(1 - n_{\bar{\mathbf{q}}\uparrow}) + n_{\bar{\mathbf{q}}\downarrow}(1 - n_{\mathbf{q}\uparrow}) \right] J_{\mathbf{q},\bar{\mathbf{q}}} G_J W_{\bar{\mathbf{q}},\mathbf{k}_2,\mathbf{k}_1,\mathbf{q}} \tag{G17}$$

$$= -\frac{1}{2} \sum_{\mathbf{k}_1,\mathbf{k}_2} S_d^+ c_{\mathbf{k}_1\downarrow}^\dagger c_{\mathbf{k}_2\uparrow} \sum_{\mathbf{q}\in\mathrm{PS}} \left(J_{\mathbf{q},\bar{\mathbf{q}}} W_{\bar{\mathbf{q}},\mathbf{k}_2,\mathbf{k}_1,\mathbf{q}} + J_{\bar{\mathbf{q}},\mathbf{q}} W_{\mathbf{q},\mathbf{k}_2,\mathbf{k}_1,\bar{\mathbf{q}}} \right) G_J \ .$$

An identical contribution is obtained from the reversed term:

$$T_{F3} G_J T_{KT2}^\dagger = \frac{1}{2} \sum_{\mathbf{k}_1,\mathbf{k}_2,\mathbf{q}} W_{\bar{\mathbf{q}},\mathbf{k}_2,\mathbf{k}_1,\mathbf{q}} \left(c_{\bar{\mathbf{q}}\uparrow}^\dagger c_{\mathbf{k}_2\uparrow} c_{\mathbf{k}_1\downarrow}^\dagger c_{\mathbf{q}\downarrow} G_J c_{\mathbf{q}\downarrow}^\dagger c_{\bar{\mathbf{q}}\uparrow} + c_{\mathbf{q}\uparrow}^\dagger c_{\mathbf{k}_2\uparrow} c_{\mathbf{k}_1\downarrow}^\dagger c_{\bar{\mathbf{q}}\downarrow} G_J c_{\bar{\mathbf{q}}\downarrow}^\dagger c_{\mathbf{q}\uparrow} \right) J_{\mathbf{q},\bar{\mathbf{q}}} S_d^+$$

$$= -\frac{1}{2} \sum_{\mathbf{k}_1,\mathbf{k}_2} S_d^+ c_{\mathbf{k}_1\downarrow}^\dagger c_{\mathbf{k}_2\uparrow} \sum_{\mathbf{q}\in\mathrm{PS}} \left(J_{\mathbf{q},\bar{\mathbf{q}}} W_{\bar{\mathbf{q}},\mathbf{k}_2,\mathbf{k}_1,\mathbf{q}} + J_{\bar{\mathbf{q}},\mathbf{q}} W_{\mathbf{q},\mathbf{k}_2,\mathbf{k}_1,\bar{\mathbf{q}}} \right) G_J \ . \tag{G18}$$

Net renormalisation to the Kondo interaction

Combining the results from eqs. G12, G13, G17 and G18, as well as using the properties $J_{\bar{\mathbf{q}},\mathbf{k}_1} J_{\mathbf{k}_2,\bar{\mathbf{q}}} = J_{\mathbf{q},\mathbf{k}_2} J_{\mathbf{k}_1,\mathbf{q}} = J_{\mathbf{k}_2,\mathbf{q}} J_{\mathbf{q},\mathbf{k}_1}$ and $J_{\mathbf{q},\bar{\mathbf{q}}} W_{\bar{\mathbf{q}},\mathbf{k}_2,\mathbf{k}_1,\mathbf{q}} = J_{\bar{\mathbf{q}},\mathbf{q}} W_{\mathbf{q},\mathbf{k}_2,\mathbf{k}_1,\bar{\mathbf{q}}}$, the total renormalisation in the momentum-resolved Kondo coupling $J^{(j)}$ at the jth step amounts to

$$\Delta J_{\mathbf{k}_1,\mathbf{k}_2}^{(j)} = - \sum_{\mathbf{q}\in\mathrm{PS}} \frac{J_{\mathbf{k}_2,\mathbf{q}}^{(j)} J_{\mathbf{q},\mathbf{k}_1}^{(j)} + 4 J_{\mathbf{q},\bar{\mathbf{q}}}^{(j)} W_{\bar{\mathbf{q}},\mathbf{k}_2,\mathbf{k}_1,\mathbf{q}}}{\omega - \frac{1}{2}|\varepsilon_j| + J_{\mathbf{q}}^{(j)}/4 + W_{\mathbf{q}}/2} \tag{G19}$$

[1] N. F. Mott, Proceedings of the Physical Society. Section A **62**, 416 (1949).
[2] K. Held, R. Peters, and A. Toschi, Phys. Rev. Lett. **110**, 246402 (2013).
[3] R. M. Martin, L. Reining, and D. M. Ceperley, *Interacting Electrons: Theory and Computational Approaches* (Cambridge University Press, 2016).
[4] A. Georges and G. Kotliar, Physical Review B **45**, 6479 (1992).
[5] A. Georges, G. Kotliar, W. Krauth, and M. J. Rozenberg, Reviews of Modern Physics **68**, 13 (1996).
[6] A. Mukherjee and S. Lal, New Journal of Physics **22**, 063007 (2020).
[7] A. Mukherjee and S. Lal, New Journal of Physics **22**, 063008 (2020).
[8] A. Mukherjee and S. Lal, Nuclear Physics B **960**, 115170 (2020).
[9] A. Mukherjee and S. Lal, Nuclear Physics B **960**, 115163 (2020).
[10] S. Patra and S. Lal, Phys. Rev. B **104**, 144514 (2021).
[11] S. Pal, A. Mukherjee, and S. Lal, New Journal of Physics **21**, 023019 (2019).
[12] H. R. Krishna-murthy, J. W. Wilkins, and K. G. Wilson, Phys. Rev. B **21**, 1003 (1980).
[13] K. G. Wilson, Rev. Mod. Phys. **47**, 773 (1975).
[14] R. Bulla, T. Costi, and T. Pruschke, Rev. Mod. Phys. **80**, 395 (2008).
[15] A. Mukherjee, N. S. Vidhyadhiraja, A. Taraphder, and S. Lal, New Journal of Physics **25**, 113011 (2023).
[16] A. Georges, G. Kotliar, W. Krauth, and M. J. Rozenberg, Reviews of Modern Physics **68**, 13 (1996).
[17] S. P. Anirban Mukherjee and S. Lal, Journal of High Energy Physics **2021**, 10.1007/JHEP04(2021)148 (2021).
[18] A. Mukherjee, A. Mukherjee, N. S. Vidhyadhiraja, A. Taraphder, and S. Lal, Phys. Rev. B **105**, 085119 (2022).
[19] S. Patra, A. Mukherjee, and S. Lal, New Journal of Physics **25**, 063002 (2023).
[20] A. M. Tsvelick and P. B. Wiegmann, Journal of Statistical Physics **38**, 125 (1985).
[21] V. J. Emery and S. Kivelson, Phys. Rev. B **46**, 10812 (1992).
[22] C. Varma, P. B. Littlewood, S. Schmitt-Rink, E. Abrahams, and A. Ruckenstein, Physical Review Letters **63**, 1996 (1989).
[23] P. Coleman, L. B. Ioffe, and A. M. Tsvelik, Phys. Rev. B **52**, 6611 (1995).
[24] A. J. Schofield, Phys. Rev. B **55**, 5627 (1997).
[25] S. Patra, A. Mukherjee, A. Mukherjee, N. S. Vidhyadhiraja, A. Taraphder, and S. Lal, Journal of Physics: Condensed Matter **35**, 315601 (2023).
[26] D. L. Cox and M. Jarrell, **8**, 9825 (1996).
[27] N. Andrei and A. Jerez, Phys. Rev. Lett. **74**, 4507 (1995).

[28] C. Varma, Z. Nussinov, and W. Van Saarloos, Physics Reports **361**, 267 (2002).

[29] P. W. Anderson, Phys. Rev. Lett. **18**, 1049 (1967).

[30] K. Yamada and K. Yosida, Progress of Theoretical Physics **59**, 1061 (1978), https://academic.oup.com/ptp/article-pdf/59/4/1061/5315849/59-4-1061.pdf.

[31] K. Yamada and K. Yosida, Progress of Theoretical Physics **62**, 363 (1979).

[32] D. Gazizova and J. P. F. LeBlanc, Emergent nearest-neighbor attraction in the fully renormalized interactions of the single-band repulsive hubbard model at weak coupling (2023), arXiv:2307.02360 [cond-mat.str-el].

[33] A. Stoyanova, *Delocalized and correlated wave functions for excited states in extended systems*, Ph.D. thesis, University of Groningen (2006).

[34] R. M. Martin, Physical Review Letters **48**, 362 (1982).

[35] P. Phillips, Annals of Physics **321**, 1634 (2006).

[36] D. E. Logan, A. P. Tucker, and M. R. Galpin, Phys. Rev. B **90**, 075150 (2014).

[37] D. E. Logan and M. R. Galpin, Journal of Physics: Condensed Matter **28**, 025601 (2015).